

The emission of volatile compounds from leaf litter

Leonie Derendorp

ISBN: 978-94-6191-286-2

The emission of volatile compounds from leaf litter

De emissie van vluchtige stoffen door blad
materiaal

(met een samenvatting in het Nederlands)

PROEFSCHRIFT

ter verkrijging van de graad van doctor aan de Universiteit Utrecht op
gezag van de rector magnificus, prof.dr. G.J. van der Zwaan, ingevolge
het besluit van het college voor promoties in het openbaar te
verdedigen op

maandag 18 juni 2012 des middags te 2.30 uur

door

Leonie Derendorp

geboren op 16 september 1984 te Moordrecht

Promotoren: Prof. dr. T. Röckmann
Prof. dr. M. C. Krol
Co-promotor: Dr. R. Holzinger

CONTENTS

Contents	i
1 Introduction	1
1.1 Trace gases in the atmosphere	1
1.1.1 Hydrocarbons	1
1.1.2 Hydrogen and carbon monoxide	2
1.1.3 Methyl chloride	4
1.2 VOC emissions from leaf litter	5
1.3 Leaf litter production and decomposition	7
1.3.1 The role of volatile compounds in the decomposition of plant litter	8
1.4 Goal and outline	9
2 C₂–C₅ hydrocarbons from leaf litter	11
2.1 Introduction	13
2.2 Experimental methods	14
2.2.1 Plant materials	14
2.2.2 Analytical setup	15
2.2.3 Emission rate measurements	15
2.2.4 Setup temperature experiments	17

2.2.5	Setup UV experiments	17
2.2.6	Description of the experiments	19
2.3	Results and discussion	22
2.3.1	Heat induced C ₂ –C ₅ hydrocarbon emissions from leaf litter	22
2.3.2	UV induced C ₂ –C ₅ hydrocarbon emissions from leaf litter	27
2.4	Environmental importance	37
2.4.1	Global budgets	37
2.4.2	Local atmospheric chemistry	39
2.5	Conclusions	40
3	H₂ and CO emissions from leaf litter	43
3.1	Introduction	44
3.2	Experimental methods	45
3.2.1	Plant material	45
3.2.2	Measurement system	46
3.2.3	Experiment description	46
3.3	Results and discussion	47
3.3.1	Emissions of H ₂ and CO induced by heating of sequoia leaf litter	47
3.3.2	Emissions of H ₂ and CO induced by UV radiation	50
3.4	Conclusions	52
4	CH₃Cl emissions: laboratory experiments	55
4.1	Introduction	57
4.2	Experimental methods	58
4.2.1	Plant materials	58
4.2.2	Experimental setup	60
4.2.3	Methyl chloride emission rate measurements	60
4.2.4	Chloride content determination	61
4.2.5	Methoxyl group content determination	62
4.2.6	Calculations and statistics	62

4.3	Results and discussion	63
4.3.1	Comparison of the static- and dynamic system	63
4.3.2	Variation in CH ₃ Cl emission rates between plant species	67
4.3.3	Influence of the chloride and methoxyl group content of the leaf litter on CH ₃ Cl emissions.	68
4.3.4	The temperature dependence of CH ₃ Cl emissions	72
4.3.5	The temporal evolution of the CH ₃ Cl emission rates from leaf litter	77
4.4	Implications for atmospheric chemistry and climate change	78
4.5	Conclusions	79
5	CH₃Cl fluxes: field experiments	81
5.1	Introduction	82
5.2	Experimental methods	83
5.2.1	Location of the field experiments	83
5.2.2	Chamber and flux measurements	83
5.2.3	Laboratory measurements	85
5.2.4	Measurement of the CH ₃ Cl mixing ratio	85
5.2.5	Calculations and statistics	85
5.3	Results and discussion	86
5.3.1	Soil uptake at different locations	86
5.3.2	Methyl chloride emissions from leaf litter	90
5.4	Conclusions	94
6	Modeling the CH₃Cl budget	97
6.1	Introduction	98
6.1.1	Biomass burning	99
6.1.2	Tropical vegetation	100
6.1.3	Ocean	101
6.1.4	Fungi	102
6.1.5	Salt marshes	102

6.1.6	Wetlands, peatlands and rice paddies	102
6.1.7	Anthropogenic sources	103
6.1.8	Oxidation by the OH radical	103
6.1.9	Goal	103
6.2	Methods	104
6.2.1	The model	104
6.2.2	Sources	105
6.2.3	Observations	109
6.2.4	Emission scenarios for the forward simulations	110
6.2.5	Setup for the inversions	112
6.3	Results and discussion	113
6.3.1	Forward simulations using emission scenarios	113
6.3.2	Inversions	117
6.3.3	Sensitivity study	122
6.3.4	Validation	126
6.4	Summary and conclusion	129
7	Conclusion and outlook	131
8	Samenvatting	135
	Dankwoord	139
	Curriculum Vitae	141
	Bibliography	143

1.1 Trace gases in the atmosphere

The Earth's atmosphere mainly consists of nitrogen (N_2 , 78%) and oxygen (O_2 , 21%), but also argon (1%) and variable amounts of water vapor are present. In addition, there are thousands of other compounds present in the atmosphere in small quantities, which are called trace gases. Although their quantities are small, these trace gases have a strong influence on air quality and the global climate. The most abundant atmospheric trace gas is carbon dioxide (CO_2), an important greenhouse gas with a mixing ratio of ~ 380 ppm ($\mu\text{mol mol}^{-1}$). Also methane (CH_4) and nitrous oxide (N_2O) are strong greenhouse gases and influence the radiative balance of the Earth. Other abundant trace gases include molecular hydrogen (H_2) with a mixing ratio of ~ 500 ppb (nmol mol^{-1}) and carbon monoxide (CO) with a typical mixing ratio of ~ 100 ppb. In addition to H_2 and CO , the compounds studied in this thesis are hydrocarbons and methyl chloride (CH_3Cl). The environmental relevance of these compounds is discussed in this chapter.

1.1.1 Hydrocarbons

Hydrocarbons are compounds that consists entirely of carbon and hydrogen atoms. There are different types of hydrocarbons. Alkanes are compounds with only single bonds. Each carbon atom is connected to four other carbon or hydrogen atoms. The smallest hydrocarbons is methane, which is also an alkane. In alkenes, some carbon atoms are only attached to three carbon or hydrogen atoms. As a result, some carbon

atoms are connected to each other via a double bond. An example of an alkene is ethene, which is emitted by vegetation. Hydrocarbons with a triple bond are called alkynes. An example is ethyne, which is formed during combustion processes. Other types of hydrocarbons include cyclic hydrocarbons and aromatic hydrocarbons.

The surface mixing ratio of methane in the atmosphere is approximately 1.7-1.8 ppm. However, for most hydrocarbons in the atmosphere the mixing ratios are lower. Typical mixing ratios vary from ppt's (pmol mol^{-1}) for reactive compounds up to several ppb's for less reactive compounds. For example, Seinfeld and Pandis (2006) reported typical mixing ratios of 27 ppb for ethane, 56 ppb for propane and 42 ppb for butane.

Although the mixing ratios of hydrocarbons in the atmosphere are low, they play an important role in tropospheric chemistry. Hydrocarbons are oxidized by ozone, OH and nitrate radicals, and therefore influence the cycles of these oxidizing species. In addition, non-methane hydrocarbons are important precursors for tropospheric ozone in the presence of NO_x and influence HO_x chemistry (Chameides et al., 1988; Sauvage et al., 2009; Yates et al., 2010; Pozzer et al., 2010). The oxidation of hydrocarbons results in the production of carbonyl compounds, which can also be involved in the formation of secondary organic aerosols (Cahill et al., 2006; Claeys et al., 2004; Holzinger et al., 2005; DiCarlo et al., 2004). A schematic overview of the oxidation of hydrocarbons by the OH radical is shown in Fig. 1.1.

The sources of hydrocarbons in the atmosphere can be natural or anthropogenic. Ethane has mainly anthropogenic sources and is emitted during industrial processes, the combustion of biofuels and fossil fuels, biomass burning and waste treatment (Stein and Rudolph, 2007). Compounds with mainly natural sources are isoprene and monoterpenes. They are emitted by living vegetation in response to changing temperatures and levels of light intensity. Other compounds are emitted from both natural and anthropogenic sources. For example, ethene is released from urban areas and during biomass burning, but also vegetation, oceans and the soil emit ethene. Especially vegetation is an important ethene source, with an estimated contribution of 1/3 to the total ethene emission (Poisson et al., 2000).

1.1.2 Hydrogen and carbon monoxide

Hydrogen is an interesting compound as it may be used as an energy carrier in the future as a replacement for fossil fuels. However, during the use, storage and production of H_2 , a small fraction of the H_2 may leak to the atmosphere and thereby enhance the atmospheric H_2 mixing ratio. In the atmosphere, H_2 reacts with the OH radical. Enhanced H_2 levels therefore lead to a lower level of OH radicals, and consequently

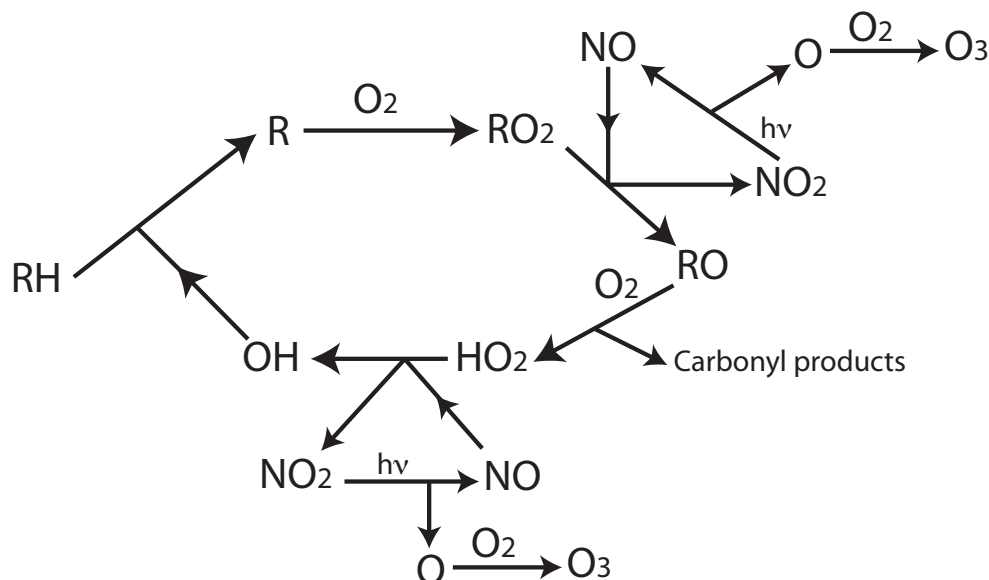


Figure 1.1: Schematic overview of the oxidation of hydrocarbons (RH) in the troposphere. After oxidation by the OH radical, the resulting hydrocarbon radical (R) reacts with molecular oxygen (O_2) to form a hydrocarbon peroxide (RO_2). This peroxide reduces to a hydrocarbon oxide (RO) due to reactions with NO that also leads to the formation of NO_2 . The hydrocarbon oxide reacts again with O_2 , which leads to the formation of carbonyl compounds and HO_2 . The carbonyl compounds may participate in the formation of aerosols, whereas HO_2 is recycled to OH via a reaction with NO. The NO_2 that is formed in several steps can be photolyzed leading the recycling of NO and the formation of ozone (O_3). This overview was derived from Seinfeld and Pandis (2006).

less OH is available for the removal of other pollutants from the atmosphere. In addition, enhanced H_2 mixing ratios lead to the increased formation of stratospheric water vapor, which leads to the formation of stratospheric clouds and consequently the enhanced destruction of stratospheric ozone. Important sources of H_2 are the oxidation of methane and non-methane hydrocarbons, biomass burning, the combustion of fossil fuels and the fixation of nitrogen in the ocean and biosphere. The main sink of H_2 is uptake by the soil. In addition, H_2 is removed from the atmosphere by oxidation with the OH radical. The global atmospheric burden of H_2 is estimated between 141 and 172 Tg, whereas estimates for the atmospheric lifetime vary between 1.4 and 2.3 yr (Pieterse et al., 2011; Ehhalt and Rohrer, 2009).

Carbon monoxide is the main sink for the OH radical. Approximately 40% of all OH reacts with CO. Variations in the atmospheric level of CO therefore lead to variations in the available amount of OH, which in turn leads to variations in the levels of other atmospheric pollutants that are normally oxidized by OH. In addition, CO is an important precursor of tropospheric ozone when NO_x are present. The main sources of

CO are biomass burning, the combustion of fossil fuels during transport and industrial processes, and residential cooking and heating. Carbon monoxide is also produced in the atmosphere during the oxidation of methane and non-methane hydrocarbons. The main sink of CO is oxidation by the OH radical, but a small fraction is lost from the atmosphere via deposition (Seinfeld and Pandis, 2006; Spivakovsky et al., 2000).

1.1.3 Methyl chloride

Methyl chloride is the most abundant natural chlorine-containing compound in the atmosphere. Approximately 16% of the total amount of tropospheric chlorine originates from CH_3Cl (Graedel and Keene, 1995; Butler, 2000; World Meteorological Organization, 2010). Atmospheric concentrations of CH_3Cl generally range between 500 and 600 ppt and Khalil and Rasmussen (1999) estimated the average atmospheric CH_3Cl mixing ratio at 540 ppt. The largest concentrations are observed in the Tropics, and the lowest are found in the polar regions. Seasonal variations of the CH_3Cl mixing ratio are mainly due to varying levels of the OH radical. The atmospheric lifetime of CH_3Cl is approximately 1.3 yr. Because of this relatively long lifetime, part of the CH_3Cl emitted at the surface is transported into the stratosphere. In the stratosphere, the chlorine atoms are released through photolysis. These chlorine atoms are responsible for the catalytic destruction of stratospheric ozone (Butler, 2000). Anthropogenic emissions of ozone depleting substances have been strongly reduced since the Montreal Protocol was introduced in 1987. As a consequence, compounds with natural sources have become relatively more important as a source of chlorine to the stratosphere. This is illustrated in Fig. 1.2. In 1990 the destruction of stratospheric ozone was at its maximum value and mainly caused by compounds emitted from anthropogenic sources. As a consequence of the Montreal Protocol, the emissions from anthropogenic sources are decreasing. In the future, most of the stratospheric ozone destruction is expected to be caused by compounds emitted by natural sources, including CH_3Cl . Therefore, understanding the global CH_3Cl budget and assessing how it will change in a changing climate is of great importance.

There are substantial uncertainties in the atmospheric CH_3Cl budget. For many years only half to two-thirds of the CH_3Cl sinks ($\sim 4 \text{ Tg yr}^{-1}$) could be balanced with known sources of CH_3Cl (Butler, 2000; Graedel and Keene, 1995; Keene et al., 1999). However, many sources, mainly natural, have now been identified that can balance or even outweigh the total global sink strength (Keppler et al., 2005; Saito and Yokouchi, 2008; World Meteorological Organization, 2010), but it remains uncertain which sources are most important for the atmospheric budget and what parameters and processes control the emissions. The main sink for CH_3Cl is oxidation by the OH radical in the

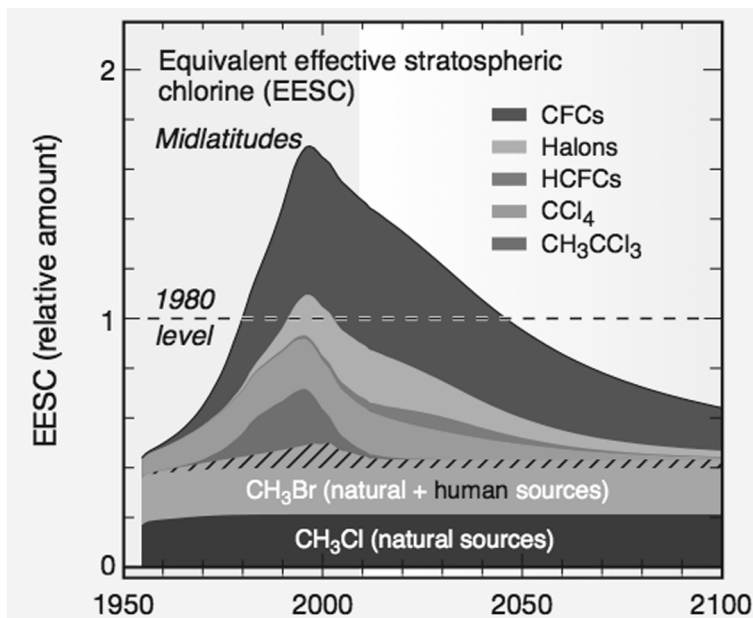


Figure 1.2: Equivalent effective stratospheric chlorine from 1950 and predicted up to the year 2100. Edited from World Meteorological Organization (2010).

troposphere, but also the soil is a significant sink of CH_3Cl (Keppler et al., 2005; Khalil and Rasmussen, 2000; Rhew et al., 2010). Known sources include tropical plants (Yokouchi et al., 2002, 2007), biomass burning (Lobert et al., 1999), industry (McCulloch et al., 1999), wood rotting fungi (Harper, 1985; Anke and Weber, 2006), oceans (Moore, 2000; Ooki et al., 2010), salt marshes (Rhew et al., 2000; Rhew and Mazéas, 2010), soil (Keppler et al., 2000), rice paddies (Khan et al., 2011; Redeker et al., 2000) and leaf litter (Hamilton et al., 2003).

1.2 The emission of volatile compounds from leaf litter

Leaf litter emits volatile compounds into the atmosphere, where those compounds may influence the atmospheric chemistry on local and regional scales and may effect the global climate. Numerous chemical species that can be released from leaf litter have been identified, but large uncertainties in the amounts that are released and the factors that control the emissions still exist. In a laboratory experiment on volatile compound emissions from leaf litter of deciduous trees, Isidorov and Jdanova (2002) identified over 70 different compounds belonging to different classes including C_4 – C_{10} hydrocarbons, terpenes and oxygenated compounds, but the emissions were not quantified. Isidorov and Jdanova (2002) suggested that most compounds were emitted due

to the action of litter decomposing microorganisms. This was confirmed by Leff and Fierer (2008), who also observed that volatile organic compound (VOC) emissions from decomposing litter are mainly due to microbial activity. In addition, Gray et al. (2010) showed that methanol is the main compound emitted during plant litter decomposition, and that biotic sources of VOCs are more important than abiotic sources.

Several other compounds have been identified that are emitted via an abiotic process. Methyl bromide (CH_3Br) emissions from leaf litter are not mediated by enzymatic or microbial activity, but depend on both temperature and the bromine content of the plant material (Wishkerman et al., 2008). Similar results were obtained for methyl chloride (CH_3Cl) emissions from dead and senescent leaves (Hamilton et al., 2003; Keppler et al., 2004; Yassah et al., 2009). The emissions of CH_3Cl were depending on temperature and the chloride content of the plant material. Hamilton et al. (2003) and Keppler et al. (2004) suggested that CH_3Cl is formed in leaf litter through reaction between pectin methoxyl groups and chloride ions, but the precise formation mechanism is unknown. In addition, field measurements of CH_3Cl emissions have been performed on leaf litter at different locations in a tropical rainforest (Blei et al., 2010) and from needle and leaf litter in a temperate deciduous forest in Scotland (Blei and Heal, 2011). Blei and Heal (2011) concluded that the extent to which leaf and needle litter fluxes are the product of abiotic chemical reactions and/or microbial/fungal activity is unknown and requires further investigation.

Carbon monoxide (CO) is emitted by leaf litter upon irradiation with ultraviolet (UV) light, and the emission rate depends on both the intensity and wavelength of the radiation. Thermally induced CO emissions have also been observed and the emission rates increased with temperature (Schade et al., 1999; Tarr et al., 1995). In addition, acetone and methanol are emitted from leaf litter. The emissions increased with temperature, but the total emission was found to be independent of temperature (Warneke et al., 1999).

Several hydrocarbons that are emitted by leaf litter and the factors influencing the emissions have been identified. Methane is emitted from leaf litter, dry and fresh detached leaves, and plant structural components (e.g., lignin and pectin). The emission of methane is influenced by temperature and UV radiation (Keppler et al., 2009; Vigano et al., 2008, 2009, 2010; McLeod et al., 2008; Messenger et al., 2009; Bruhn et al., 2009). In addition to methane, McLeod et al. (2008) also detected emissions of ethane and ethene from citrus pectin and detached tobacco leaves when irradiated with UV radiation. In addition, monoterpene emissions from needle and leaf litter were observed during field experiments in Poland and Finland (Hellén et al., 2006; Isidorov et al., 2010).

For some VOCs leaf litter is estimated to be an important source for their global budget.

For example, the global annual emission of acetone and methanol from degrading leaves is estimated to be 6 – 8 Tg for acetone and 18 – 40 Tg for methanol, which is a significant (>10 %) contribution to the global budget of these compounds (Warneke et al., 1999). According to estimates by Hamilton et al. (2003) the global source of CH_3Cl from leaf litter ranges from 0.3 up to 2.5 Tg yr^{-1} , which corresponds to up to 60% of the CH_3Cl budget (Keppler et al., 2005).

1.3 Leaf litter production and decomposition

Leaf litter is a potentially important source of volatile compounds, because it is available at the Earth's surface in large quantities. Matthews (1997) estimated the size of the global plant litter pool at 160 Pg dm ($1\text{Pg} = 10^{15}\text{ g}$; dm = dry matter). This estimate of plant litter includes litter of leaves, fine wood and roots. Also the annual production of leaf litter is substantial. Each year, between 75 and 135 Pg dm yr^{-1} of plant litter is produced. This includes both above and below ground plant litter. The contribution of above ground litter, including leaf litter, to the total plant litter production is estimated at 44 - 49 Pg dm yr^{-1} (Matthews, 1997). An estimate of the spatial distribution of the annual above ground plant litter production is shown in Fig. 1.3. This figure clearly indicates that the production of plant litter is largest in the tropical regions.

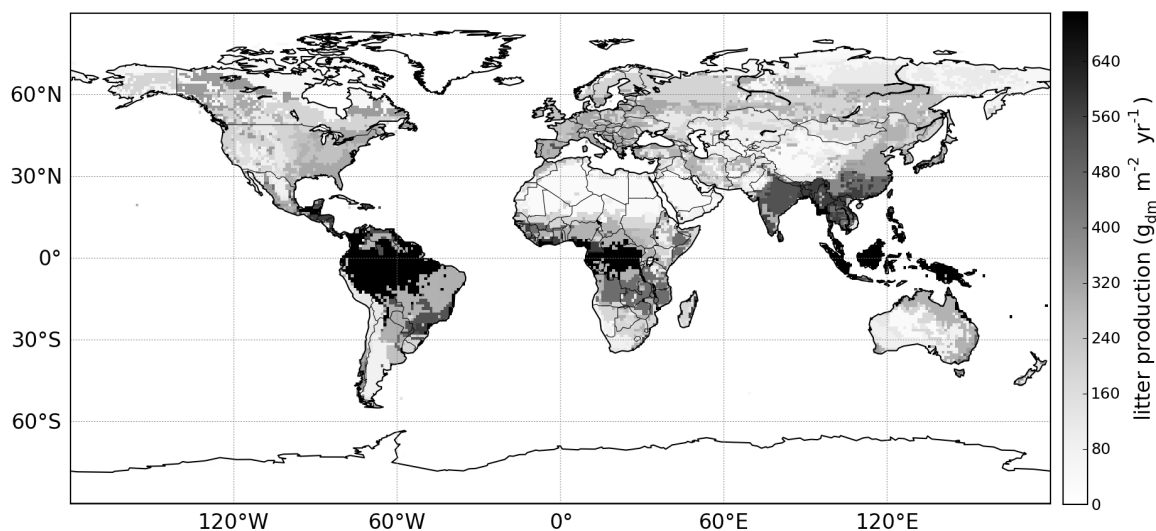


Figure 1.3: Estimate of the annual aboveground litter production based on data from Matthews (1997).

1.3.1 The role of volatile compounds in the decomposition of plant litter

Decomposition of plant litter is the main process by which carbon is cycled between plants, soil and the atmosphere. During the decomposition process carbon dioxide is produced and released into the atmosphere. In mesic ecosystems with a moderate and well balanced water supply, the decomposition of plant litter is mainly due to microbial communities. Consequently, the decomposition is controlled by temperature and precipitation. Also litter quality, defined as the carbon to nitrogen ratio (C:N ratio) or the lignin to nitrogen ratio (lignin:N ratio) of the litter, is an important factor for the decomposition rate of plant litter. The litter quality is low, when the lignin content is high. Lignin is the main structural compound of wood and has a complex, heterogeneous chemical structure, which is difficult to degrade by microbial communities. Therefore, in mesic ecosystems the decomposition rate of plant litter with a high lignin content is low. (Ayres et al., 2009; Brandt et al., 2007).

In contrast, in arid ecosystems there are additional processes involved in the decomposition of plant litter. Arid ecosystems cover approximately one third of Earth's land surface and are characterized by high temperatures, high levels of solar radiation and a low availability of moisture. These factors limit microbial activity and the decomposition of plant litter by microbial communities. However, the decomposition of plant matter is faster than expected based on temperature, precipitation and litter quality, which indicates that in addition to microbial plant litter decomposition there are other decomposition processes in arid ecosystems (Brandt et al., 2009; Day et al., 2007; Austin and Vivanco, 2006). The formation of volatile compounds from plant litter has been identified as an important mechanism for the decomposition of plant litter in these ecosystems. Volatile compounds are formed when plant litter is exposed to UV radiation. The high levels of UV radiation in these arid areas enhance the production of volatile compounds (Day et al., 2007). In addition, the quality of plant litter in these ecosystems is often low, i.e. the lignin content is high. Lignin is a good absorber of UV radiation and photo degradation is favored for plant litter with a high lignin content. Brandt et al. (2009) measured the production CO_2 from plant litter in a desert grassland in New Mexico, and concluded that a significant fraction of the litter mass loss was caused by CO_2 production as a consequence of photo degradation. This indicates that for arid ecosystems a significant fraction of the carbon that is stored in plant litter is not cycled via the soil, but is directly released into the atmosphere.

1.4 Goal and outline

This thesis describes the experiments in which the emission of several volatile compounds from leaf litter was measured and the factors that influence the emissions were investigated. Afterwards, the significance of the emissions for local atmospheric chemistry and the global budgets of the compounds were determined. The environmental importance of the emissions was either estimated using a simple upscaling method or using a global chemistry transport model. The volatile compounds investigated in this thesis were C₂–C₅ hydrocarbons, CH₃Cl, H₂ and CO. This thesis includes work from five papers:

1. L. Derendorp, R. Holzinger, A. Wishkerman, F. Keppler and T. Röckmann, *Methyl chloride and C₂–C₅ hydrocarbon emissions from dry leaf litter and their dependence on temperature*, Atmos. Environ., 45(18), pp. 3112–3119, 2011
2. L. Derendorp, R. Holzinger and T. Röckmann, *UV induced C₂–C₅ hydrocarbon emissions from leaf litter*, Environ. Chem. 8(6), pp. 602–611, 2011
3. L. Derendorp, J. B. Quist, R. Holzinger and T. Röckmann, *Emissions of H₂ and CO from leaf litter of Sequoiadendron giganteum, and their dependence on UV radiation and temperature*, Atmos. Environ., 45 (39) pp. 7520–7524, 2011.
4. L. Derendorp, A. Wishkerman, F. Keppler, C. McRoberts, R. Holzinger and T. Röckmann, *Methyl chloride emissions from halophyte leaf litter: dependence on temperature and chloride content*, Chemosphere, doi:10.1016/j.chemosphere.2011.12.035, 2012,
5. L. Derendorp, M. C. Krol, T. Röckmann, J. W. Elkins, R. Wang and M. Maione, *Modeling methyl chloride: the importance of leaf litter emissions*, in preparation.

In order to avoid excessive repetitions, the content of the papers has been re-grouped by compound or compound class in the different chapters of this thesis. Each chapter starts with a general introduction on the respective compounds. In Chapter 2, the emission of C₂–C₅ hydrocarbons from leaf litter is described. Laboratory experiments were performed to determine the effect of UV radiation intensity and wavelength, humidity and temperature on the emission rates. Also the temporal evolution of the C₂–C₅ hydrocarbon emissions was investigated. This chapter includes the respective results from papers 1 and 2.

The measurements of H₂ and CO emissions from leaf litter that were published in paper 3 are presented in Chapter 3. This chapter discusses the influence of UV radiation and temperature on the emission of H₂ and CO from leaf litter of *Sequoiadendron*

giganteum. Previous studies already showed that CO can be emitted from leaf litter upon heating or UV irradiation and these results are confirmed by our measurements. Emissions of H₂ from leaf litter have not been measured before and were investigated in this study for the first time.

A large part of this thesis focusses on CH₃Cl. Chapter 4 describes two laboratory studies in which the emission of CH₃Cl from leaf litter was measured and the factors that control emissions were investigated. In the first laboratory study, the emission of CH₃Cl from several plant species was measured and the dependence of the emissions on temperature was determined. Methyl chloride was emitted in significant amounts from leaf litter of various plant species, but large variations between plant species were observed. These variations were further examined in the second laboratory study with leaf litter of halophytes, plant species that are able to live in salty environments and that have high levels of chlorine in their leaves. This chapter includes the respective results from the papers 1 and 4. Chapter 5 describes a limited number field experiments in which the emission of CH₃Cl from leaf litter was measured (unpublished results). In addition, the uptake of CH₃Cl by the soil was measured. Chapter 6 describes a study in which the atmospheric CH₃Cl budget is modeled. Forward simulations with a global chemistry transport model were done to assess the global relevance of leaf litter as a source of CH₃Cl. In addition, inversions were performed to estimate the global net emission of CH₃Cl for different geographical regions. The results from this modeling study are described in paper 5.

CHAPTER 2

THE DEPENDENCE OF C₂–C₅ HYDROCARBON EMISSIONS ON TEMPERATURE AND UV RADIATION

Hydrocarbons play an important role in tropospheric chemistry. They are oxidized by ozone, OH and nitrate radicals and therefore influence the atmospheric levels of these oxidizing species. Hydrocarbons also react with halogens when present. In addition, they are important precursors for tropospheric ozone in the presence of NO_x and influence HO_x chemistry. Hydrocarbon oxidation products can also be involved in the formation of secondary organic aerosols. This study investigated the emission of several C₂–C₅ hydrocarbons from leaf litter of different plant species and their dependence on temperature and UV radiation. The emission rates of ethane, ethene, propane, propene and n-pentane increased with temperature between 20 and 100 °C. Hydrocarbon emission rates up to 0.88 ng gdw⁻¹ h⁻¹ were measured at 20 °C, whereas at 70 °C emission rates increased up to 650 ng gdw⁻¹ h⁻¹ depending on plant species. The Arrhenius relation can be used to describe the temperature dependence of hydrocarbon emissions, although deviations from this relation were observed at high temperature. The emissions were not due to enzymatic activity, which was indicated by emission rates that continuously increased with increasing temperature, and activation energies that were higher than 50 kJ mol⁻¹. At constant temperature, the emission rate decreased in time. At high temperatures (80–100 °C) this was noticeable on a timescale of hours, while at low temperatures (20–30 °C) the decrease was very slow and only visible on a timescale of months.

When leaf litter was irradiated with UV, the emission rates of C₂–C₅ hydrocarbons increased linearly with the intensity of the UV radiation within the ambient range of UV intensities. UVB radiation (280–320 nm) was more efficient in the generation of hydrocarbons from leaf litter than UVA (320–400 nm). In absence of oxygen, no emissions of C₂–C₅ hydrocarbons were ob-

served. When leaf litter was placed in humid air, emission rates approximately tripled compared to emissions from leaf litter in dry air. A simple upscaling showed that C₂–C₅ hydrocarbon emissions from leaf litter induced by UV radiation or heating of the litter are likely insignificant for their global budgets. However, hydrocarbon emissions from leaf litter might have a small influence on atmospheric chemistry on the local scale.

This chapter is based on:

- L. Derendorp, R. Holzinger, A. Wishkerman, F. Keppler and T. Röckmann, *Methyl chloride and C₂–C₅ hydrocarbon emissions from dry leaf litter and their dependence on temperature*, Atmos. Environ., 45(18), pp. 3112-3119, 2011
- L. Derendorp, R. Holzinger and T. Röckmann, *UV induced C₂–C₅ hydrocarbon emissions from leaf litter*, Environ. Chem. 8(6), pp. 602-611, 2011

2.1 Introduction

Hydrocarbons play an important role in tropospheric chemistry, as these compounds are oxidized by ozone, OH and nitrate radicals, and therefore influence the levels of these oxidizing species. In addition, they are important precursors for tropospheric ozone in the presence of NO_x and influence HO_x chemistry (Chameides et al., 1988; Yates et al., 2010; Pozzer et al., 2010). The oxidation products of direct leaf litter emissions can also be involved in the formation of secondary organic aerosols (Cahill et al., 2006; Claeys et al., 2004).

Leaf litter has been identified as a source hydrocarbons to the atmosphere. Several hydrocarbons emitted by leaf litter have been identified in previous studies and the factors that influence the emissions have been investigated. Most studies focussed on the emission of methane from leaf litter, dry and fresh detached leaves, and plant structural components (e.g. lignin and pectin) (Keppler et al., 2009; Vigano et al., 2008, 2009, 2010; McLeod et al., 2008; Messenger et al., 2009; Bruhn et al., 2009). The emission of methane was depending on temperature and influenced by UV radiation. Also emissions of ethane and ethene were observed when citrus pectin and detached tobacco leaves were irradiated with UV (McLeod et al., 2008). In addition, emissions of monoterpenes and several other hydrocarbons were emitted from a Scots pine forest floor in the boreal region (Finland). Monoterpenes were the main emitted compounds, and it was suggested that decaying plant material on the forest floor was the main source of the emissions (Hellén et al., 2006). Monoterpene emissions from needle litter were also measured during litter bag experiments in Poland. The emission rates from needle litter in the first stage of decomposition were comparable to the live needles of the same trees, suggesting that needle litter is an important source of monoterpenes (Isidorov et al., 2010).

In this study the focus was on the emission of C₂–C₅ hydrocarbons from leaf litter. C₂–C₅ hydrocarbons are expected to be formed in leaf litter through peroxidation of the poly-unsaturated fatty acids (PUFAs) of the membranes lipids, which are present in walls of plant cells. The process requires oxygen and can be initiated by radicals or enzymes. Peroxidation of PUFAs leads to the formation of lipid hydroperoxides, which can subsequently decompose to hydrocarbons, aldehydes and alcohols. Decomposition of lipid hydroperoxides occurs due to heating or reaction with the transition metals iron or copper (Halliwell and Gutteridge, 2008; John and Curtis, 1977; Dumelin and Tappel, 1977; Konze and Elstner, 1978).

The goal of this study was to investigate the environmental importance of leaf litter as a source of C₂–C₅ hydrocarbons to the atmosphere. For some VOCs (e.g. CH₃Cl (Hamilton et al., 2003; Keppler et al., 2004), methanol and acetone (Warneke et al.,

1999)) leaf litter has previously been identified as a globally important source, but the emission of many C₂–C₅ hydrocarbons from leaf litter has not been measured before. In laboratory experiments under controlled conditions, we investigated which hydrocarbons were emitted, and how C₂–C₅ hydrocarbon emissions were influenced by temperature and UV radiation. To determine the influence of temperature, emission rates were measured between 20 and 70 °C and Arrhenius plots were used to quantify the temperature dependence of the emissions. Measurements were performed on both ground and whole leaf material. In addition, the temporal evolution of the emission rates was determined at different temperatures. To determine the effect of UV radiation on the emission of C₂–C₅ hydrocarbons from leaf litter, it was examined whether UVA or UVB is more efficient in generating C₂–C₅ hydrocarbon emissions from leaf litter. Also, the combined effect of UV radiation and humidity on the emissions was determined, as well as whether UV induced C₂–C₅ hydrocarbons could be formed in absence of oxygen. Last, the temporal evolution of hydrocarbon emissions from leaf litter when irradiated with UV was investigated. A simple upscaling method was used to estimate the influence of C₂–C₅ hydrocarbon emissions from leaf litter on their global budgets and atmospheric chemistry.

2.2 Experimental methods

2.2.1 Plant materials

Leaf litter of sequoia (*Sequoiadendron giganteum*), rice (*Oryza sativa*), maize (*Zea mays* spp.), cherry prinsepia (*Prinsepia sinenses*), birch (*Betula jacquemontii*) and beech (*Fagus orientalis*) was collected in the botanical garden of the Johannes Gutenberg University in Mainz (Germany). Sweetgum (*Liquidambar styraciflua*) was collected in Moordrecht (The Netherlands). Sequoia, cherry prinsepia, birch, sweetgum and beech are typical forest plants in continental and mediterranean climates, whereas rice and maize are important agricultural crops. The leaf litter was air-dried at 25 °C for two months in a fume hood. After drying, part of the plant material was stored in plastic zip bags, while the other part was ground with a coffee grinder to homogenize the plant material and stored in 50 mL vials sealed with parafilm (Sigma-Aldrich, Germany). All leaf litter was stored at ambient temperature. For cherry prinsepia and beech only ground plant material was available, while for sweetgum and birch only whole (unground) leaf litter was used.

2.2.2 Analytical setup

Dry plant material (0.5 - 3 g) was inserted into a cylindrical UV-transparent quartz tube (suprasilTM) of 350 mL volume. At one end the quartz tube could be opened via a conically tapered ground glass joint. To prevent the tube from opening during the experiments, a clip was used to fix the tube, without using grease. For measurements with ground litter, a flat glass plate was fully covered with plant material and inserted into the tube, while whole leaf litter was directly placed in the tube. The tube was continuously flushed with synthetic air (AirProducts 22655, Zero 4.8, The Netherlands) or nitrogen gas (AirProducts 26508, BIP 5.7, The Netherlands) via a mass flow controller at a flow rate of 50 mL min⁻¹. Air coming out of the quartz tube was flushed into a gas chromatograph (GC) via a Nafion humidity exchanger (Perma Pure, MD-050-72P-2, NJ, USA) and another mass flow controller at a flow rate of 33.3 mL min⁻¹. Excess air was vented. 1/4 inch PFA teflon lines were used to connect different parts of the system. The temperature of the leaf litter was monitored in the quartz tube on the surface of the leaves with a thermocouple. Parts of the system that did not require exposure to UV radiation were covered with aluminum foil.

2.2.3 Emission rate measurements

A gas chromatograph (Varian star 3600 CX, CA, USA) equipped with a flame ionization detector was used to measure mixing ratios of several C₂–C₅ hydrocarbons. Air from the quartz tube was cryotrapped at a flow rate of 33.3 mL min⁻¹ at -170 °C in the sample pre-concentration trap (SPT), which was filled with glass beads. The SPT was chilled with liquid nitrogen and the temperature was regulated via a solenoid valve and a thermostat. Depending on the required sample size, the trapping time was 15 or 30 min, which corresponds to a sampled volume of 0.5 and 1.0 L, respectively. After trapping, the SPT was heated to 150 °C within 5 s to release the sample to the column of the gas chromatograph. A 10 m CP-SIL 5CB column followed by a 50 m silicaPLOT column were used, both with an inner diameter of 0.53 mm. The temperature of the column was initially 40 °C for 5 min, then increased to 225 °C at a rate of 6.5 °C min⁻¹. The total run on the gas chromatograph was completed in 40 min. After the run, an additional 15 min were required to cool down the system for the next measurement. The chromatograms were evaluated for ethane, ethene, ethyne, propane, propene, *i*-butane, *n*-butane, *i*-pentane, and *n*-pentane.

The gas chromatograph was regularly calibrated with reference gases (Praxair SI91597, Belgium, for ethane, ethene, ethyne, propane, propene, *i*-butane, *n*-butane, *i*-pentane and *n*-pentane with mixing ratios of 50, 31, 31, 30, 31, 20, 20, 20, and 20 ppb (nmol mol⁻¹),

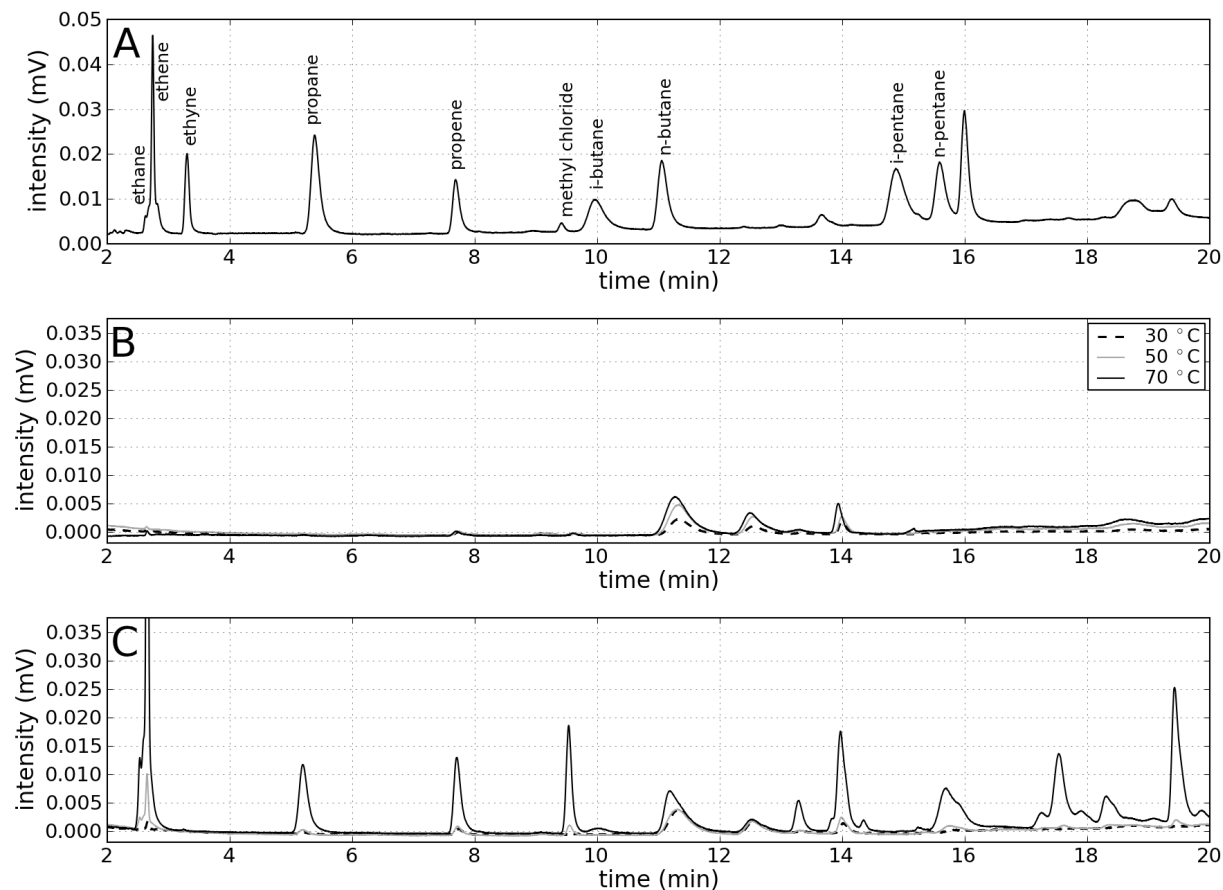


Figure 2.1: (A) Example of a measurement of the reference gas in which the target compounds are labelled. (B) Blank measurements at 30, 50, and 70 °C. (C) Example chromatograms of an experiment with whole maize leaf litter at the same three temperatures.

respectively, and AiR Environmental CC262873, CO, USA, for ethane and propane with mixing ratios of 206 and 103 ppb, respectively). Fig. 2.1a shows an example of a chromatogram with the reference gases. Only the first twenty minutes of the chromatogram are shown, since all reported compounds eluted within this time.

The emission rates of the different hydrocarbons were calculated according to Eq. (2.1)

$$ER_x = \frac{C_x M_x F_{\text{chamber}}}{V_m A} \quad (2.1)$$

where ER_x is the emission rate of compound x , C_x its mixing ratio, M_x its molar mass, F_{chamber} the flow rate through the quartz tube, V_m the molar volume of an ideal gas. A

is either the dry mass or the surface area of the leaf litter. For experiments in which the temperature dependence of the emission rates is determined, the emissions were scaled with the mass of the leaf litter, and A is the dry weight of the plant sample. For experiments in which the effects of UV radiation were investigated, the emission rates were scaled to the surface area of the leaves, and A is the area of the leaves directly exposed to UV radiation. For ground litter a flat glass plate inside the quartz tube was fully covered with plant material, and the area of this glass plate was used to calculate the emission rates. For measurements on whole litter the quartz tube was generally completely filled with litter, and the area of the quartz tube was used. Mixing ratios were determined after correction for a system blank (Fig. 2.1b).

The detection limit of the mixing ratio, defined as three times the standard deviation of the noise, was ~ 2 ppt for each of the C_2 – C_5 hydrocarbons in a 1 L sample. For experiments in which the influence of temperature on the emissions is investigated, this corresponds to an emission rate of $\sim 0.007 \text{ ng gdw}^{-1}\text{h}^{-1}$ for 1 g of plant material. For experiments in which UV effects are investigated, this corresponds to ~ 2.5 and $1.0 \text{ ng m}^{-2}\text{h}^{-1}$ for ground and whole leaf litter, respectively.

2.2.4 Setup temperature experiments

A heating wire connected to an adjustable power supply was wrapped around the quartz tube to vary the temperature inside the tube. The temperature was monitored in the tube on the surface of the leaves with a thermocouple. Stable temperatures were generally obtained within ten minutes, and remained stable during the measurements. The quartz tube was covered with aluminum foil to exclude outside light or UV radiation.

2.2.5 Setup UV experiments

UV lamps were placed above the quartz tube to expose leaf litter to radiation of different intensities and wavelengths. Four different lamps were used: Vitalux (Osram, 300W, emitting in both the UVA and UVB range with a UVA/UVB ratio of 7), TL01 (20W, Philips, The Netherlands, emitting in a narrow UVB range), TL09 (20W, Philips, The Netherlands, emitting mainly in the UVA range), and TL12 (20W, Philips, The Netherlands, emitting in a broad UVB range). In experiments with the TL lamps, 7 lamps (tubes) were placed next to each other to obtain homogeneous radiation intensity, while in experiments with the Vitalux lamp (point source) only one lamp was used. Relative emission spectra of the lamps are shown in Fig. 2.2. In one experi-

mental series, filters were placed between the UV lamp and the quartz tube to create additional variation in the wavelengths of the radiation received by the leaf litter. A cellulose diacetate filter and a glass filter (WG305, Schott, Germany) were used. The cellulose diacetate filter mainly removed wavelengths below 290 nm, whereas the glass removed 70% of the radiation at 300 nm, 35% at 310 nm, and 20% at 320 nm (Fig. 2.2). The intensity of the UV radiation was varied by placing the quartz tube including leaf litter at different distances from the UV lamp. The UVA and UVB intensity were measured with a Waldmann UV meter 585-100 (Waldmann, Schweningen, Germany). For each lamp type, calibration of the Waldmann UV meter was performed with a calibrated standard UV-visible spectroradiometer (model 752, Optronic Laboratories Inc, USA). In absence of reliable action spectra for C₂–C₅ hydrocarbon release from leaf litter upon UV irradiation, the UV strength is reported as the non-weighted integral over the UVA or UVB range. To avoid heating of the leaf litter because of heat from the lamps, a ventilator was placed next to the quartz tube. As a result, the leaf temperature stayed below 30°C. The leaf temperature was measured with a thermocouple on the surface of the whole and ground leaf litter.

When the Vitalux lamp was used to irradiate the leaf litter, heating of the plant material in the quartz tube was observed (generally up to 30 °C when the tube was close to the lamp), even though a ventilator was placed next to the tube for cooling. In experiments where the temperature dependence of hydrocarbon emissions from leaf litter was determined, activation energies were calculated (Sect. 2.3.1). These activation energies were used to correct for heat induced emissions. For plant species of which the activation energy was not determined, an activation energy of 100 kJ mol⁻¹ was assumed. The correction for heat induced emissions was generally less than 5% of the measured emission rate when leaf litter was irradiated with UV. Therefore, potential errors from temperature differences between thermocouple and the leaf surface are negligible for the present study.

Because the Vitalux lamp was a point source, a small UV gradient along the quartz tube was observed. Therefore, the average of six UVA and UVB measurements performed at six positions around the quartz tube was used.

A small fraction of the UV radiation was absorbed by the Suprasil tube. In the UVA range 9% of the radiation was absorbed, while in the UVB range the absorption was 11%. The absorbance was constant over the full range of UV intensities used in the experiments, and corrected UV intensities are reported.

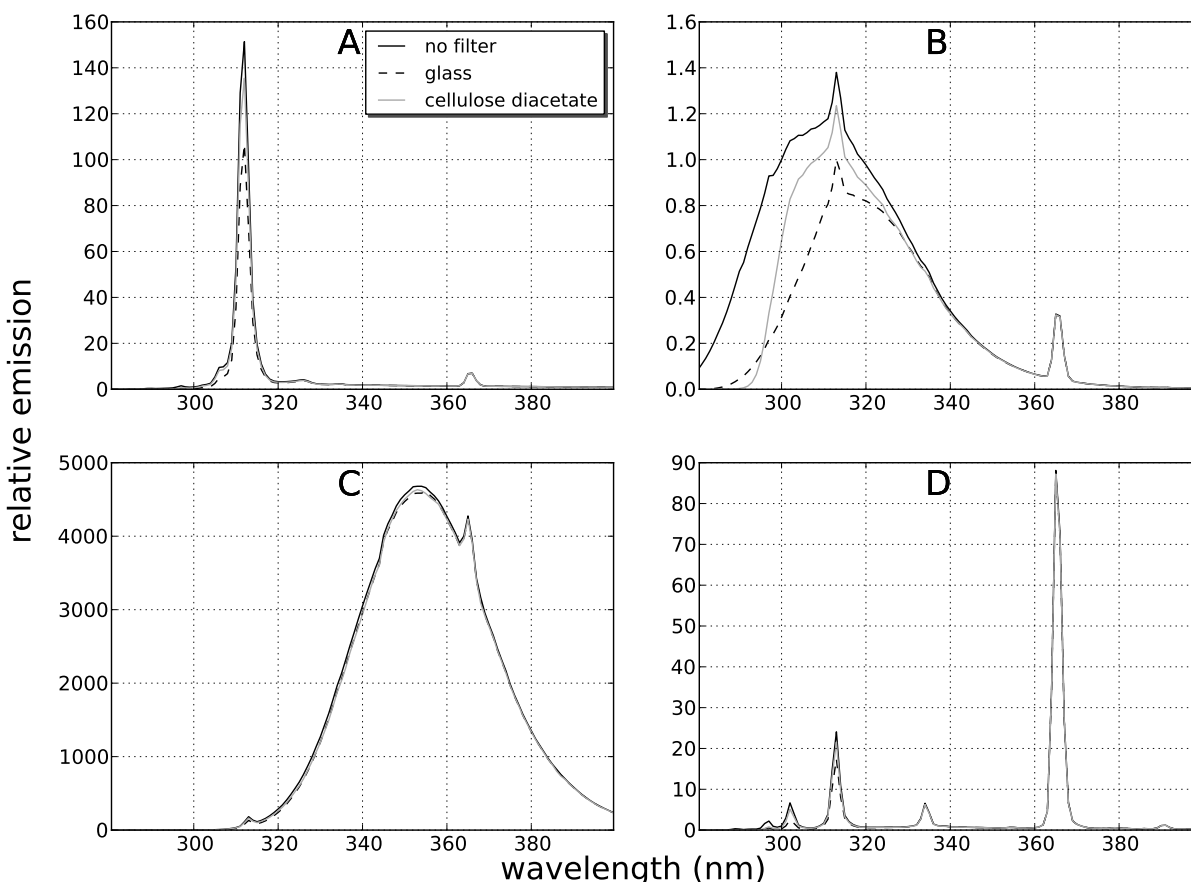


Figure 2.2: Emission spectra of the (A) TL01 lamp, (B) TL12 lamp, (C) TL09 lamp, and (D) Vitalux lamp between 280 and 400 nm (UVA and UVB) in combination with different filters. The emissions of the lamps without using filters are normalized to 1 at 300 nm.

2.2.6 Description of the experiments

2.2.6.1 Heating of leaf litter

Experiments were performed to determine the dependence of C_2 – C_5 hydrocarbon emissions from leaf litter on temperature. In addition, the temporal variation of the emissions was investigated. The plant species used for the different experiments were randomly chosen.

For sequoia, rice, maize, cherry prinsepia and beech, ground or whole leaf litter was placed in the quartz tube and heated from 20 to 70 °C in steps of 10 °C. During the experiment the tube was continuously flushed with synthetic air. At each temperature level the emission rates of the different hydrocarbons were measured three times in a

row. The average and standard deviation of the three measurements is reported. The standard deviation is used to indicate the spread in the emission rate measurements at a certain temperature. The measurements at each temperature level took ~ 4.5 hrs. In total, the measurements at all temperature levels of one experiment took ~ 27 hrs. The temperature was decreased to ambient level during the night, typically for 16 hrs. The same leaf litter sample was used during an experiment.

To quantify the overall temperature dependence of the emission rates, activation energies were calculated with the Arrhenius equation (Eq. 2.2)

$$k = A \exp \left(\frac{-E_a}{RT} \right) \quad (2.2)$$

where k is the reaction rate coefficient, A the pre-exponential factor, E_a the activation energy, R the gas constant, and T the temperature. In case of a pseudo-first order reaction, i.e., when the amount of precursor is very large compared to the fraction of this precursor that reacts to yield a hydrocarbon, k is proportional to the emission rate ER . The activation energy can then be determined directly from the slope (E_a/R) of the Arrhenius plot, a plot of $\ln(ER)$ as function of the inverse temperature (Atkins and de Paula, 2002). Linear regression analysis using weighted least squares was used to fit the data.

To follow the temporal evolution of the emission rates, long term heating experiments were carried out. Whole maize leaves were placed in the quartz tube and heated to 80 or 100 °C in an atmosphere of synthetic air. The emission rates of the different C₂–C₅ hydrocarbons were regularly measured over the course of several days.

To determine whether long term storage of the leaf litter has an effect on the emission rates, measurements of the emission rate at temperatures between 20 and 70 °C were performed on whole sequoia leaf litter after drying the litter. Ten months later, this experiment was repeated with whole sequoia litter of the same batch that was not used in other experiments.

2.2.6.2 Irradiation of leaf litter with UV

Four experiment series were performed to determine the dependence of C₂–C₅ hydrocarbon emissions from leaf litter on the wavelength and intensity of the UV radiation, on humidity, and to examine the temporal evolution of the emissions when continuously irradiated with UV. The plant species used in the different experiment series were randomly chosen. Measurements of the emission rate were generally performed in triplicate. The average of three measurements is reported, whereas the standard

deviation is used to indicate the spread in the individual emission rate measurements around its mean value.

To determine the wavelength dependence of C₂–C₅ hydrocarbon emissions from leaf litter, whole birch leaf litter was placed in the quartz tube that was continuously flushed with synthetic air. Emission rates were measured for leaf litter irradiated with UV from each combination of lamps (Vitalux, TL01, TL09 or TL12) and filters (no filter, cellulose diacetate, or glass). The tube was placed at a fixed distance from the lamp and filters were placed between the lamp and the quartz tube. The intensity of the UVA and UVB radiation was measured for each lamp-filter combination.

The emission rates of C₂–C₅ hydrocarbons were measured as a function of UV intensity for ground and whole leaves of maize, sequoia and rice. The leaves were placed in the quartz tube and synthetic air was used to flush the tube. The Vitalux lamp was used to irradiate the leaves. By placing the tube at distances between 50 and 20 cm from the lamp the UVB intensity was varied between 1 and 7 Wm⁻², whereas the UVA intensity varied between 8 and 45 Wm⁻². Measurements without UV radiation were also performed.

To determine the combined effect of humidity and UV radiation on the C₂–C₅ hydrocarbon emission rates, and the dependence of the emissions on oxygen, maize leaves were placed in the quartz tube and flushed with either nitrogen gas, dry synthetic air, or humid synthetic air. Saturated humid synthetic air was generated by bubbling synthetic air through a flask with demineralized water at a temperature of 22°C before entering the quartz tube. The emission rate as a function of UV intensity was determined for each carrier gas, according to the procedure outlined above.

The temporal evolution of hydrocarbon emissions from leaf litter when irradiated with UV was determined for leaf litter of sweetgum. Whole sweetgum leaves were placed in the quartz tube, which was flushed with synthetic air. The Vitalux lamp was used to irradiate the leaf litter continuously for 356 days. The quartz tube was placed at such a distance from the lamp that the UV intensities received by the leaf litter were initially 23 and 4.5 Wm⁻² for UVA and UVB, respectively. In the course of the experiment, the intensities decreased to 16 and 2.3 Wm⁻² UVA and UVB, respectively, because of degradation of the emission efficiency of the lamp. Measurements of the emission rates were generally performed at least once a week.

2.3 Results and discussion

2.3.1 Heat induced C₂–C₅ hydrocarbon emissions from leaf litter

The emission rates of several C₂–C₅ hydrocarbons were measured as function of temperature for rice, maize, beech, cherry prinsepia and sequoia leaves. As an example, chromatograms of the emissions from whole maize leaves at 30, 50 and 70 °C are shown in Fig. 2.1c. Emissions of ethane, ethene, propane, propene and *n*-pentane were clearly elevated compared to the blanks shown in Fig. 2.1b. The blank contribution of the different compounds was generally small at all temperatures, except in the case of *n*-butane. At the elution time of *n*-butane a large peak was observed in the blank. This peak was probably not *n*-butane, but a different, unidentified co-elutant. For some plant species the emissions of ethane and propane at low temperatures were too low to accurately calculate the emission rates. We did not see evidence for emission of *i*-butane, *n*-butane and *i*-pentane from dry leaves. These compounds were either not formed or their emission rates were below our detection limit. Ethyne emissions were only observed for a few plant species at high temperature (70 °C).

2.3.1.1 Temperature dependence of C₂–C₅ hydrocarbon emissions from leaf litter

Emission rate as a function of temperature

Figure 2.3 shows the emission rate (ng gdw⁻¹h⁻¹) as a function of temperature for ethane, ethene, propane, and propene for selected plant species. The other plant species showed similar results. The C₂–C₅ hydro-carbon emission rates increased continuously with temperature between 20 and 70 °C. This indicates that the release of C₂–C₅ hydro-carbons from dry leaf litter was not due to enzymatic activity. If the release was due to enzymatic activity, emission rates would be expected to increase with temperature until a maximum emission rate at 30–40 °C, followed by a decline at higher temperatures due to denaturation of enzymes (Atkins and de Paula, 2002; Campbell and Reece, 2002).

For each plant species, the emission rates of alkenes were larger than the emission rates of alkanes at all temperatures. At high temperatures the emission rates for whole leaves were generally higher than for ground leaves, whereas at low temperatures, similar emission rates were observed for both whole and ground leaves. This resulted in a weaker temperature dependence of the emission rates for ground leaves compared to whole leaves (see also the section on Arrhenius plots).

At the highest temperatures, a systematic decrease of the emission rates was observed

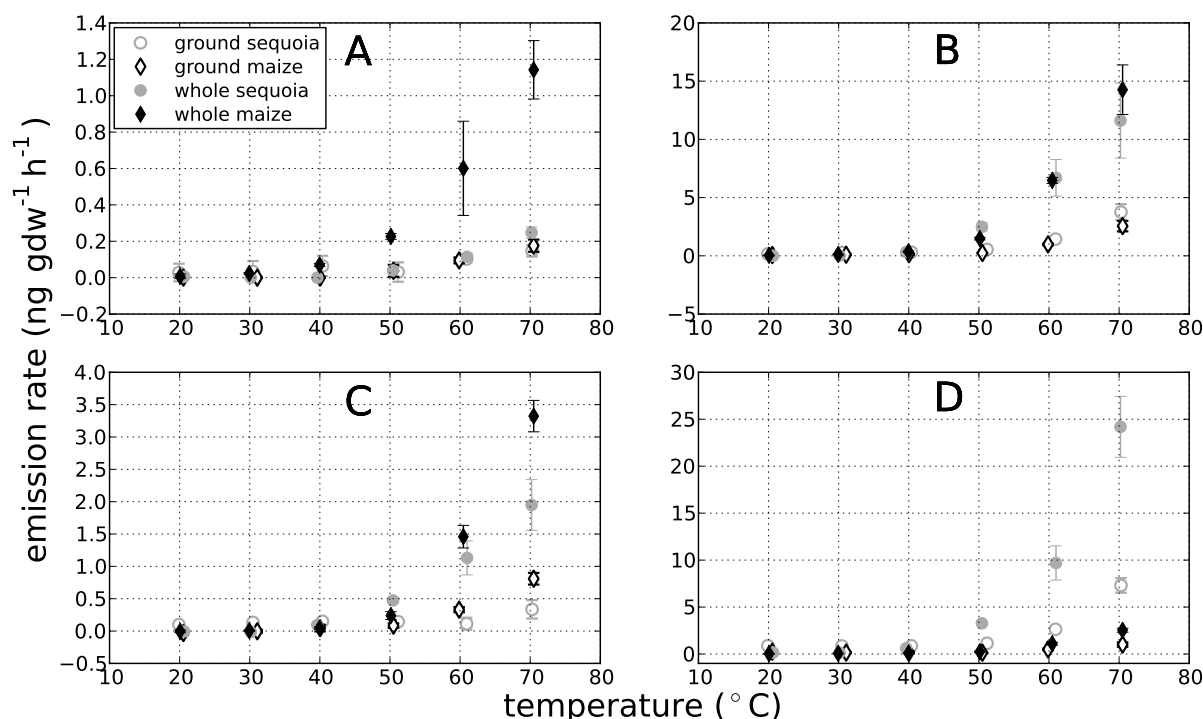


Figure 2.3: Emission rate as function of temperature for (A) ethane, (B) ethene, (C) propane and (D) propene from selected plant species. Emissions from the other plant species show similar temperature dependencies. Note the different scales of the emission rates for the different compounds.

during the 4.5 hours required to perform three measurements at the respective temperature. This resulted in relatively large standard deviations, and reflects the changing conditions for C_2 – C_5 hydrocarbon emissions at these temperatures and timescales.

An overview of the emission rates at 30 °C for all plant species used in the experiments is shown in Table 2.1. For all emitted C_2 – C_5 hydrocarbons, variations in the emission rates between different plant species were observed. At low temperature, the variations were relatively small. For example, ground sequoia emitted $0.86 \text{ ng gdw}^{-1}\text{h}^{-1}$ propene, whereas ground maize emitted $0.15 \text{ ng gdw}^{-1}\text{h}^{-1}$ at 30 °C. However, the variability increased at higher temperature. The highest hydrocarbon emission rate was measured for ethene. At 70 °C, whole rice emitted $653 \text{ ng gdw}^{-1}\text{h}^{-1}$ ethene, whereas the lowest ethene emission rate was $1 \text{ ng gdw}^{-1}\text{h}^{-1}$ for ground prinsepia (data at 70 °C not shown). Note that these differences should only tentatively be interpreted as indications for differences between plant species, since intra-species variation was not examined in this project.

CHAPTER 2. C₂–C₅ HYDROCARBONS FROM LEAF LITTER

Table 2.1: C₂–C₅ hydrocarbon emission rates ± 1 standard deviation (ng gdw⁻¹h⁻¹) at 30 °C for the examined plant species. For some plant species, the emissions of ethane and propane at 30 °C were too low to accurately determine the emission rates, and are indicated as not detected (n.d.).

plant species	ethane	ethene	propane	propene	<i>n</i> -pentane
ground sequoia	0.03±0.06	0.28±0.08	0.13±0.01	0.86±0.20	0.11±0.06
ground maize	n.d.	0.10±0.01	n.d.	0.15±0.04	0.07±0.03
ground rice	n.d.	0.13±0.06	0.04±0.02	0.13±0.08	0.04±0.01
ground cherry prinsepia	n.d.	0.07±0.02	0.08±0.03	0.18±0.03	0.25±0.17
ground beech	0.02±0.03	0.04±0.02	0.04±0.03	0.22±0.07	0.07±0.01
whole sequoia	n.d.	0.02±0.003	n.d.	0.15±0.02	0.15±0.06
whole maize	0.02±0.003	0.12±0.01	0.01±0.001	0.06±0.01	0.10±0.01
whole rice	n.d.	0.68±0.1	0.07±0.06	0.10±0.03	0.08±0.02

Arrhenius plots

Figure 2.4 shows Arrhenius plots for ethene emissions from ground and whole leaves of maize and sequoia. For the other hydrocarbon similar results were obtained. An overview of the activation energies for ethane, ethene, propane, propene and *n*-pentane emissions from whole leaves is shown in Table 2.2. The Arrhenius plots were made with the assumption that the pseudo-first order approximation can be applied. This seems a reasonable assumption, because the amount of precursor in a leaf (PUFA), is generally much larger than the trace amounts of hydrocarbons that were emitted (Hopkins, 1999; Hatanaka, 1993).

Table 2.2: Activation energies (kJ mol⁻¹) for emissions of C₂–C₅ hydrocarbons from different plant species (whole leaf measurements). The uncertainties are derived from the uncertainty in the slope of the Arrhenius plot, which was obtained by linear regression.

plant species	ethane	ethene	propane	propene	<i>n</i> -pentane
whole sequoia	85.5±8.5	151.6±5.0	100.1±4.8	113.3±2.8	30.1±3.2
whole maize	84.7±3.8	109.7±2.5	116.7±6.7	91.4±2.5	70.4±2.2
whole rice	78.0±12.6	191.6±8.6	102.8±7.6	120.4±8.4	83.8±5.8

Indeed, the Arrhenius plot for ethene emissions from whole maize leaves exhibits an approximately linear relationship. However, for whole rice leaves (data not shown) and whole sequoia leaves large deviations from the Arrhenius relation were observed.

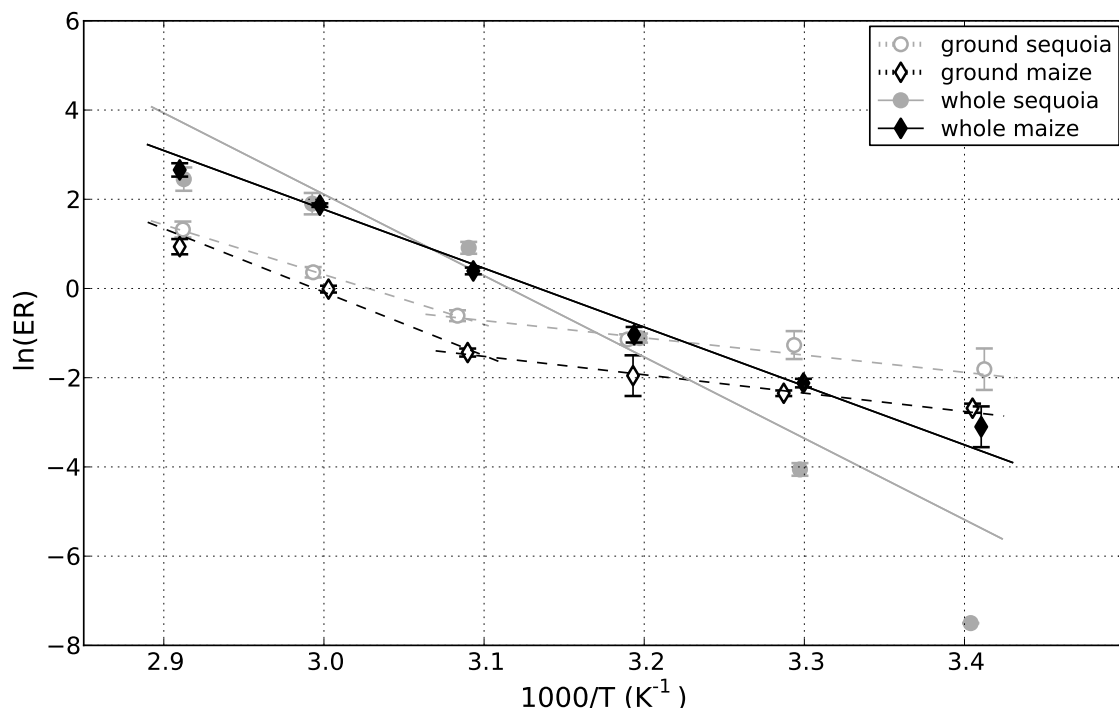


Figure 2.4: Arrhenius plot for ethene emissions from maize and sequoia leaf litter in the temperature range 20–70 °C.

$\ln(\text{ER})$ curves towards lower values at higher temperature compared to the expected linear relation between $\ln(\text{ER})$ and the inverse temperature, which shows that the pseudo first order assumption was probably not valid for these plant species. This is in agreement with the decrease in emission rate that occurred at high temperature during the 4.5 h period needed for the measurements at the respective temperature level. The decay of the hydrocarbon emission rates from whole leaf litter at high temperature is tentatively interpreted as depletion of a pool of precursors, either PUFAs or lipid hydroperoxides. As the amount of PUFAs in leaves is generally several orders of magnitude larger than the trace amounts of hydrocarbons that were released, we probably observed depletion of the pool of lipid hydroperoxides.

In contrast, for hydrocarbon emissions from ground leaf litter (Fig. 2.4, dashed lines), $\ln(\text{ER})$ curves towards higher values at higher temperatures compared to the expected linear relation between $\ln(\text{ER})$ and the inverse temperature. This cannot be explained by decreasing emission rates during the experiments. To illustrate this behaviour, two separate linear fits are made through the data at low (20–50 °C) and high (50–70 °C) temperatures. The different slopes of these fits suggest that different formation and re-

lease processes were important in the two temperature regions. Different mechanisms of lipid hydroperoxide decomposition might be important at different temperatures, since decomposition occurs either due to heating or due to reaction with transition metals. Grinding of the leaves makes the leaf material more porous and can effect the diffusion of formed hydrocarbons out of the leaf litter. Diffusion of oxygen, required for the lipid peroxidation, into the leaf can also be affected by the grinding process.

The activation energies (Table 2.2) were generally higher than 50 kJ mol⁻¹. This indicates, in addition to the continuous increase of the emission rate with temperature, that the emissions were caused by an abiotic process and were not due to enzymatic activity (Schönknecht et al., 2008).

2.3.1.2 The temporal evolution of the hydrocarbon emission rates from leaf litter

High temperature

Section 2.3.1.1 noted that a decrease in emission rate was observed during subsequent measurements at high temperatures. This was further examined in an experiment where the emission rates of the different C₂–C₅ hydrocarbons were followed over the course of several days for maize leaves at high temperature (80 and 100 °C). The results are shown in Fig. 2.5 for ethene as an example, but similar results were found for the other C₂–C₅ hydrocarbons.

The C₂–C₅ hydrocarbon emission rates show an initial peak, then a sharp decrease to lower values within several hours, followed by a much slower decay in the following hours. However, decline of the emission rates to levels below our detection limit was not observed within the 170 h duration of the experiment. As described in Sect. 2.3.1.1, the decline of the C₂–C₅ hydrocarbon emission rates was probably caused by depletion of the lipid hydroperoxide pool. Higher emission rates were observed at 100 than at 80 °C during the whole experiment, but the largest differences were observed in the initial stage of the experiment. After 100 hrs the emission rates decreased to low values at both temperatures.

Ambient temperature

The effect of long term storage of the leaf litter on the emissions was assessed by performing measurements of the emission rate as a function of temperature for whole leaf litter of sequoia directly after drying of the batch, and ten months later. The leaf litter was stored at ambient temperature. Both measurement series are compared in Fig. 2.6. After ten months, the emission rates still increased exponentially with temperature, but the values were lower than directly after drying. In the low temperature regions,

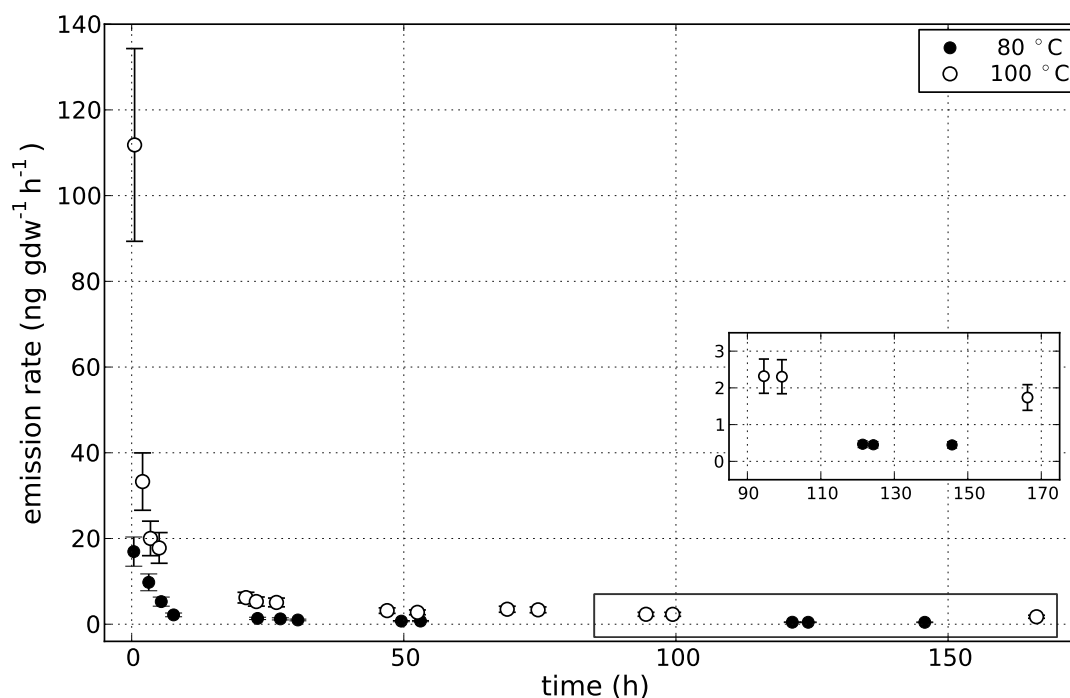


Figure 2.5: Emission rate of ethene as a function of heating time for whole maize leaves at 80 and 100 °C. The inset illustrates the low emission rates between 85 and 170 h.

the emission rates were still of comparable magnitude, but at higher temperatures the emission rates were approximately 60–90% lower than directly after drying of the leaf batch.

This comparison shows that the decline of the emission rates that was observed at high temperature also occurs at ambient temperature, but on a much longer time scale. Whereas at 80 or 100 °C the decline of the emission rate was visible within several hours, at ambient temperature the decline in emission rate was only visible on a timescale of months or years.

2.3.2 UV induced C₂–C₅ hydrocarbon emissions from leaf litter

2.3.2.1 Hydrocarbon emissions induced by UV radiation

For the hydrocarbons that could be detected with our experimental setup, Table 2.3 gives an overview of the typical range of emission rates that was observed when leaf litter was irradiated with UV. In addition, this table shows the emission rates that were

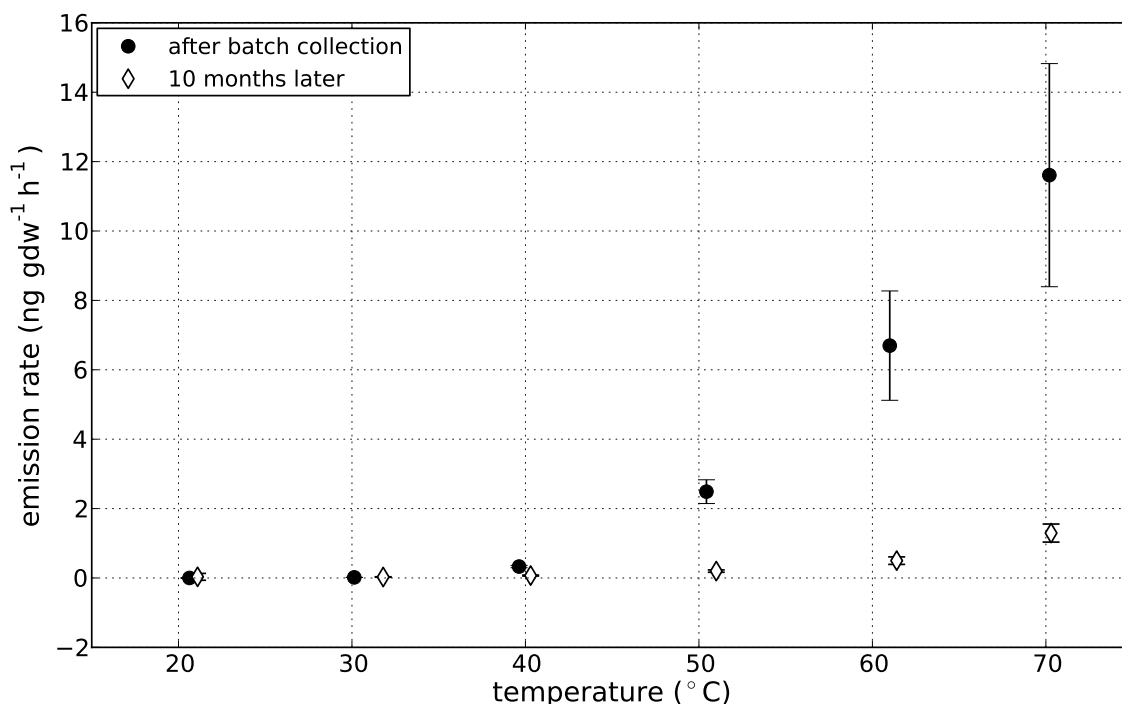


Figure 2.6: Emission rate of ethene as a function of temperature for whole sequoia leaves directly after drying of the leaf batch and ten months later.

measured when leaf litter was irradiated with UVA only and UVB only, after filtering the wavelengths smaller than 290 nm with a cellulose diacetate filter (see also Sect. 2.3.2.2). The latter is environmentally most important, because at the Earth's surface wavelengths below 290 nm are absent.

Emissions of all C₂–C₅ hydrocarbons were observed, except of *i*-butane and *i*-pentane. Emissions of ethyne were generally low, but observed for most of the investigated plant species. This is in contrast to heat induced hydrocarbon emissions, where ethyne emissions were only observed for a few plant species at high temperature (80 °C)(Sect. 2.3.1.1). The highest emission rates were observed for ethene and propene. For both compounds, emission rates up to 4000 $\mu\text{g m}^{-2}\text{h}^{-1}$ were observed. The emission rates of the alkanes were lower and for e.g. ethane the emission rate varied only between 5 and 100 $\mu\text{g m}^{-2}\text{h}^{-1}$. Lower emission rates for alkanes compared to alkenes were also observed for heat induced emissions. For each compound, the emissions induced by UVB radiation were higher than the UVA induced emissions. For propane the UVB induced emission rate was only 4 time larger, whereas for propene the emission rate was even 14 times larger than the emission rate induced by UVA radiation.

Table 2.3: Typical emission rates of the measured C₂–C₅ hydrocarbons from leaf litter irradiated with UV.

compound	emission rate range ^a ($\mu\text{g m}^{-2}\text{h}^{-1}$)	emission rate due to UVA ^b ($\text{ng W}^{-1}\text{h}^{-1}$)	emission rate due to UVB ($\text{ng W}^{-1}\text{h}^{-1}$)
ethane	5 – 100	0.2	1.3
ethene	1000 – 4000	45.5	455
ethyne	0 – 30	0.2	3.2
propane	100 – 1000	4.5	19.5
propene	400 – 4000	18.2	260
<i>i</i> -butane	0	0	0
<i>n</i> -butane	100 – 1000	4.5	32.5
<i>i</i> -pentane	0	0	0
<i>n</i> -pentane	50 – 800	9.1	45.5

^a Typical range of emission rates observed in experiments where leaf litter was irradiated with the Vitalux lamp (UVA: 8–45 Wm⁻², UVB: 1–7 Wm⁻²).

^b Emission rates when leaf litter was irradiated with UVA from the TL09 lamp in combination with a cellulose diacetate filter (mainly UVA, intensity = 22 Wm⁻²). The emission rate is normalized with the UVA intensity.

^c Emission rates when leaf litter was irradiated with UVB radiation. The average emission rate of measurements with the TL01 and TL12 lamps in combination with a cellulose diacetate filter is shown (average UVB intensity = 7.7 Wm⁻²). The emission rate is normalized with the UVB intensity.

Comparison of our measured emission rates with literature values is difficult, since emission rates are often scaled to the dry weight of the leaves instead of the leaf area that was exposed to the UV radiation. For example, emissions of ethane and ethene for detached tobacco leaves up to approximately 450 and 700 ng gdw⁻¹ have been observed, respectively, after irradiating the leaves with UV for 45 hours at 3.14 Wm⁻² (McLeod et al., 2008). Ethane and ethene are also emitted from stressed, but living plants, and the emission rates vary largely between plant species (Kimmerer and Kozlowski, 1982). After freezing 30% of the leaf area, ethene emissions ranged from less than 1 nmol cm⁻² for *Zea mays* leaves up to 143 nmol cm⁻² leaf area for leaves of *Haemanthus katherinae* after 8 hrs incubation (1 nmol ethene cm⁻² during 8 hrs of incubation corresponds to $\sim 35 \mu\text{g m}^{-2}\text{h}^{-1}$). For ethane a maximum emission of 19.3 nmol cm⁻² was observed for *Tagetes erecta* (Kimmerer and Kozlowski, 1982). These emission rates for ethane and ethene for living, but stressed plants are much higher than the emission rates observed in our experiments for leaf litter. However, the large

variation between plant species is also observed in this study.

2.3.2.2 The wavelength dependence of C₂–C₅ hydrocarbon emissions from leaf litter

The emission of ethene from whole birch leaves induced by UV radiation of varying spectral composition is shown in the bottom panel of Fig. 2.7. Similar results were observed for the other C₂–C₅ hydrocarbons that were emitted by the leaf litter. Leaf litter was irradiated with UV of four different lamps, in combination with different filters. The unweighted UVA and UVB intensities received by the leaf litter for all lamp-filter combinations are shown in the top panel of Fig. 2.7. For the TL lamps, UV intensities decreased when a cellulose diacetate or glass filter was placed between the lamp and the quartz tube, mainly cutting wavelengths below 290 and 305 nm, respectively, but also a fraction of the longer wavelengths (Fig 2.2). However, for the Vitalux lamp the UV intensity increased when filters were placed between the tube and the lamp. This was likely caused by variation of the horizontal position of the tube with respect to the lamp. Because the Vitalux lamp is a point source, a small UV intensity gradient was observed below the lamp and changes in the horizontal position of the tube lead to changes in UV intensity. For the TL lamps (seven tubes in a row, homogeneous UV intensity) changes in the horizontal position of the tube with respect to the lamps did not lead to changes in the UV intensity, and changes were only caused by introduction of the filter.

Comparison of the hydrocarbon emission rate with the intensity of UVA and UVB radiation received by the leaves showed that the emission rate mainly followed the UVB intensity. A high UVB intensity generally resulted in a high emission rate, whereas a high UVA intensity induced relatively small emissions. For example, much higher emission rates were observed when the TL01 (UVB narrowband) lamp was used compared to hydrocarbon emissions induced by the TL09 (UVA) lamp. This was caused by the high intensity of the UVB radiation emitted by the TL01 lamp. The TL09 lamp emitted radiation with relatively high intensity in the UVA range, but that did not have a large effect on the emissions. The UVB intensity of the TL09 lamp was low, which resulted in relatively low emission rates.

However, the total average UVB intensity alone does not explain all variations observed in the emission rates. For example, when the UVB broadband lamp TL12 without filter was used to irradiate the leaf litter, a much higher emission rate was observed as compared to the hydrocarbon emissions that were induced by the narrow band TL01 lamp for a higher UVB intensity. Comparison of the relative emission spectra of the different lamps (Fig. 2.2) shows that TL12 is the only lamp that emits a large fraction

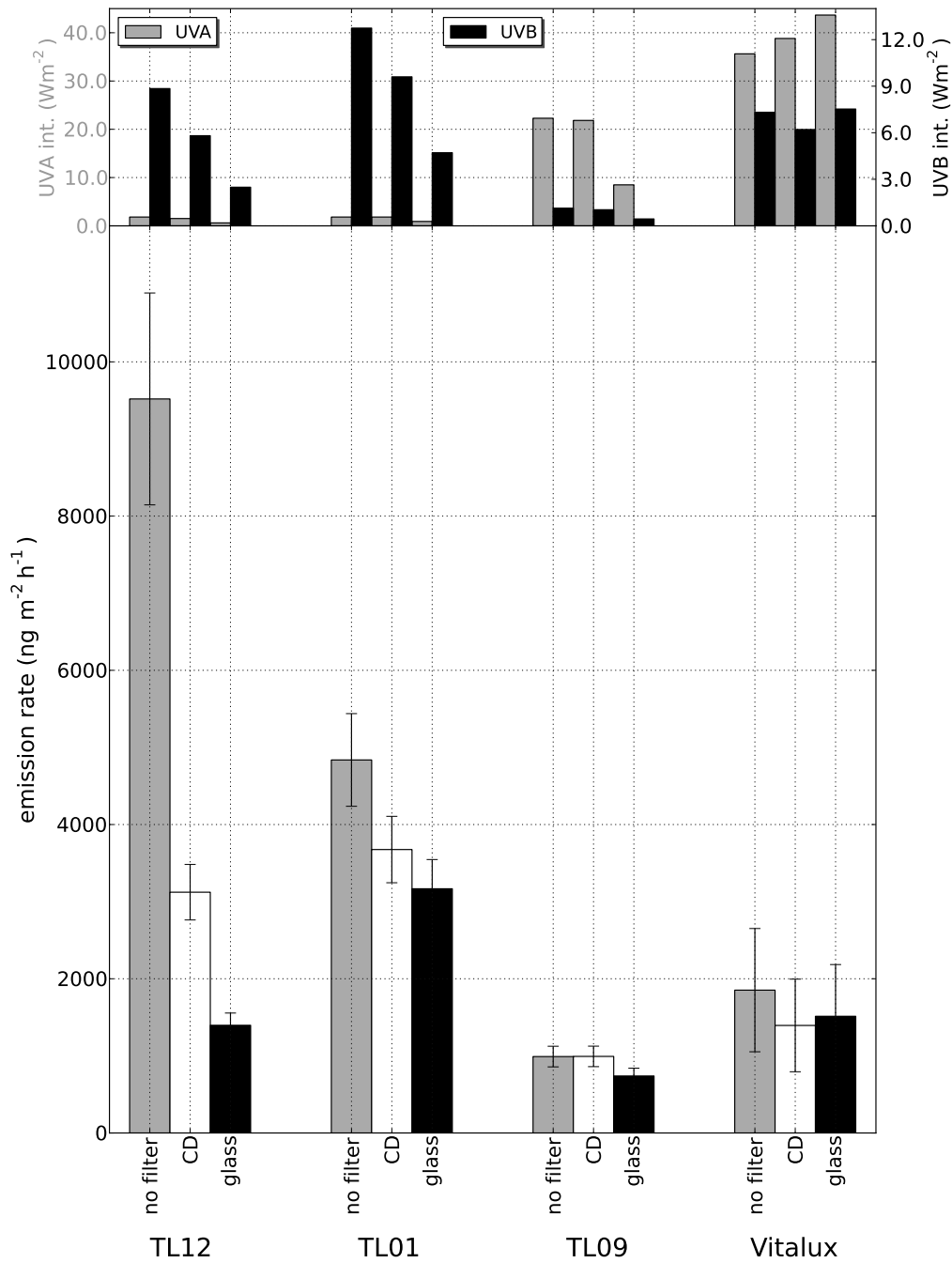


Figure 2.7: Top: intensity of the unweighted UVA (grey) and UVB (black) radiation received by the leaf litter for each lamp-filter combination. Bottom: ethene emission rates for birch leaf litter when irradiated with UV from each combination of lamp (TL12, TL01, TL09 and Vitalux) and filter (no filter, cellulose diacetate (CD) and glass).

its radiation between 280 and 300 nm. This suggests that especially these wavelengths are effective in producing hydrocarbon emissions. Placing a cellulose diacetate or glass filter between the lamp and the leaf litter strongly reduced the amount of radiation with wavelengths below 290 and 305 nm, respectively. Therefore, when leaf litter was irradiated with TL12 in combination with one of these filters, a much stronger reduction in emission rate was observed as compared to the other lamps. This confirms that short wavelengths are most efficient in generating hydrocarbon emissions from leaf litter.

2.3.2.3 Emission rate as a function of UV intensity: comparison between whole and ground leaf litter

Different UV intensities are received by different locations on Earth. Generally, the highest UV intensities are found in the Tropics. Typical tropical UVB levels at noon are 4 Wm⁻², whereas in the midlatitudes noon UVB levels are typically 2 Wm⁻² (Bernhard et al., 1997). The influence of the UV intensity on the emission rate of C₂–C₅ hydrocarbons was investigated for both whole and ground leaf litter of three plant species irradiated with the Vitalux lamp. Whole leaf litter better represents natural conditions, but there can be significant inhomogeneity within a batch of leaves. Grinding of the leaves improves the homogeneity of the sample, but also changes the structure of the leaf litter.

The emissions of selected hydrocarbons are shown in Fig. 2.8 for whole and ground leaf litter of rice, sequoia and maize. The emission rates are reported as a function of the total unweighted UVB intensity, because the results in Sect. 2.3.2.2 showed that the UVB intensity has a stronger influence on the emission rates than the UVA intensity.

For all C₂–C₅ hydrocarbons and plant species that were investigated the emission rates increased linearly with the UVB intensity between 0 and 7 Wm⁻². The emission rates from ground leaves were generally higher than from whole leaves, likely due to the increased roughness of the ground samples, which increased the effective surface area of the leaf litter at which the hydrocarbons could be formed. However, the difference between ground and whole leaves varied between plant species and individual compounds emitted from a certain plant sample. For example, there was only a small difference between *n*-pentane emissions from ground and whole sequoia, but a relatively large difference in propane emissions from whole and ground rice leaves. Also the variations between plant species were larger for ground compared to whole leaves. For example, ethene emission rates from ground litter at 5 Wm⁻² ranged from ~ 1000 to 3000 ng m⁻²h⁻¹ between the different plant species, whereas the ethene emission rates from whole litter only varied between 600 and 900 ng m⁻²h⁻¹ for these species

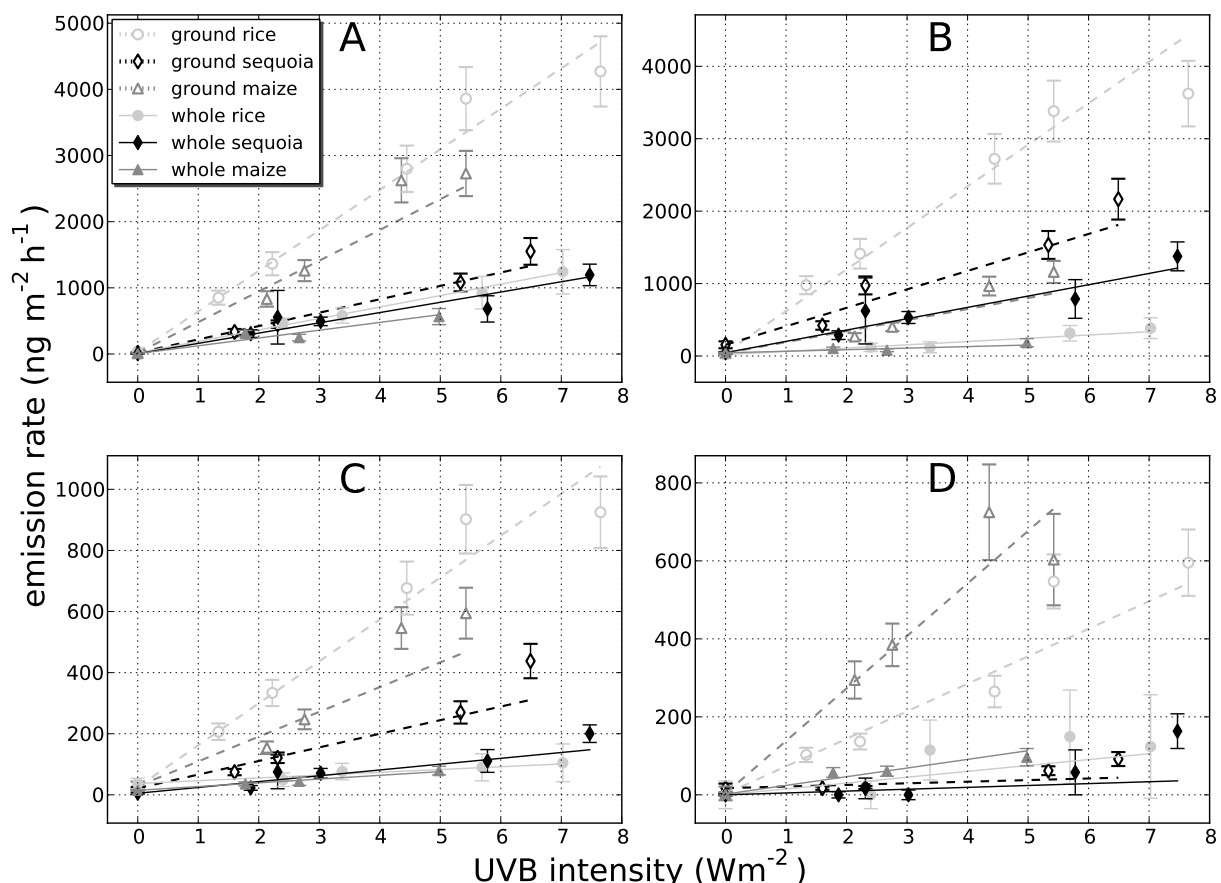


Figure 2.8: Emission rate as a function of UVB intensity for (A) ethene, (B) propene, (C) propane and (D) n-pentane emissions from whole and ground leaves of rice, sequoia and maize.

at the same UVB intensity. Although differences in the emission rates between plant species were expected, these differences should be interpreted with caution since only one plant per species was examined. Higher emissions from ground compared to whole leaves are in contrast to heat induced C₂–C₅ hydrocarbon emissions from leaf litter, where lower emissions were observed from ground leaves (Sect. 2.3.1.1). Apparently, heat and UV radiation induced C₂–C₅ hydrocarbon emissions via different mechanisms. Grinding improved the homogeneity of the leaf litter sample, but also altered the structure of the leaves. This strongly influenced the emission rates and measurements on ground leaves will not be representative for leaf litter emissions in real ecosystems.

2.3.2.4 The effect of humidity and oxygen on the emission rates

The experiments in sections 2.3.2.2 and 2.3.2.3 were carried out in dry synthetic air, whereas in nature the air is humid. Therefore, the combined effect of humidity and UV radiation on the hydrocarbon emission rates was examined. We also tested the dependence of the emissions on oxygen, since hydrocarbons are thought to be formed in leaf litter through the oxygen requiring lipid peroxidation process (Halliwell and Gutteridge, 2008; John and Curtis, 1977; Dumelin and Tappel, 1977; Konze and Elstner, 1978). The hydrocarbon emission rates as a function of UVB intensity were determined for whole maize leaves in nitrogen gas, dry synthetic air and humid synthetic air while being irradiated with the Vitalux lamp. As an example the results for ethene are shown in Fig. 2.9. Similar results were obtained for the other C₂–C₅ hydrocarbons emitted by the leaf litter.

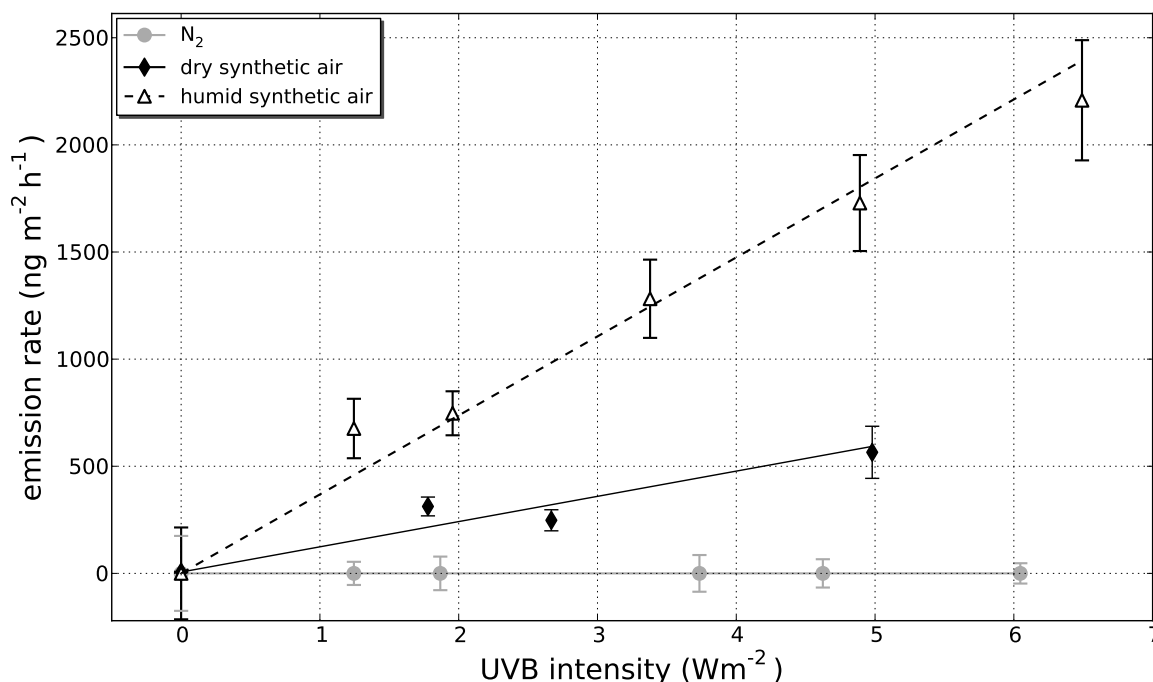


Figure 2.9: Ethene emission rate as a function of UVB intensity for whole maize leaves in nitrogen, dry- and humid synthetic air. The Vitalux lamp was used for irradiation of the leaf litter.

In absence of oxygen, no C₂–C₅ hydrocarbon emissions were observed. This is in agreement with the hypothesis that hydrocarbons are formed through the oxygen requiring lipid peroxidation process. Apparently, there are no significant formation pathways for hydrocarbons that operate in the absence of oxygen.

For both maize leaves in humid or in dry synthetic air, a linear increase of the emission rate with UVB intensity was observed. However, the emission rates were approximately three times higher in humid air than in dry air over the full UV range. For example, at a UVB intensity of 4 Wm^{-2} (typical for the Tropics at noon), an ethene emission rate of $500 \text{ ng m}^{-2}\text{h}^{-1}$ was observed for maize leaves in dry synthetic air, whereas in humid synthetic air an emission rate of $1500 \text{ ng m}^{-2}\text{h}^{-1}$ was observed. A possible explanation is that the combination of UV radiation and moisture in the air caused an increased formation of reactive oxygen species, which reacted on the surface of the leaves leading to the increased formation of $\text{C}_2\text{--C}_5$ hydrocarbons. When assessing the environmental importance of UV induced hydrocarbon emissions, humidity should be taken into account, as it has a large effect on the emissions.

2.3.2.5 The temporal evolution of $\text{C}_2\text{--C}_5$ hydrocarbon emissions from leaf litter

In experiments where the $\text{C}_2\text{--C}_5$ hydrocarbon emissions as a function of temperature were measured (Sect. 2.3.1), it was observed that the emission rates decline within several hours when the leaves were heated to high temperature ($80 - 100^\circ\text{C}$). In contrast, UV induced $\text{C}_2\text{--C}_5$ hydrocarbon emissions did not decline rapidly. Whole sweetgum leaves were continuously irradiated with the Vitalux lamp for 356 days. The UV intensities were initially 23 and 4.5 Wm^{-2} for UVA and UVB, respectively, but decreased throughout the experiment to 16 and 2.3 Wm^{-2} , respectively, because of aging of the lamp. The initial UVB intensity is a typical level for the Tropics at noon (Bernhard et al., 1997; Vigano et al., 2008). In Sect. 2.3.2.3 it was observed that the hydrocarbon emission rates depend linearly on UVB intensity. Therefore, to correct for the decreasing UV intensity during the experiment, the emission rates ($\text{ng m}^{-2}\text{h}^{-1}$) are normalized with the intensity of the UVB radiation (Wm^{-2}), resulting in emission rates in units of $\text{ng W(UVB)}^{-1}\text{h}^{-1}$. The results are shown in Fig. 2.10 for ethene, propane and *n*-pentane.

For most $\text{C}_2\text{--C}_5$ hydrocarbons, an increase of the emission rate was observed in the first weeks, followed by a slow decline in the following weeks. For ethene, a maximum emission rate was observed after ~ 20 days, whereas for propane the maximum emission rate was already observed after ~ 10 days. In contrast, for ethane (not shown) and *n*-pentane the decline of the emission rate started directly at the beginning of the experiment, and no initial emission rate increase was observed. At the end of the experiment, the emissions of all measured $\text{C}_2\text{--C}_5$ hydrocarbon were still substantial. For example, after 356 days the *n*-pentane emission rates was $\sim 10 \text{ ng W(UVB)}^{-1}\text{h}^{-1}$, corresponding to $\sim 23 \text{ ng m}^{-2}\text{h}^{-1}$. This is much higher than our detection limit of $1 \text{ ng m}^{-2}\text{h}^{-1}$.

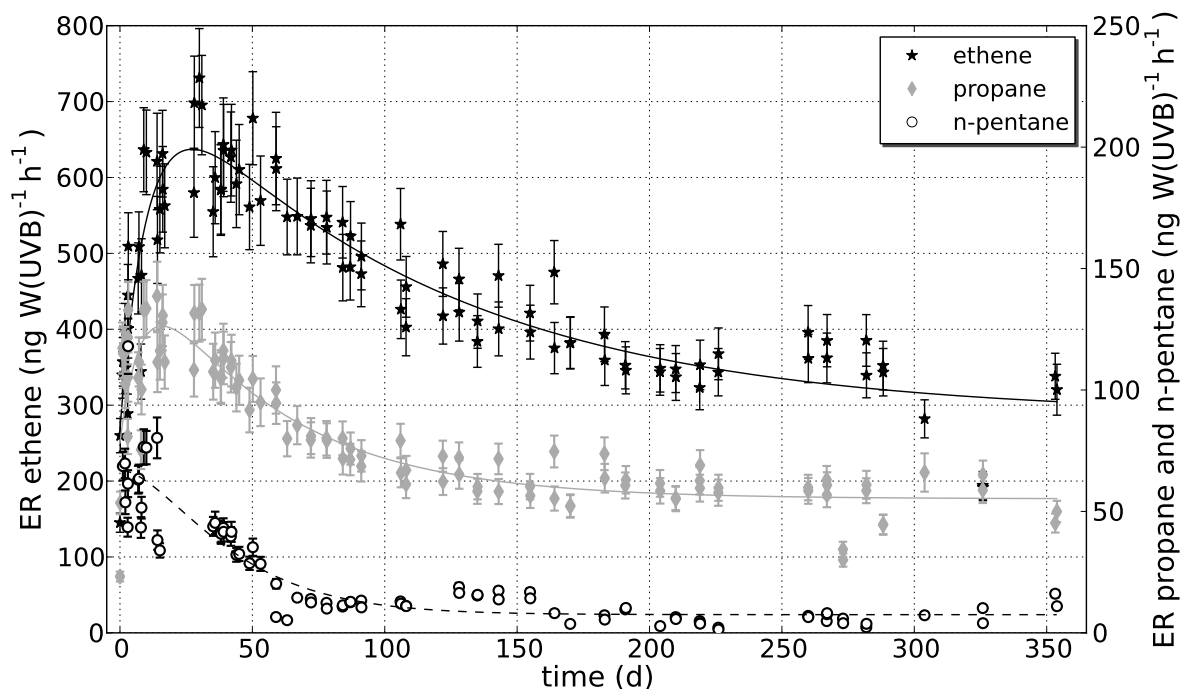


Figure 2.10: Temporal evolution of the emission rates (ER) of ethene, propane and *n*-pentane for sweetgum leaves when continuously irradiating the leaf litter with the Vitalux lamp (UVA intensity: 23 - 16 Wm^{-2} , UVB intensity: 4.5 - 2.3 Wm^{-2}). Note that the emission rates of propane and *n*-pentane are shown on the secondary y-axis.

The increase of the emission rate in the first days could be caused by additional drying of the plant material during the experiment. Before the experiment, the leaf litter was already dried at 25 °C for two months in ambient air. During the experiment, the leaf litter temperature was $\sim 28^\circ\text{C}$ due to the heat of the Vitalux lamp and the leaf litter sample lost another 13% of mass. Possibly a large fraction of this mass loss was due to the additional loss of moisture. The increase of the emission rates due to drying of the leaf litter is in agreement with observations by Brandt et al. (2007) where they observed that UV had a stronger effect on litter decomposition in dryer ecosystems. After some days of irradiation the material is then completely dry, and the hydrocarbon emission rates decline because of degradation of the leaf litter. It is not clear why for ethane and *n*-pentane no initial increase of the emission rate was observed. Possibly ethane and *n*-pentane are formed via a different mechanism than the other C₂–C₅ hydrocarbons.

At the end of the experiment, leaf parts that were directly exposed to UV radiation (unshaded leaves) were clearly bleached compared to the shaded leaf parts. This confirmed the influence of UV radiation on the degradation of leaf litter. When leaf litter

is irradiated with UV, the radiation will be absorbed by chromophores in the leaf litter. This likely results in the formation of reactive oxygen species, which degrade the leaf litter, for example via the lipid peroxidation process as hypothesized in Sect. 2.3.2.4 (Halliwell and Gutteridge, 2008). Also the chromophore itself can be attacked by reactive oxygen species, resulting in bleaching of the chromophores. As a consequence, less radiation is absorbed, which leads to a decreased formation of reactive oxygen species and a decreased formation of C₂–C₅ hydrocarbons, and could explain the decreasing emission rates that were observed after 20 days.

2.4 Environmental importance of hydrocarbon emissions from leaf litter

2.4.1 Global budgets

Since leaf litter is available at many locations at the Earth's surface, a simple upscaling was applied to assess the significance of C₂–C₅ hydrocarbon emissions from leaf litter for the global budgets of these compounds. Global annual emissions of C₂–C₅ hydrocarbons induced by heating or UV radiation are calculated separately. The goal of this upscaling is to estimate an upper limit for hydrocarbon emissions from leaf litter.

For heat induced emissions, the emissions measured at 30 °C were assumed to continue for one year at a constant rate. The annual global source of heat induced C₂–C₅ hydrocarbons from leaf litter was calculated according to

$$\text{total source} = \text{emission rate}(30\text{ }^{\circ}\text{C}) \cdot \text{yearly decaying biomass} \quad (2.3)$$

where 7.0×10^{16} g was used as the amount of biomass decaying each year (Warneke et al., 1999).

This estimate should be seen as the upper limit for the source of C₂–C₅ hydrocarbons from leaf litter, because a) 30 °C is much higher than the annual global mean temperature, b) the timing of litter fall and the availability of leaf litter throughout the year was not taken into account, c) performing the experiments in synthetic air possibly optimized the emission rates by maximizing the air-to-leaf gradient of hydrocarbons, and d) the emission rates at 30 °C were assumed to be constant, whereas the results in Sect. 2.3.2.5 showed that the emission rates decreased throughout the year.

The emission rates reported in Table 2.1 were used for the calculation after conversion

to units of ng gdw⁻¹yr⁻¹. The total source was calculated for all plant species in Table 2.1 and for each hydrocarbon, the observed range for ground and whole leaf litter is reported in Table 2.4. In these computations, the uncertainties of the emission rates shown in Table 2.1 have been taken into account by error propagation. The estimated ranges are relatively large, because of the large variations of the emission rates between the different plant species and the substantial uncertainties in the individual emission rate measurements. For each hydrocarbon, the estimate of the total global annual source is included in the bottom part of Table 2.4.

Table 2.4: Estimates of the upper limit of the annual global source strength (Tg yr⁻¹) of C₂–C₅ hydrocarbon emissions from dry leaf litter due to heating or UV radiation. For heat induced emissions, the estimates are based on measurements on both whole and ground leaf litter. For the UV induced emissions, the upscaling was performed using both weighted and unweighted UV intensities. Estimates of the total global annual source of each hydrocarbon are included in the bottom part of the table.

		ethane	ethene	propane	propene	<i>n</i> -pentane
temperature	ground leaves	0–0.06	0.01–0.22	0–0.09	0.03–0.65	0.02–0.26
	whole leaves	0–0.01	0.01–0.48	0–0.08	0.03–0.10	0.04–0.13
UV radiation	unweighted UV	0.006	1.4	0.12	0.63	0.25
	weighted UV	0.003	0.65	0.06	0.29	0.11
total global source		8.2 ^a ; 9.6 ^a ; 12.4 ^b	40.3 ^b	10.7 ^b	23.0 ^b	4.4 ^c

^a Stein and Rudolph (2007)

^b Poisson et al. (2000)

^c Pozzer et al. (2010)

A similar estimate of the upper limit of C₂–C₅ hydrocarbon emissions from leaf litter was made for UV induced emissions. Although unweighted UV intensities are reported throughout the manuscript, the upscaling was done using the unweighted UVA and UVB intensities as well as the UV intensity weighted with the erythral action spectrum (UVE)(McKinlay and Diffey, 1987) to examine the sensitivity of the estimate for the weighting of the UV radiation. The UVE action spectrum assumes that shorter UV wavelengths cause more damage than longer wavelengths. For the upscaling with the unweighted UVA and UVB intensities, the measurements presented in Table 2.3 (3rd and 4th column) were used. It was assumed that leaf litter is irradiated with UV for 12 hrs per day for 365 days per year and that typical UVA and UVB intensities are 45 and 1.6 Wm⁻², respectively (<http://rredc.nrel.gov/solar/spectra/am1.5/>, Bruhn et al. (2009)). The total vegetated area of the Earth (116×10¹² m², Matthews (1997)) was used for the extrapolation to the global scale. When applying this upscal-

ing to calculate the upper limit for UV induced hydrocarbon emissions from leaf litter, the largest emission was found for ethene (1.41 Tg yr^{-1}), whereas the annual emission of ethane from leaf litter was only 0.01 Tg yr^{-1} . When using the erythemally weighted UV intensity for the extrapolation, a global annual emission of 0.64 Tg yr^{-1} was estimated for ethene, whereas the emission of ethane was only 0.003 Tg yr^{-1} . The results for the other hydrocarbons are shown in Table 2.4. All estimates should be considered as upper limits, because upper limits for vegetated area, UV intensity and UV duration have been used. In addition, variation in UV intensity due to clouds, and a decrease of the UV intensity at higher latitudes and solar zenith angles was not taken into account.

This method only gives an estimate for upper limit of actual global emissions. However, the results presented in Table 2.4 do show that for most of the $\text{C}_2\text{--C}_5$ hydrocarbons leaf litter is an insignificant source on the global scale. For example, for ethene leaf litter contributes at most for 3.5% of the total emissions, whereas for ethane the maximum contribution is only 1%. The largest contribution was estimated for *n*-pentane, where highest estimate leads to a contribution of 6% of the global estimated source.

2.4.2 Local atmospheric chemistry

Although the emissions of $\text{C}_2\text{--C}_5$ hydrocarbons from leaf litter are not significant for the global hydrocarbon budgets, the emission may be important for the atmosphere's oxidation capacity on local scales. The largest emissions were found for ethene and propene when leaf litter was irradiated with UV or heated. Ethene and propene have a relatively short lifetime and are locally oxidized by the OH radical. The significance of $\text{C}_2\text{--C}_5$ hydrocarbon emissions from leaf litter on a local scale is estimated by comparing the number of reactions between OH and $\text{C}_2\text{--C}_5$ hydrocarbons emitted by leaf litter with the number of reactions between OH and background levels of carbon monoxide. Similar assumptions as for the global estimate were used.

Summed over all $\text{C}_2\text{--C}_5$ hydrocarbons, unweighted UVA and UVB induced an emission of 2.4 and $24 \text{ nmol W}^{-1}\text{h}^{-1}$, respectively, which corresponds to a total emission of $144 \text{ nmol m}^{-2}\text{h}^{-1}$ for typical UVA and UVB intensities (number are derived from Table 2.3 after conversion to units of $\text{nmol W}^{-1}\text{h}^{-1}$). Assuming that $\text{C}_2\text{--C}_5$ hydrocarbons emitted by leaf litter are directly oxidized by OH, and assuming a boundary layer height of 1500 m, an emission rate of $144 \text{ nmol m}^{-2}\text{h}^{-1}$ corresponds to a reactivity with OH of $\sim 16000 \text{ reactions cm}^{-3}\text{s}^{-1}$. The contribution of the heat induced $\text{C}_2\text{--C}_5$ hydrocarbon emissions to this reactivity is negligible (not shown). For comparison, the reactivity due to background levels of carbon monoxide (100 ppb, $[\text{OH}] = 1 \times 10^6 \text{ molec. cm}^{-3}$) is $370000 \text{ reactions cm}^{-3}\text{s}^{-1}$. So $\text{C}_2\text{--C}_5$ hydrocarbon emissions from leaf litter may have a small ($\sim 4\%$) effect on local atmospheric chemistry in re-

gions of strong sources.

2.5 Conclusions

Ethane, ethene, propane, propene and *n*-pentane were emitted from dry leaf litter at ambient temperatures, and the emission rates increased with temperature between 20 and 70 °C. Increased emissions were also observed when leaf litter was irradiated with UV. No emissions of *i*-butane, *n*-butane and *i*-pentane were detected, whereas ethyne emissions were only detected when litter was irradiated with UV. The emission rates varied largely between leaf litter of different plant species. In addition, differences were observed between whole and ground leaf litter. When leaf litter was heated to high temperature, higher emissions were observed for whole leaves, whereas UV radiation induced higher hydrocarbon emissions from ground leaf litter.

The temperature dependence of the hydrocarbon emission rates can be described by the Arrhenius equation, although deviations were observed at higher temperature. The emission of hydrocarbons from leaf litter was not due enzymatic activity, which was indicated by the continuous increase of the emission rates with increasing temperature, and activation energies that were higher than 50 kJ mol⁻¹. Emissions induced by heating to higher temperatures (80 or 100°C) did not persist for long times, but decreased already within hours. At ambient temperature the hydrocarbon emission rates also decreased in time, but the decline of the emission rate was only visible on a timescale of months to years.

When leaf litter was irradiated with UV, the emission rates increased linearly with the UV intensity within the ambient range of UV intensities. Especially UVB radiation with short wavelengths was very efficient in generating C₂–C₅ hydrocarbon emissions. When leaf litter in humid air was exposed to UV radiation, the emission rates approximately tripled compared to the emission rates measured for leaves in dry air. Without oxygen no C₂–C₅ hydrocarbons were emitted from the leaf litter. UV induced hydrocarbon emissions continue for a long period, and a decline of the emission rates was visible only on a time scale of months.

The extrapolation of the laboratory measurements clearly suggests that leaf litter is an insignificant source of C₂–C₅ hydrocarbons on a global scale. Locally, C₂–C₅ hydrocarbon emissions from leaf litter may have a small effect on local OH levels in regions with strong sources.

Acknowledgements

This work was funded by the Netherlands Organization for Scientific Research (NWO) under grant number 865.07.001. Asher Wishkerman and Frank Keppler (Max Planck Institute for Chemistry, Germany) are kindly acknowledged for supplying leaf litter from the Johannes Gutenberg University in Mainz (Germany) for the experiments, and Huib van Weelden (Utrecht University Medical Center, the Netherlands) is acknowledged for supplying the UV lamps.

CHAPTER 3

EMISSIONS OF H₂ AND CO FROM LEAF LITTER OF SEQUOIADENDRON GIGANTEUM, AND THEIR DEPENDENCE ON UV RADIATION AND TEMPERATURE

Senescent and dead plant material releases carbon monoxide (CO), methane and larger hydrocarbons upon heating or irradiation with UV, but emissions of hydrogen (H₂) have not been reported. This study investigated whether leaf litter is able to emit H₂ and which factors control the possible emissions. In addition, the emission of CO from leaf litter was measured and compared to previous studies. H₂ was released from leaf litter of sequoia (Sequoiadendron giganteum) in detectable amounts at temperatures above 45°C, whereas CO was also emitted at ambient temperature. The emission rates of both H₂ and CO increased with temperature according to the Arrhenius relation. UV radiation can induce emissions of both H₂ and CO. However, UV induced H₂ was only emitted under anoxic conditions. Emissions of CO were higher in synthetic air, but strongly reduced in the absence of oxygen.

This chapter is based on:

- L. Derendorp, J. B. Quist, R. Holzinger and T. Röckmann, *Emissions of H₂ and CO from leaf litter of Sequoiadendron giganteum, and their dependence on UV radiation and temperature*, Atmos. Environ., 45 (39) pp. 7520–7524, 2011.

3.1 Introduction

Many volatile compounds are released from plant matter during its decomposition. The emissions are often influenced by UV radiation and depend on temperature. Carbon dioxide is the main compound emitted during plant litter decomposition, but many other compounds are also released, for example methanol and acetone (Warneke et al., 1999), methane (Vigano et al., 2008; McLeod et al., 2008; Bruhn et al., 2009), C₂–C₅ hydro-carbons (McLeod et al. (2008), Chapter 2) and CH₃Cl (Hamilton et al. (2003); Keppler et al. (2004), Chapter 4). Carbon monoxide is also emitted by senescent and dead brown leaves, dead grass and leaf litter (Schade et al., 1999; Tarr et al., 1995; Sanhueza et al., 1994, 1998; Zepp et al., 1996). Globally, 50-170 Tg yr⁻¹, is released from dead plant matter (Schade and Crutzen, 1999). The emission of CO is strongly influenced by UV radiation, and depends on both the intensity and wavelength of the radiation. Schade et al. (1999) showed that the CO emission rate increases quadratically with UV intensity, and that UVA is most effective in generating CO emissions from leaf litter, whereas Tarr et al. (1995) showed that also UVB is important. The photo-production of CO is higher in leaf litter than in live vegetation. This is either due to chemical changes in the leaf occurring during senescence resulting in the formation of compounds that are more prone to photochemical decomposition, or due to the lack of a protective mechanism to prevent photochemical damage in dead plant matter (Tarr et al., 1995). In addition, CO emission rates rise with temperature according to the Arrhenius relation (Schade et al., 1999). Oxygen promotes the production of CO, whereas the presence or absence of CO₂ has no effect on the CO emission rate. This suggests that CO from leaf litter is formed through a physical rather than a metabolic mechanism. Direct photodegradation of plant cellular material might be responsible for the release of CO from dead plant material (Tarr et al., 1995; Schade et al., 1999; Bauer et al., 1980).

Emissions of molecular hydrogen (H₂) from dead plant matter have not been reported before. However, H₂ can be released from the plant structural component cellulose upon irradiation with UV (Sionkowska et al., 2002). Known sources of H₂ to the atmosphere include biomass burning, fossil fuel combustion, biological N₂ fixation and photochemical production. H₂ is oxidized in the atmosphere by the OH radical, but the main sink is uptake by soils (e.g. Ehrlert and Rohrer (2009); Pieterse et al. (2011); Novelli et al. (1999)).

Leaf litter may influence the soil fluxes of H₂ and CO. Soils are able to simultaneously take up and emit both H₂ and CO. Although the soil generally acts as a sink for both H₂ and CO, the direction and magnitude of the flux is determined by factors like soil type, soil organic matter content and soil temperature. Soil moisture, vegetation

cover and plant litter on the soil surface also have a significant effect on the soil flux, because they limit the diffusion of atmospheric air into the soil (Conrad and Seiler, 1985b; Schade et al., 1999; Sanhueza et al., 1998).

The uptake of H_2 is caused by the enzymatic activity of soil hydrogenases, whereas CO uptake is caused by microorganisms. The uptake of CO is identified as a first-order process with uptake rates being proportional to the atmospheric CO mixing ratio. The soil can also be a source of H_2 and CO. H_2 is produced and released from soils during biological N_2 fixation, whereas CO production in soils is due to the abiotic oxidation of soil organic matter (Conrad and Seiler, 1982, 1985b; Sanhueza et al., 1998).

The production rate of CO can exceed its consumption rate in deserts or savannas with arid conditions. In those ecosystems, the high temperatures and low soil moisture content promote the production of CO by the oxidation of soil organic matter, but limit CO uptake due to the inactivation of microorganisms. As a result, these soils act as a net source of atmospheric CO (Conrad and Seiler, 1982, 1985a,b). Field measurements have shown that CO emissions from leaf litter can compensate for the uptake of CO by the soil. For example, CO emissions from leaf litter in tropical savanna can be up to an order of magnitude higher than the soil uptake during daytime in the dry season (Schade et al., 1999).

This study examined whether H_2 can be emitted from leaf litter, and whether leaf litter can be an environmentally important source of H_2 , for example by partly compensating for the soil sink. Laboratory experiments were performed to determine whether the H_2 emissions were influenced by, or depending on oxygen, temperature and UV radiation. In addition, as a reference compound the emission of CO from leaf litter was measured and compared to previous studies.

3.2 Experimental methods

3.2.1 Plant material

Leaf litter of sequoia (*Sequoiadendron giganteum*) was collected in the botanical garden of the Johannes Gutenberg University in Mainz (Germany). The leaf litter was air-dried at 25 °C for two months in a fume hood. After drying, the plant material was stored in plastic zip bags at room temperature (~ 22 °C).

3.2.2 Measurement system

Sequoia leaf litter (0.5 - 3.0 g) was placed in a quartz tube (Suprasil™) with a volume of 350 mL that was continuously flushed with N₂, synthetic air or ambient air at a flow rate of 50 mL min⁻¹. Part of the gas leaving the quartz tube was flushed into a reduction gas analyzer (Peak Laboratories LLC, CA, USA) at a flow rate of 8 mL min⁻¹ to measure the mixing ratios of H₂ and CO. The temperature in the quartz tube could be varied via a heating wire connected to an adjustable power supply that was wrapped around the tube. The temperature of the leaf litter was measured with a thermocouple in the quartz tube on the leaf surface. In measurements where the temperature dependence of the emission rates was determined, the tube was covered with isolation material and aluminum foil to exclude UV radiation and visible light. The influence of UV radiation on the emission rates was determined by placing the quartz tube including leaf litter under a Vitalux UV lamp (Osram, 300W) that emits in both the UVA and UVB range. Varying UV intensities were obtained by placing the tube at different distances from the lamp. Details on the UV setup can be found in Sect. 2.2.5. The reduction gas analyzer was regularly calibrated with a reference gas with a H₂ mixing ratio of 548.1 ± 1.5 ppb and a CO mixing ratio of 222.5 ± 0.2 ppb. The response of the reduction gas analyzer was linear with respect to the H₂ and CO mixing ratios over the measurement range employed in the experiments.

3.2.3 Experiment description

3.2.3.1 Emission rate as a function of temperature

To determine the temperature dependence of H₂ and CO emissions from leaf litter, dry sequoia leaves were placed in the quartz tube. The temperature of the leaf litter was increased from 20 to 80 °C, while the emission rates were measured every 3.5 minutes. During the temperature increase, the quartz tube was continuously flushed with either N₂, synthetic air or ambient air to determine whether heat induced emissions of H₂ and CO from leaf litter were influenced by, or depending on oxygen, background concentrations of H₂ and CO, or other trace gases in the air. The experiments were performed in duplicate. Emission rates were calculated using to Eq. (2.1) and the temperature dependence of the emission rates was quantified by the activation energy that was calculated using the Arrhenius equation (Eq. 2.2). After the experiment, the leaf litter was cooled to 20°C, followed by another temperature increase to 80°C to check if the emission rates measured during the first and second temperature increase were comparable.

3.2.3.2 Emission rate as a function of UV radiation intensity

H₂ and CO emission rates were measured as a function of UV intensity by placing the quartz tube including sequoia leaf litter at distances between 20 and 50 cm from a Vitalux lamp. The emission rates were measured 5 to 7 times at each UV level. To determine the dependence of UV induced emissions on oxygen, emission rates as a function of UV intensity were measured while the quartz tube with leaf litter was flushed with either N₂ or synthetic air. Because the Vitalux lamp is a point source, a small UV gradient along the quartz tube could not be avoided. Therefore, at each UV level the UVA and UVB intensity were measured with a Waldmann UV meter 585-100 (Waldmann, Schweningen, Germany) at six positions around the quartz tube. The average of these six UV measurements was used. A small fraction of the UV radiation was absorbed by the quartz tube. The absorption was 9 and 11% for the UVA and UVB range, respectively, and was constant over the full range of UV intensities used in the experiments. The sum the UVA and UVB intensity corrected for absorption by the glass is reported, since studies by Schade et al. (1999) and Tarr et al. (1995) showed that, at least for CO formation, both UV ranges are important. Unweighted UV intensities are reported, because no reliable action spectrum for H₂ and CO emissions from leaf litter is available. Fifteen percent of the UV radiation was UVB, which is similar to the natural radiation. The UV intensity was varied between 8 and 46 Wm⁻², which are intensities that can be found under natural conditions. The emission rates were calculated according to Eq. (2.1). Although a ventilator was placed next to the quartz tube to avoid heating of the leaf litter because of the heat of the lamp, temperatures up to 32°C were observed at the highest UV intensities. Activation energies calculated with Eq. 2.2 were used to correct for these heat induced emissions, and the emissions rates were normalized to emission rates at 20°C.

3.3 Results and discussion

3.3.1 Emissions of H₂ and CO induced by heating of sequoia leaf litter

Typical emission rates of H₂ and CO at temperatures between 20 and 80 °C are shown in Fig. 3.1 for sequoia leaf litter in N₂, synthetic- or ambient air.

Emissions of H₂ were detectable for leaf litter in N₂, synthetic and ambient air, i.e., with background H₂ levels, but only when the leaf litter was heated to at least 45 °C. Although air temperatures of 45°C are rarely reached, high soil surface temperatures

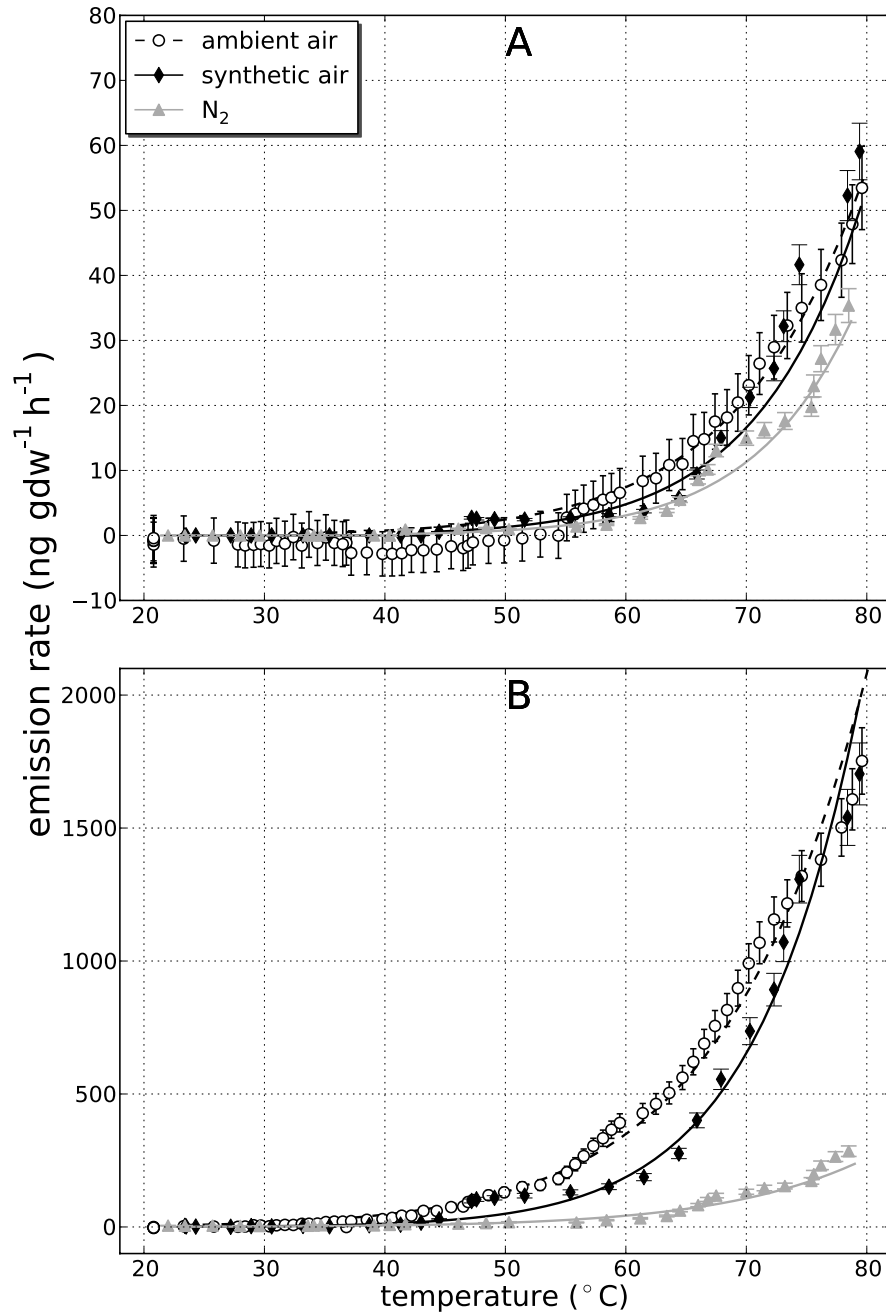


Figure 3.1: Emission rate of (A) H_2 and (B) CO as a function of temperature for sequoia leaf litter in N_2 , synthetic air and ambient air. Measurements are indicated by the marker symbols, whereas the Arrhenius fits (Eq. 2.2) are shown as lines. The error bars show the overall uncertainty of the emission rate calculated using error propagation.

are more often observed. For example, on a sunny day a surface temperature of 52°C was measured for a soil covered with brown, summer-dormant grass in Texas (Brady and Weil, 1999). In ambient air, the H₂ mixing ratio for the blank measurements was slightly higher than when leaf litter was placed in the quartz tube at temperatures below 50°C. Although the uncertainties are large, this indicates that H₂ might have been taken up by the leaf litter at these temperatures. After heating the leaf litter to 80°C for one time, the uptake of H₂ below 50°C was no longer observed in the second run (not shown), indicating that the uptake was probably due to biological activity. For temperatures of 45°C and higher, the H₂ emission rates increased with temperature according to the Arrhenius relation. The H₂ emission rates were of similar magnitude in synthetic- and ambient air, and emission rates of 55 - 60 ng gdw⁻¹h⁻¹ were observed at 80 °C. In N₂, the H₂ emission rate was lower: only 35 ng gdw⁻¹h⁻¹ was emitted at 80°C. This shows that the release of H₂ from leaf litter was not influenced by background H₂ concentrations and other trace gases. Anoxic conditions slightly reduced the H₂ emissions at high temperature in absence of UV radiation.

Carbon monoxide emissions were observed over the full temperature range (20-80°C) for leaf litter in all three carrier gases. The emission rates increased with increasing temperature according to the Arrhenius relation, although for sequoia leaf litter in synthetic- and ambient air at high temperature, the measured emission rates were lower than expected from the Arrhenius relation. The emission of CO was much lower for leaf litter in N₂ than in either synthetic- or ambient air. This indicates that CO emissions depend on the availability of oxygen. However, there are low emission of CO for leaf litter in N₂, which suggests that there may be an additional non-oxygen dependent pathway for CO formation. Alternatively this emission can result from oxygen that was still in the leaf (Tarr et al., 1995). Flushing the leaves for some days with N₂ prior to the experiment would probably decrease the oxygen level in the leaves, which should further decrease the CO emission rate in N₂. The emissions in synthetic and ambient air show similar results, which indicates that the presence of other trace gases and background concentrations of CO do not have a large influence on the CO emission rates.

The activation energies as derived from the Arrhenius equation (Eq. 2.2) are given in Table 3.1 for H₂ and CO emissions from leaf litter in N₂, synthetic- and ambient air. For H₂ emissions from leaf litter, the activation energies were of similar magnitude in all gases, whereas for CO the activation energy for leaf litter in synthetic air was higher than for leaf litter in the other carrier gases. The activation energies for both H₂ and CO emissions from leaf litter in all three gases were higher than 50 kJ mol⁻¹, which indicates that the emissions were not due to biotic activity (Schönknecht et al., 2008). In addition, the emissions increased with temperature up to 80 °C, which indicates as

well that the emissions originated from an abiotic process. Carbon monoxide can also be produced in soils due to the oxidation of soil organic matter and Conrad and Seiler (1985b) concluded that this was also an abiotic process. An overview of activation energies for CO emissions from plant litter measured in other studies is shown in Table 3.2. For comparison, the activation energies for the production of CO by soils have been added to this table. The activation energie for CO measured in this study is much larger than previously observed for leaf litter by Schade et al. (1999) and Zepp et al. (1996), but similar to values observed for CO emissions from soil. Soil CO production is also strongly reduced in absence of oxygen (Conrad and Seiler, 1985a), indicating that similar CO formation processes possibly exist in soils and leaf litter.

Table 3.1: *Activation energies (kJ mol⁻¹) for H₂ and CO emissions from sequoia leaf litter in N₂, synthetic- or ambient air. The activation energies and their uncertainties are derived from the least squares fit to the data in Fig. 3.1.*

	H ₂	CO
N ₂	123.6 ± 8.7	88.5 ± 5.4
synthetic air	118.0 ± 10.2	118.7 ± 4.8
ambient air	108.0 ± 6.8	87.7 ± 1.5

Table 3.2: *Comparison of the activation energy (kJ mol⁻¹) for CO emissions from sequoia leaf litter measured in this study with other studies where CO emissions from soil and plant litter have been measured.*

study	substrate/soil	Activation energy
Conrad and Seiler (1982)	soil	93
Conrad and Seiler (1985b)	soil	83 - 102
Conrad and Seiler (1985a)	soil	80 - 110
Schade et al. (1999)	leaf litter	66 ± 3
Zepp et al. (1996)	leaf litter	34.6
Zepp et al. (1996)	standing dry grass	88.4
Zepp et al. (1996)	soil	76.6
Hellebrand and Schade (2008)	composting of hay	65
This study	leaf litter	89 - 119

3.3.2 Emissions of H₂ and CO induced by UV radiation

Typical emission rates of H₂ and CO as a function of UV intensity are shown in Fig. 3.2 for leaf litter in N₂ or synthetic air. UV induced emissions of H₂ were observed

for leaf litter in a N_2 atmosphere; under these conditions the emission rate strongly increased with UV intensity. The H_2 emission rate varied from close to zero at 8 Wm^{-2} up to $\sim 0.6 \mu\text{g m}^{-2}\text{h}^{-1}$ at 35 Wm^{-2} . However, when leaf litter was placed in synthetic air, UV radiation did not induce any H_2 emission over the full UV range. Apparently the presence of oxygen or reactive oxygen species inhibited the formation of H_2 .

UV induced CO emissions from leaf litter were observed in both N_2 and synthetic air. In both carrier gases the CO emission rates increased with UV intensity. The emission rate was higher for leaf litter in synthetic air than in N_2 . In synthetic air, a CO emission rate of $25 \mu\text{g m}^{-2}\text{h}^{-1}$ was observed at 35 Wm^{-2} , whereas in N_2 the CO emission rate was only $15 \mu\text{g m}^{-2}\text{h}^{-1}$ at a similar UV intensity.

Irradiation of the leaf litter caused heating of the litter up to 32°C even though a ventilator was placed next to the tube with leaf litter for cooling. The UV induced CO emissions were corrected for heat induced emissions using the activation energies calculated in Sect. 3.3.1. Fig. 3.2b (dashed lines) also shows the UV induced CO emissions without the correction for heat induced emissions. Because of the different activation energies for CO emissions from leaf litter in N_2 and synthetic air, differences between the CO emission rates induced by UV radiation strongly reduced after temperature correction, and a similar dependence on UV intensity was observed for both cases. H_2 emissions were not observed at 32°C and no correction for heat induced emissions had to be applied.

UV induced CO emissions have been measured before by Schade et al. (1999) for dry savanna grass irradiated with a solar simulator in laboratory experiments. They observed CO emission rates from close to zero without UV radiation up to $300 \times 10^9 \text{ molec. cm}^{-2}\text{s}^{-1}$ at 900 Wm^{-2} , which corresponds to an emission rate of $500 \mu\text{g m}^{-2}\text{h}^{-1}$. The highest UV intensity used in our experiment was only $\sim 48 \text{ Wm}^{-2}$, and the CO emission rate was $160 \mu\text{g m}^{-2}\text{h}^{-1}$ at this intensity without the correction for heat induced emissions. After this correction, the emission rate was $30 \mu\text{g m}^{-2}\text{h}^{-1}$. Extrapolation of this emission rate to an UV intensity of 900 Wm^{-2} yields an emission rate of $560 \mu\text{g m}^{-2}\text{h}^{-1}$, which is in very good agreement with the emission rate reported by Schade et al. (1999). Tarr et al. (1995) examined the effect of senescence on CO photoproduction and showed that the emissions increased when transforming from living to senescent to dead plant matter. For fallen brown leaves, the CO emission rates ranged between 120 and $330 \times 10^9 \text{ molec. cm}^{-2}\text{s}^{-1}$ at 650 Wm^{-2} . This corresponds to $200 - 500 \mu\text{g m}^{-2}\text{h}^{-1}$ and is also in agreement with our measurements.

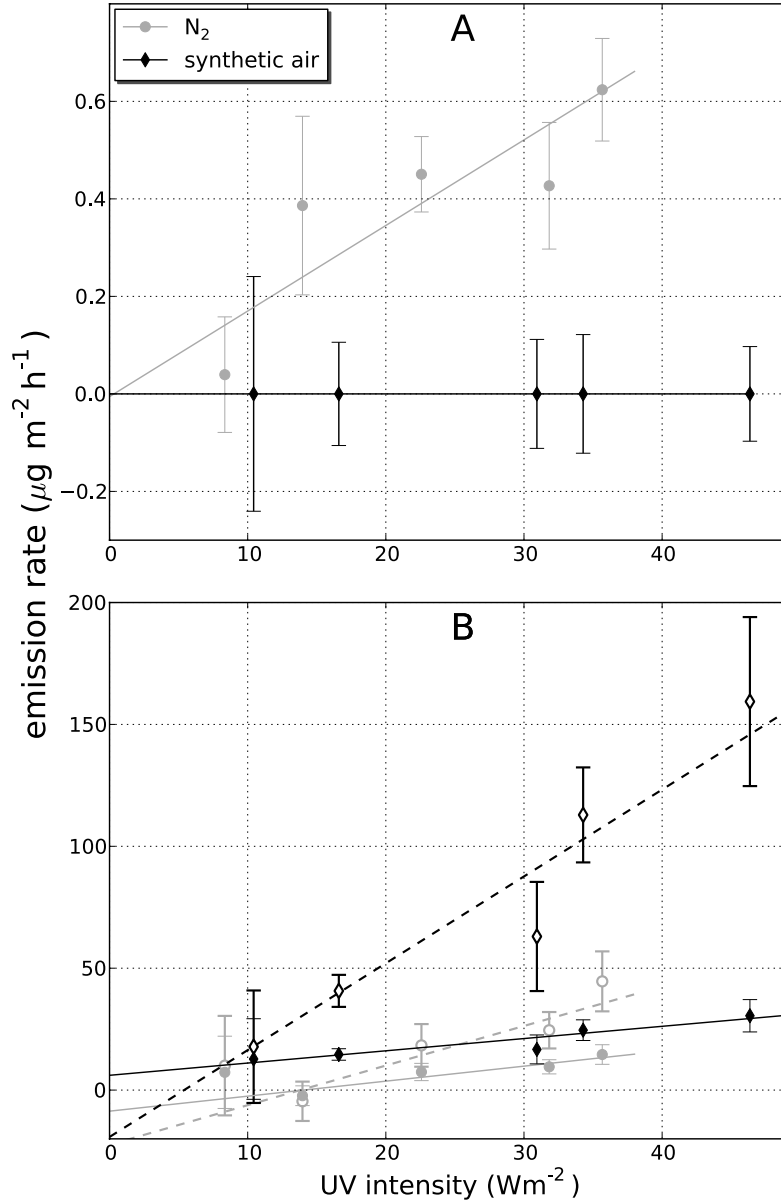


Figure 3.2: Emission rate of (A) H₂ and (B) CO as a function of UV intensity (solid markers and lines) for leaf litter in N₂ and synthetic air. In (B) the open markers and dashed lines indicate the CO emission rates before correcting for heat induced emissions using the activation energies as observed in Sect. 3.3.1. Heat induced H₂ emissions were only observed at temperatures of 45°C and higher, so no correction was applied for H₂. The error bars represent the standard deviation of the measurements at each UV level.

3.4 Conclusions

In this study the environmental importance of leaf litter as a source of H₂ was investigated. Sequoia leaf litter has the capability to emit H₂, but only in environments with

temperatures above 45°C. Although such high air temperatures are rarely reached, they are more easily observed at the soil surface. Above 45°C, the H₂ emission rate increased with temperature following the Arrhenius relation under both oxic and anoxic conditions. UV radiation generated H₂ emissions only under anoxic conditions. The emission rate increased linearly with the UV intensity. In contrast, CO emissions from leaf litter occurred under common natural conditions. The emission of CO occurred at ambient temperature, but CO emissions were also induced by UV radiation. As for H₂, CO emissions increased with temperature following the Arrhenius relation, and increased linearly with UV intensity.

Only one plant species (*Sequoiadendron giganteum*) was measured in this study, which is globally only a minor species. We acknowledge that other plant species might give different results. However, the CO emission rates measured for this species during irradiation with UV compared well with previous studies.

Acknowledgements

This work was funded by the Netherlands Organization for Scientific Research (NWO) under grant number 865.07.001. Asher Wishkerman and Frank Keppler (Max Planck Institute for Chemistry, Germany) are kindly acknowledged for supplying leaf litter from the Johannes Gutenberg University in Mainz (Germany) for the experiments, and Huib van Weelden (Utrecht University Medical Center, the Netherlands) is acknowledged for supplying the UV lamps.

CHAPTER 4

METHYL CHLORIDE LABORATORY EXPERIMENTS: DEPENDENCE OF CH₃CL EMISSIONS FROM LEAF LITTER ON TEMPERATURE, CHLORIDE- AND METHOXYL GROUP CONTENT

Leaf litter has been identified as a potentially important source of CH₃Cl, but the factors controlling the emissions are unclear. Two studies were performed in which CH₃Cl emission rates from leaf litter were measured. During the initial study emissions of CH₃Cl from dry leaf litter of various plant species were investigated. These measurements were simultaneously performed with the measurements of the C₂–C₅ hydrocarbon emissions from leaf litter described in Chapter 2. Large variations in the CH₃Cl emission rate between different plant species were observed. In the temperature range 20–100 °C, the CH₃Cl emission rate strongly increased with temperature. At 20 °C, emission rates between 0.03 and 0.85 ng gdw⁻¹h⁻¹ were observed, whereas at 70 °C the emission rates increased up to 18 µg gdw⁻¹h⁻¹. The temperature dependence of the CH₃Cl emission rate can be described by the Arrhenius relation. The emissions were not due to enzymatic activity, which was indicated by emission rates that continuously increased with increasing temperature, and activation energies that were higher than 50 kJ mol⁻¹. At constant temperature, the CH₃Cl emission rate decreased in time. At high temperatures (80–100 °C) this was noticeable on a timescale of hours, while at low temperatures (20–30 °C) the decrease was slow and visible on a timescale of months. A simple upscaling showed that the emission of CH₃Cl from leaf litter might be significant for its global budget.

The follow up study focussed on leaf litter of twelve halophyte species, and investigated the temperature dependence of the CH₃Cl emission rates, and the dependence of the CH₃Cl emissions on the chloride- and methoxyl group content of the plant material. Emission rates varied be-

tween halophyte species up to two orders of magnitude. As observed in the initial experiments, the emissions were not due to biological activity, and increased with temperature following the Arrhenius relation. The activation energies were similar for all investigated plant species, indicating that even though emissions vary largely between plant species, their response to changing temperatures is similar. The chloride- and methoxyl group contents of the leaf litter samples were determined, but those parameters were not significantly correlated to the CH_3Cl emission rate.

This chapter is based on:

- L. Derendorp, R. Holzinger, A. Wishkerman, F. Keppler and T. Röckmann, *Methyl chloride and C_2 – C_5 hydrocarbon emissions from dry leaf litter and their dependence on temperature*, *Atmos. Environ.*, 45 (18) pp. 3122-3199, 2011
- L. Derendorp, A. Wishkerman, F. Keppler, C. McRoberts, R. Holzinger and T. Röckmann, *Methyl chloride emissions from halophyte leaf litter: dependence on temperature and chloride content*, *Chemosphere*, doi:10.1016/j.chemosphere.2011.12.035, 2012

4.1 Introduction

Leaf litter was first identified as a potentially significant source of CH_3Cl in laboratory experiments by Hamilton et al. (2003). Methyl chloride emissions were measured from dead and senescent plant material of several plant species at temperatures between 30 and 50 °C. The emission rates were strongly temperature dependent. In addition, a strong correlation between the CH_3Cl emission rate and the chloride content of the leaf litter was observed. The formation of CH_3Cl was identified as an abiotic process and occurs in dead and senescent plant material (woody and foliar). Methyl chloride is formed through a reaction between chloride ions and methoxyl groups that originate from the plant component pectin. Keppler et al. (2004) measured CH_3Cl emission rates between 150 and 300 °C from freeze-dried, milled biomass, and confirmed that emission rates strongly increased with temperature.

A limited number of field measurements of the CH_3Cl flux from leaf litter has been performed. Blei et al. (2010) found large differences in the CH_3Cl emission rate between different locations in a tropical rainforest in Malaysian Borneo. In contrast, for needle and leaf litter in a temperate deciduous forest in Scotland, the temporal variation of the net CH_3Cl fluxes was significantly greater than the spatial variation (Blei and Heal, 2011). Most of the year the flux of CH_3Cl was slightly negative, except for a large, positive emission peak in autumn that coincided with the fall of fresh leaf litter and elevated fungal activity at that time of year. Another positive emission event was observed in March, although much smaller than in autumn. This corresponded with a rise in ambient temperature after a prolonged winter cold period. Averaged over one year the net CH_3Cl flux from leaf litter was positive. Blei and Heal (2011) found no significant correlation between the net CH_3Cl flux and the ambient air temperature (up to 16 °C) or leaf litter water content.

Due to the limited amount of measurements on CH_3Cl emissions from leaf litter and the large variation in CH_3Cl emission rates between different plant species, estimates of the global source of CH_3Cl from leaf litter are highly uncertain (0.3 - 2.5 Tg yr⁻¹, Hamilton et al. (2003)). However, the estimated range implies that the emissions can be possibly important for the global CH_3Cl budget. In addition, the extent to which leaf and needle litter fluxes are the product of abiotic chemical reactions and/or microbial/fungal activity is unknown and requires investigation as suggested by Blei and Heal (2011).

The goal of these laboratory studies was to investigate the emission of CH_3Cl into the atmosphere by leaf litter of different plant species and to examine the factors that control the emissions. The influence of temperature and the chloride- and methoxyl group content of the leaf litter on the emissions was investigated. The emission rates

were measured at temperatures between 20 and 70 °C and the activation energies were calculated to quantify the temperature dependence of the emissions. In the initial experiment, measurements were performed on both ground and whole leaf material. In addition, the temporal evolution of the emission rates was determined at different temperatures. The dependence of the CH₃Cl emission rates on the chloride- and methoxyl group content of the leaf litter was investigated in a follow-up study on halophyte leaf litter. Hamilton et al. (2003) already observed a correlation between the CH₃Cl emission rate and the tissue chloride content. However, they mainly investigated leaf litter from trees of Northern Ireland with chloride contents below 15000 ppm. In this study halophytes of different vegetation forms and collected in different geographical zones with chloride contents in the range of 4500 - 50000 ppm are investigated. Because CH₃Cl is formed through the reaction between pectin methoxyl groups and chloride ions, we also investigate the influence of the total methoxyl group content on the emission rates, although this is not expected to have a large effect at ambient temperatures. A simple upscaling method was used to assess the environmental importance of leaf litter as a source of CH₃Cl.

4.2 Experimental methods

4.2.1 Plant materials

For the initial study on CH₃Cl emissions from leaf litter, the same plant materials were used as for the measurements of C₂–C₅ hydrocarbon emissions (Sect. 2.2.1) except birch and sweetgum litter. For the follow-up study on halophytes, fresh leaf litter of twelve halophyte species was collected in Uzbekistan, Mauritania or Botswana. All leaf samples were air-dried followed by freeze-drying. Prior to the experiment the leaf litter samples were ground to pass through a 1 mm sieve. For all halophyte species, the sampling location, family, vegetation form and salt tolerance mechanism are indicated in Table 4.1. Samples of *Cressa cretica* and *Traganum nudatum* were collected at two locations and because of insufficient material were ground together.

Table 4.1: Overview of the plant species, sampling location, family, vegetation form, and salt tolerance mechanism of the halophytes used in this study. In the remainder of this manuscript the plant species names will be abbreviated (column 2).

plant species	abbrev- viation	sampling- location	latitude, lon- gitude (°)	family	vegetation salt tolerance mechanism form
<i>Tamarix hispida</i> wild	TAMH	Uzbekistan	43.50, 59.41	Tamaricaceae	shrub salt secreting glands ^a
<i>Astragalus</i> sp.	ASTR	Uzbekistan	44.00, 58.80	Fabaceae	N/A
<i>Tamarix leptostachys</i> bunge	TAML	Uzbekistan	44.00, 58.80	Tamaricaceae	shrub salt secreting glands ^a
<i>Haloxylon persicum</i> bunge ex boiss	HAPE	Uzbekistan	43.83, 59.27	Amaranthaceae	shrub accumulation of organic solutes, especially soluble sugars (osmoregulation) ^b
<i>Calligonum</i> sp.	CALL	Uzbekistan	44.00, 58.80	Polygonaceae	N/A
<i>Cynodon dactylon</i>	CYDA	Botswana	-20.46, 25.93	Poaceae	grass salt gland, accumulation of glycine betaine (osmoregulation) ^c
<i>Aerva persica</i>	AEPE	Mauritania	18.89, -15.66	Amaranthaceae	subshrub facultative halophyte, mechanism unknown ^d
<i>Cressa cretica</i>	CRCR	Mauritania	19.87, -16.23 and 19.91, -16.29	Convolvulaceae	shrub salt secreting glands ^a
<i>Panicum</i> sp.	PASP	Botswana	-20.46, 25.93	Poaceae	grass N/A
<i>Spergularia rubra</i>	SPRU	Botswana	-20.46, 25.93	Caryophyllaceae	weed, perennial N/A
<i>Sporobolus spicatus</i>	SPSP	Mauritania	19.91, -16.29	Poaceae	grass salt secreting gland ^e
<i>Traganum nudatum</i>	TRNU	Mauritania	18.89, -15.66 and 19.91, -16.29	Chenopodiaceae	subshrub N/A

^a Kasera and Mohammed (2010)

^b Song et al. (2006)

^c Marcum (1999)

^d Dagar and Gurbachan (2007)

^e Ramadan (2001)

4.2.2 Experimental setup

For the initial study the plant system as described in Sect. 2.2.2 was used. This plant system is referred to as the dynamic system. For the study on halophyte leaf litter, a static system was used (Fig. 4.1). The two plant systems will be compared in Sect. 4.3.1. For the static system, ground leaf litter (0.05 to 0.3 g) was placed in a 40 ml vial closed with a screw cap containing a PTFE/silicon septum (Supelco, Sigma Aldrich, PA, USA) and was heated for 14 to 18 hrs at 30, 40 or 50 °C. After heat treatment, the samples were cooled down to room temperature ($\sim 20^\circ\text{C}$), and the CH₃Cl mixing ratio in the vial was measured within 8 hrs. Directly before measuring the CH₃Cl mixing ratio, two capillaries (fused silica, inner diameter: 0.53 mm, SGE, Australia), each connected to a needle, were inserted into the vial via the septum (Fig. 4.1). Via these capillaries, the air in the vial was flushed with 500 ml nitrogen gas (AirProducts 26508, BIP 5.7, The Netherlands) into a gas chromatograph with cryotrap (see Sect. 2.2.3) to measure the CH₃Cl mixing ratio. A Nafion humidity exchanger (Perma Pure, MD-050-72P-2, NJ, USA) was placed between the vial and the gas chromatograph to remove moisture that might have been present in the vial. For each plant species, three replicates and three blank measurements were performed at each temperature (30, 40 and 50°C). Blanks were made by following the procedure outlined above, but without leaf litter in the vial. For each measurement a new vial with a new septum was used.

4.2.3 Methyl chloride emission rate measurements

The CH₃Cl emission rates were measured simultaneously with the C₂–C₅ hydrocarbon emissions (Sect. 2.2.3). A reference gas (AiR Environmental CC262873, CO, USA) with a CH₃Cl mixing ratio of 103 ppb was used for calibration of the gas chromatograph for CH₃Cl. For a 1 L sample, the CH₃Cl detection limit was ~ 4 ppt.

For experiments with the dynamic system, the CH₃Cl emission rate was calculated using Eq. 2.1. For experiments with the static system, CH₃Cl emission rates were calculated at each temperature for all plant species according to Eq. 4.1

$$ER = \frac{CMvol_{vial}}{V_m m_{dw} \Delta t} \quad (4.1)$$

where ER is the emission rate, C is the CH₃Cl molar mixing ratio in the vial after heat treatment and after blank correction, M the molar mass of CH₃Cl (50.5 g mol^{-1}), vol_{vial} the volume of the vial (40 mL), V_m the molar volume of an ideal gas at standard temperature and pressure (24.5 L mol^{-1}), m_{dw} the dry weight of the leaf litter and Δt the heating period of the leaf litter. The emission rates are reported in $\text{ng gdw}^{-1} \text{h}^{-1}$

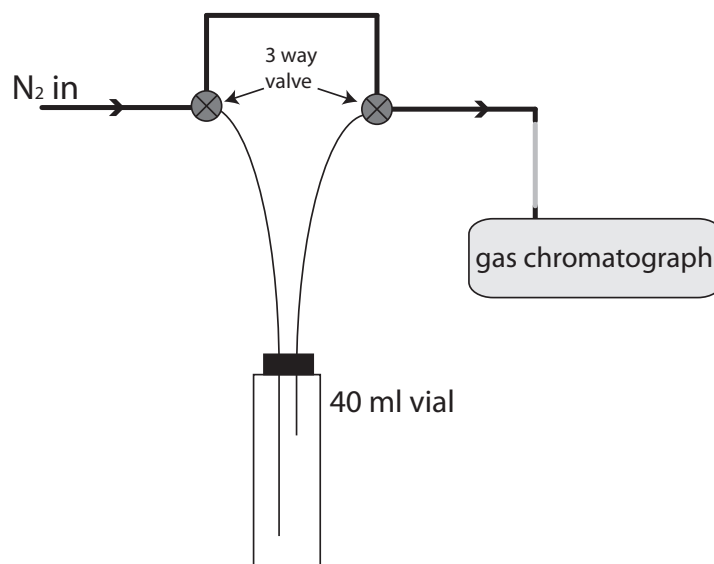


Figure 4.1: Schematic overview of the static plant system. Leaf litter is placed in the 40 mL vial, which is sealed with a screw cap with a septum at the top. Thin black lines indicate the capillaries that were inserted into the vial via a needle. Thick black lines indicate 1/8 inch steel tubing, whereas the grey thick line before the gas chromatograph indicates the nafion humidity exchanger. The flow rate into the gas chromatograph was 33 mL min^{-1} . The three way valves can be put in a position to directly flush nitrogen gas into the gas chromatograph, or flush nitrogen gas via the vial into the gas chromatograph.

(gdw = gram dry weight). The time between cooling down the vial with leaf litter and the actual measurement was not taken into account, because the emissions at 20°C were very small compared to the emissions at higher temperature.

4.2.4 Chloride content determination

The total chlorine content of the halophyte samples was measured using X-ray fluorescence (XRF) as described in Cheburkin and Shotykh (1996). Since fresh leaf litter was used in all experiments, it is reasonable to assume that most chlorine was in the form of chloride ions (Leri and Myneni, 2010). The leaf litter was not washed in order to mimic the natural conditions. No distinction between internal and external salt was made. In general we assumed that most of the chloride should be internal, but for e.g. the *Tamarix* species, which use salt secreting glands as part of their tolerance mechanism, a significant fraction of the salt is considered to be external. The chloride contents of the leaf litter samples is reported in % mass. The percentage coefficient of variation of the method was 6.7%.

4.2.5 Methoxyl group content determination

For determination of the methoxyl group content of the halophyte leaf litter, the method as described by Wishkerman et al. (2008) was used. Triplicate samples (~10 mg each) were placed in a glass vial (14 mL) and ethyl cellulose (50 μ L, 6 mg mL⁻¹ in chloroform) was added as internal standard. After evaporation of the solvent, hydriodic acid, 57% (1 mL) and distilled water (100 μ L) were added, and the vial was sealed with a screw cap containing a PTFE/silicone septum. For quantification, a series of standards were prepared in a similar fashion to the samples except that the distilled water was replaced by aqueous methanol solutions of known concentration. For quality control purposes, samples of methyl D-galactopyranoside with known methoxyl content were analyzed with each sample batch. Samples were heated at 130 °C for 30 min and the headspace (50 μ L) was monitored for methyl and ethyl iodide content by gas chromatography/mass spectrometry (GC/MS) using a 6890GC/5973N system (Agilent Technologies, Palo Alto CA, USA). The MS was employed in the selected ion monitoring (SIM) mode measuring ion currents at m/z 142 and 156. The GC oven was equipped with a 12.5 m \times 0.25 mm \times 8 μ m Chrompack CP-Poraplot Q capillary column (Varian, Oxford, UK) and programmed at 80 °C for 1 min and then ramped at 10 °C min⁻¹ to a final temperature of 200 °C. Helium (1.5 mL min⁻¹) was employed as the carrier gas with an injection split ratio of 100:1. The recovery for methyl D-galactopyranoside (quality control) was $97.1 \pm 1.2\%$, and the percentage coefficient of variation of the method was $\pm 1.9\%$. The methoxyl group content of the leaf litter samples is reported as a percentage of the sample mass.

4.2.6 Calculations and statistics

In general, measurements were performed in triplicate. The average of the three measurements is reported and the standard deviation is used to indicate the spread of the emission rate measurements around its mean value. The temperature dependence of the emission rates was quantified by using the Arrhenius equation (Eq. 2.2) to calculate the activation energy. The slopes of the Arrhenius plots for the different plant species (proportional to the activation energy) were tested for similarity using analysis of covariance (ANCOVA) (Zar, 2007). The F-statistic was calculated and compared to critical values of the F-distribution. Alternatively, the temperature dependence of the emissions was quantified using the Q₁₀ temperature coefficient (Eq. 4.2), a measure of the rate of change of the emission rate due to a 10°C temperature increase.

$$Q_{10} = \left(\frac{ER_2}{ER_1} \right)^{\left(\frac{10}{T_2 - T_1} \right)} \quad (4.2)$$

where ER_2 is the emission rate at temperature T_2 , and ER_1 the emission rate at temperature T_1 .

For the halophyte samples, correlation coefficients between the CH_3Cl emission rate and the chloride- or methoxyl group content of the plant material were calculated (Zar, 2007). Because the data were not normally distributed, the correlation coefficients were tested for statistical significance using the empirical bootstrap method (Dekking et al., 2005).

4.3 Results and discussion

4.3.1 Comparison of the static- and dynamic system

Methyl chloride emission rates were measured using the dynamic and the static method at temperatures between 20 and 60°C. To compare the emission rates obtained using both method, a series of measurements was performed on whole and ground sweet-gum leaf litter. The experiments performed for this comparison are listed in Table 4.2. For the static method only experiments in ambient air can be performed.

Table 4.2: Overview of the experiments that were performed to compare the static and the dynamic plant system.

number	method	litter type	carrier gas	note
1	static	ground	ambient air	
2	static	whole	ambient air	
3	dynamic	ground	ambient air	
4	dynamic	ground	synthetic air	
5	dynamic	whole	ambient air	
6	dynamic	whole	synthetic air	
7	dynamic	whole	synthetic air	repetition of experiment 6

4.3.1.1 Emission rate as a function of temperature

The CH_3Cl emission rate as a function of temperature is plotted in Fig. 4.2 for all experiment series listed in Table 4.2. Because of the different methodologies, the error

bars for experiments with the dynamic system mainly reflect changes of the emission rates in time, whereas for the static experiments the error bars reflect the variation of the emission rate within the batch of leaf litter.

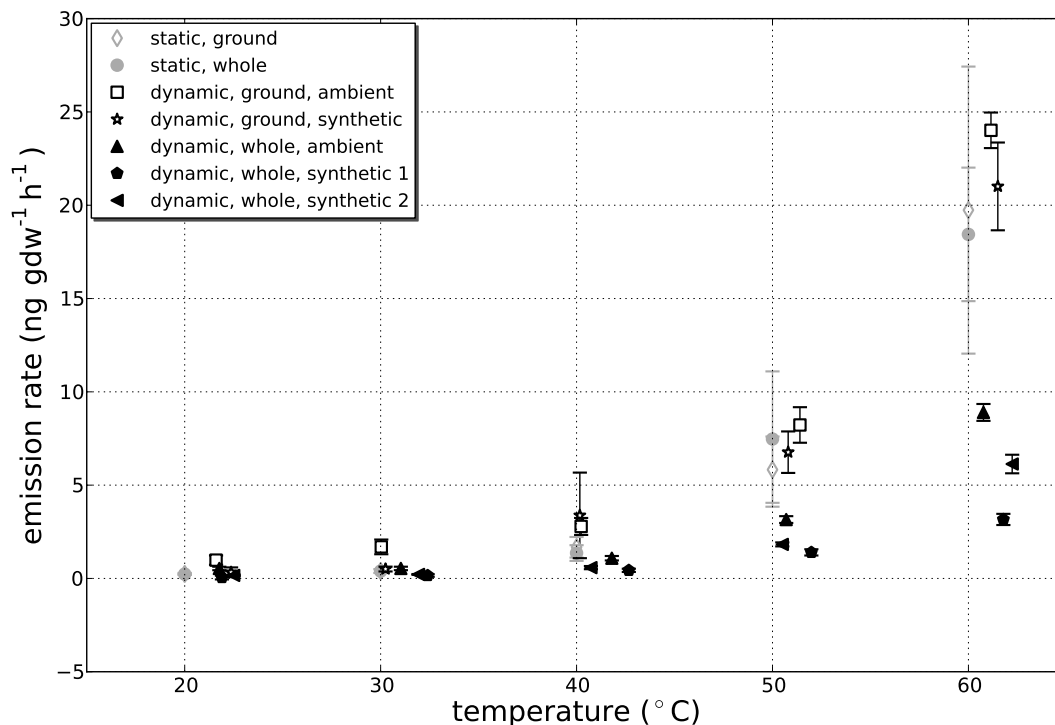


Figure 4.2: Methyl chloride emission rate as a function of temperature for all experiments of Table 4.2. The legend indicates whether the static or the dynamic method was used, and whether ground or whole sweetgum litter was used. For the experiments with the dynamic method, both synthetic and ambient air were used as carrier gas. The experiment with the dynamic method with whole leaf litter in synthetic air was performed twice (synthetic 1 and synthetic 2) and are both shown.

With the static method, comparable results were obtained at all temperatures for ground and whole leaf litter. For experiments with the dynamic system, the emissions from ground leaf litter were higher than from whole leaf litter at high temperature, but comparable at relatively low temperature. For both ground and whole leaves, the error bars increased with temperature. This was caused by a decrease of the emission rate during the 4.5 h that were required to perform three measurements at the respective temperature level. At higher temperature, the decrease of the emission rate was faster and this was reflected in a larger error bar. For the dynamic system only one leaf litter sample was used for a whole measurement series and variability within a batch of leaf

litter may lead to substantial differences between experiment series. This is illustrated by the experiment series with whole leaf litter in synthetic air using the dynamic system, which was performed twice. For those experiments, the CH_3Cl emission rates were comparable at low temperature, whereas at higher temperature deviations were observed.

The CH_3Cl emission rates at low temperatures were similar for all experiment series. However, at higher temperature (50 and 60°C) the emission rates measured with the dynamic method for whole leaves in both synthetic and ambient air were clearly lower than in the other measurement series.

4.3.1.2 Arrhenius plot

Figure 4.3 shows Arrhenius plots for the measurements of Sect. 4.3.1.1. Linear relations between $\ln(\text{ER})$ and the inverse temperature were generally observed in all experiment series. However, in some of the experiments, higher emission rates were observed at the lowest temperature ($\sim 22^\circ\text{C}$) than expected based on the linear fit. The activation energies calculated from the slope of the Arrhenius plots for CH_3Cl emission for all experiment series in Table 4.2 are shown in Table 4.3.

Table 4.3: Activation energies (kJ mol^{-1}) for CH_3Cl emissions from sweetgum leaf litter for all experiments series. The uncertainties are derived from the least squares fit through the data.

experiment	activation energy
static-ground	89.2 ± 9.8
static-whole	88.0 ± 7.3
dynamic-ground-ambient	75.5 ± 7.1
dynamic-ground-synthetic	97.5 ± 4.5
dynamic-whole-ambient	73.1 ± 11.0
dynamic-whole-synthetic 1	87.1 ± 4.8
dynamic-whole-synthetic 2	89.9 ± 5.8

4.3.1.3 Comparison: advantages and disadvantages of both plant systems

During the measurements with the dynamic system, it was observed that emission rates strongly decrease in time at high temperature. This decrease was visible within the 4.5 hrs required to repeat three measurements at a certain temperature level, and therefore it affects the measured emission rate at high temperature. In addition, compounds emitted during the period of the increase from one temperature level to the

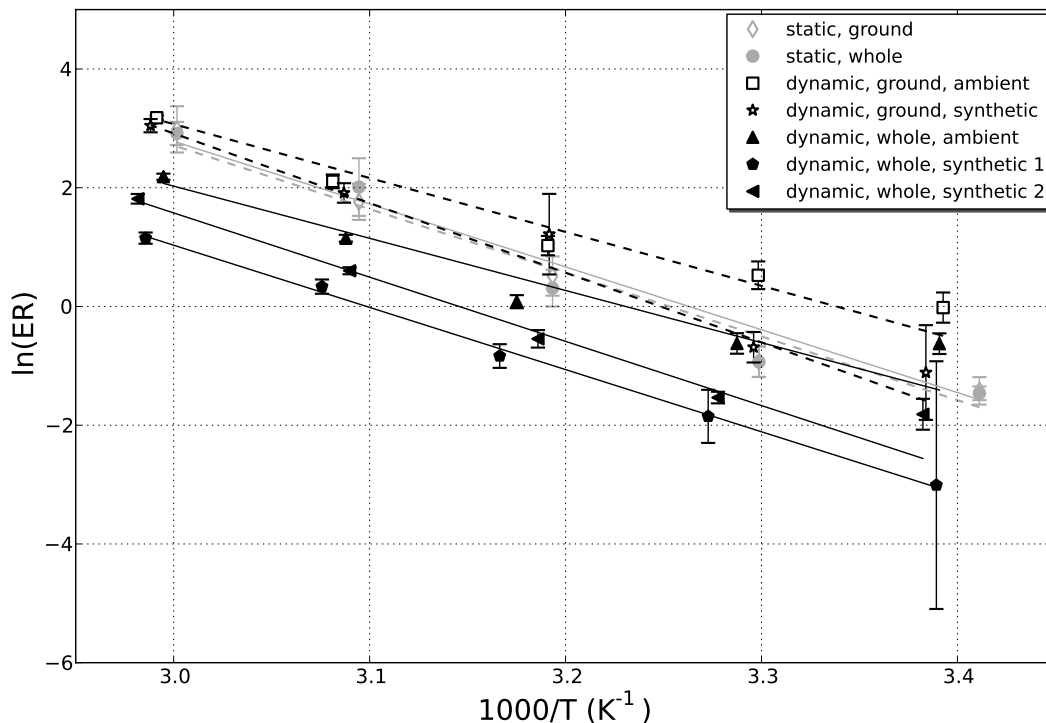


Figure 4.3: Arrhenius plot for the emission of CH₃Cl from leaf litter for all experiments in Table 4.2.

next temperature level are not detected. For the static method, leaf litter was heated for ~ 15 h, and emission rates were calculated based on the total emission during this heating period. Temporal changes of the emission rates within this heating period are not visible with this method, even though they probably do occur. Therefore, emission rates measured with the static method are not expected to scale linearly with heating period, and probably depend on the duration of the heating period.

With the static method, CH₃Cl accumulates in the vial during the heating period, resulting in a large difference between the blank measurement and the measurements with leaf litter at all temperatures. This makes it possible to measure the emissions from leaf litter in a background of ambient air. When using the dynamic system and the emissions are low, leaf litter has to be placed in synthetic air to obtain mixing ratios that are substantially different from background levels. Therefore, emissions can only be measured in ambient air with the dynamic method for compounds that are emitted at relatively high rates, while the atmospheric concentrations are relatively low. Another disadvantage is that flushing the leaf litter with synthetic air may induce

emissions of compounds that would not be emitted when background levels of those compounds are present in the air.

Both the static- and dynamic method clearly have advantages and disadvantages. However, at environmentally relevant temperatures both methods yielded similar CH_3Cl emission rates from whole and ground leaf litter.

4.3.2 Variation in CH_3Cl emission rates between plant species

In the initial experiments, the CH_3Cl emission rate was measured as a function of temperature for leaf litter of rice, maize, beech, cherry prinsepia and sequoia. An overview of the emission rates at 30 °C is shown in Table 4.4. The variability in the emission rates between the different plant species was large. The lowest emission rate ($0.04 \text{ ng gdw}^{-1}\text{h}^{-1}$) was found for whole maize leaves at 30 °C, whereas for whole rice leaves the highest emission rate of $7.3 \text{ ng gdw}^{-1}\text{h}^{-1}$ was measured. Such large variations between plant species were also observed by Hamilton et al. (2003) for CH_3Cl emissions from different plant species. The large variability between different plant species also holds at higher temperatures. Whole rice leaves, for which the highest emissions were observed, emitted CH_3Cl at a rate of $18 \mu\text{g gdw}^{-1}\text{h}^{-1}$ at 70 °C, whereas whole maize leaves emitted only $12 \text{ ng gdw}^{-1}\text{h}^{-1}$ at this temperature (data at 70 °C not shown). Note that these differences should only tentatively be interpreted as indications for differences between plant species, since intra-species variations were not examined in this project.

Table 4.4: Methyl chloride emission rates with 1 standard deviation ($\text{ng gdw}^{-1}\text{h}^{-1}$) at 30 °C for sequoia, maize, rice, beech and cherry prinsepia leaf litter.

plant species	emission rate
ground sequoia	0.27 ± 0.09
ground maize	0.39 ± 0.09
ground rice	1.87 ± 0.6
ground cherry prinsepia	0.83 ± 0.12
ground beech	0.44 ± 0.15
whole sequoia	1.28 ± 0.21
whole maize	0.04 ± 0.002
whole rice	7.3 ± 1.6

4.3.3 Influence of the chloride and methoxyl group content of the leaf litter on CH₃Cl emissions.

For leaf litter of the halophytes the influence of the chloride- and methoxyl group content of the plant material on the emission rate of CH₃Cl was investigated. An overview of the chloride- and methoxyl group content of the investigated halophyte samples is shown in Table 4.5. The methoxyl group content ranged between $0.52 \pm 0.04\%$ for TRNU and $2.52 \pm 0.12\%$ for SPRU. The chloride content of the leaf litter was high especially for species with salt secreting glands, with the highest chloride content ($4.68 \pm 0.63\%$) for TAMH. The lowest chloride content was observed for HAPE ($0.34 \pm 0.03\%$), a shrub collected in Uzbekistan.

Table 4.5: *Methoxyl group content and chloride content (% mass) of the halophyte leaf litter.*

plant species	methoxyl group content	chloride content
TAMH	1.31 ± 0.06	4.68 ± 0.63
ASTR	2.11 ± 0.43	1.20 ± 0.06
TAML	1.64 ± 0.11	3.35 ± 0.13
HAPE	1.88 ± 0.11	0.34 ± 0.03
CALL	1.37 ± 0.03	0.46 ± 0.005
CYDA	1.46 ± 0.04	0.93 ± 0.03
AEPE	1.95 ± 0.04	0.92 ± 0.04
CRCR	1.49 ± 0.05	3.20 ± 0.11
PASP	2.33 ± 0.19	0.87 ± 0.07
SPRU	2.52 ± 0.12	2.07 ± 0.21
SPSP	1.84 ± 0.11	2.21 ± 0.13
TRNU	0.52 ± 0.04	3.24 ± 0.11

Methyl chloride emission rates at 30 °C as a function of chloride- and methoxyl group content are shown in Fig. 4.4a and 4.4b, respectively. Similar results were obtained at 40 and 50°C (not shown).

Also for the halophytes, large variations in the CH₃Cl emission rates were observed between leaf litter of different species (see also Fig. 4.4 and 4.6) at all temperatures. The highest emission rates were observed for the two species of the Tamarix genus (TAMH and TAML). Emission rates of 17.2 ± 1.0 and 7.5 ± 1.0 ng gdw⁻¹h⁻¹ were observed at 30°C for TAMH and TAML, respectively, whereas for the other halophyte species the emission rates ranged from 0.18 ± 0.04 to 1.66 ± 0.07 ng gdw⁻¹h⁻¹ at this temperature. Also at higher temperature, large differences between halophyte species were observed with emission rates varying between 1.97 ± 0.10 and $189.5 \pm$

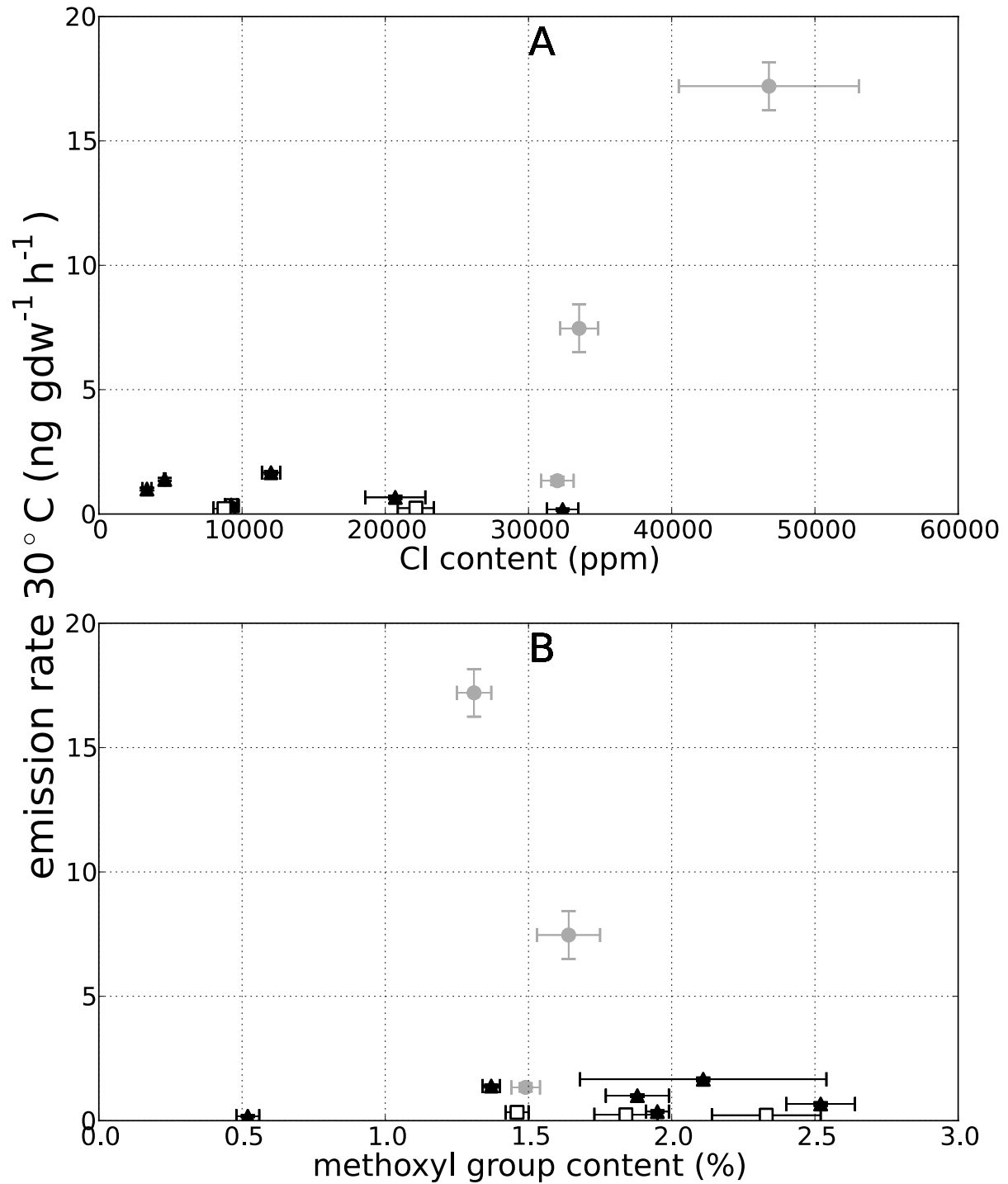


Figure 4.4: Methyl chloride emission rates at 30°C as a function of (A) chloride and (B) methoxyl group content of the leaf litter for each examined halophyte species. Shrubs with salt secreting glands are indicated by circles, grasses by squares and other vegetation forms by triangles.

2.9 ng gdw⁻¹h⁻¹ at 50°C, which is a variation of almost two orders of magnitude. In general, the highest emission rates were measured for shrubs with salt secreting glands (including the *Tamarix* species), with emission rates up to 189.5 ± 2.9 ng gdw⁻¹h⁻¹ for TAMH at 50°C. The lowest emission rates were generally measured for grasses. Even at 50°C, the emission rate ranged only from 2.3 ± 0.3 to 4.1 ± 0.1 ng gdw⁻¹h⁻¹.

Hamilton et al. (2003) measured CH₃Cl emission rates of 5.4 and 5.8 ng gdw⁻¹h⁻¹ for grasses at 50 °C, which is 1.3 to 2.5 times higher than in this study. *Batis maritima* was the plant species with the highest emission rate in their study with emission rates of 112 and 1291 ng gdw⁻¹h⁻¹ at 40 and 50°C, respectively. This is 6.5 - 7 times higher than our emission rates for TAMH. The higher emission rates measured by Hamilton et al. (2003) might reflect other growth conditions and the different plant physiology of the examined species. In addition, Hamilton et al. (2003) used whole leaf samples, whereas ground leaf samples were used in this study. This might also explain the differences between the studies.

Correlation coefficients between the CH₃Cl emission rate and the chloride content of the leaf litter ranged between 0.69 and 0.71 depending on temperature. However, these high correlation coefficients were mainly caused by the high emission rates for the two plant species of the *Tamarix* genus, which had a large chloride content. When these two plant species were excluded, the correlation coefficients decreased to values between -0.15 and 0.03 at different temperatures. Indeed, testing the statistical significance of the correlation using all measurements with the empirical bootstrap method showed that the correlations were not significant ($P = 0.49$). Hamilton et al. (2003) found that CH₃Cl emission rates were significantly correlated to the tissue chloride ion content. However, most of the plant species investigated by Hamilton et al. (2003) were leaves from trees of Northern Ireland with a chloride ion content below 15000 ppm, whereas this study investigated halophytes of different vegetation forms collected in different geographical zones. Also the chloride ion content of the litter covers a wider range. Therefore, a conclusion of the present work is that the correlation between CH₃Cl emissions and the chloride content of the plant material cannot be generalized.

The emission rates were not significantly correlated ($r = -0.22$, $P = 0.52$) with the methoxyl group content of the leaf litter at each investigated temperature. This was in agreement with our expectation that emissions do not depend on the total methoxyl group content at temperatures between 30 and 50°C, because only pectin methoxyl groups and not lignin methoxyl group are able to methylate chloride ions at these temperatures (Hamilton et al., 2003).

4.3.3.1 Discussion on the dependence of the emissions on the chloride content of the leaf litter

The absence of a statistically significant correlation between the CH₃Cl emission rate and the chloride content of the leaf litter suggests that other factors strongly influence the emissions.

Blei et al. (2010) concluded that for living vegetation in a tropical rainforest, plant species was the main factor determining the CH₃Cl emission rates. Possibly CH₃Cl emissions from leaf litter also depend on plant species or vegetation form. The lowest emission rates were observed for grasses, whereas shrubs with salt secreting glands emitted CH₃Cl with the highest rates. An influence of vegetation form on the CH₃Cl emissions may also explain the differences with the study of Hamilton et al. (2003). They measured CH₃Cl emission rates from leaf litter of Northern Ireland trees and found a significant correlation with the chloride content of the plant material, whereas in this study no significant correlation between CH₃Cl emission and chloride content was found for halophyte leaf litter of varying vegetation forms and originating from different geographical regions.

Also the stage of decomposition of the leaf litter may influence the CH₃Cl emission rate. In healthy, living leaves, the majority of the chlorine is present as chloride ions, which are required by the plant for e.g. the water splitting reaction of photosynthesis and for charge balance in the opening and closing of the stomata. When transforming from living to senescent leaves, a fraction of the chloride ions is converted from H-bonded chlorine to organo-chlorine (Myneni, 2002; Leri and Myneni, 2010). The XRF analysis used to determine the chloride content of the halophyte leaf litter does not separate these different chlorine forms, while probably not all forms are equally available for CH₃Cl formation. However, although for this study fresh leaf litter was used in all experiments, and most chlorine was likely in the form of chloride ions, there was no significant correlation between the emission rate and the chloride content. This indicates that decomposition stage is probably not the dominant factor that determines the CH₃Cl emission rate.

Another reason for the absence of a significant correlation between the CH₃Cl emission rate and the chloride content of the leaf litter may be that other factors limit the emission. Indeed, a significant dependence of the CH₃Cl emission rate on the chloride content of the plant material is probably only observed when the chloride content is the limiting factor. Hamilton et al. (2003) observed that the percentage conversion of chloride ions to CH₃Cl is relatively low in plants with high chloride content. For example, only 5% of the chloride ions was converted to CH₃Cl when they heated *Batis maritima* with a chloride content of 283 mg gdw⁻¹ from 150 to 300°C, indicating that

other factors may have limited the emission of CH₃Cl. Methyl chloride emissions are generally not limited by the methoxyl group content at ambient temperatures. However, grasses, for which the lowest emission rates were observed, usually have a low pectin and a high lignin content. Since only pectin methoxyl groups are available for CH₃Cl formation at ambient temperatures, these may have limited the CH₃Cl emission from grasses even though the total methoxyl group content was high. This may explain the low emission rates for grasses.

4.3.4 The temperature dependence of CH₃Cl emissions

For all investigated plant species, the CH₃Cl emission rate strongly increased with temperature. In the initial experiments, the emission rate as a function of temperature was measured between 20 and 70°C. For ground and whole leaf litter of maize and sequoia, the results are shown in Fig. 4.5.

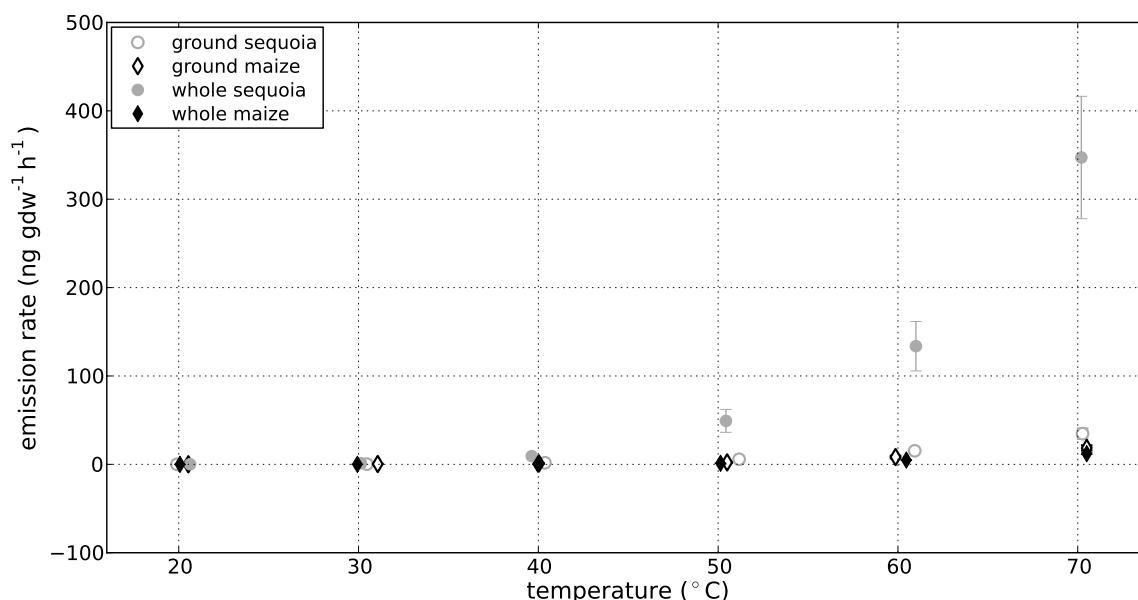


Figure 4.5: Methyl chloride emission rate as a function of temperature for ground and whole leaf litter of maize and sequoia. Emissions from the other plant species show similar temperature dependencies.

For all plant species, the emission rates increased up to 70°C, which indicates that the release of CH₃Cl from dry leaf litter was not due to biological activity as was observed for the C₂–C₅ hydrocarbon emissions from leaf litter (Sect. 2.3.1.1). Arrhenius plots for these initial experiments (not shown) generally showed a good linear relationship ($R^2 = 0.95 - 0.99$) over the full temperature range used in the measurements (20–70°C).

However, for some plant species (e.g. sequoia), slightly lower emission rates were observed at high temperature (60-70 °C) than expected based on the linear fit. This reflects the decreasing emission rates at high temperature and may indicate the beginning of the depletion of the pool of chloride ions (Hamilton et al., 2003; Keppler et al., 2004). The activation energies derived from the Arrhenius plots in these initial experiments varied between 79 ± 1 and 100 ± 3 kJ mol⁻¹ for ground leaf litter and between 119 ± 4 and 192 ± 4 kJ mol⁻¹ for whole leaf litter.

For leaf litter of the halophyte species, the CH₃Cl emission rates were measured at 30, 40 and 50°C. For all investigated halophyte species, the CH₃Cl emission rate strongly increased with temperature (Fig. 4.6). Arrhenius plots for the CH₃Cl emissions from each examined halophyte are shown in Fig. 4.7. For all plant species, the Arrhenius equation seems to describe the emission rates at all temperatures well ($R^2 > 0.97$), as was also observed in the initial experiments.

For the halophyte species, the activation energies derived from the Arrhenius plots and the Q₁₀ temperature coefficients for different temperature ranges are shown in Table 4.6.

Table 4.6: Overview of the activation energies (kJ mol⁻¹) and Q₁₀ temperature coefficients for different temperature ranges for CH₃Cl emissions from halophyte leaf litter.

plant species	activation energy	Q ₁₀ (30-40°C)	Q ₁₀ (40-50°C)	Q ₁₀ (30-50°C)
TAMH	102.4 ± 9.9	2.6 ± 0.2	4.2 ± 0.2	3.3 ± 0.2
ASTR	118.1 ± 6.3	3.8 ± 0.4	5.0 ± 0.7	4.4 ± 0.4
TAML	101.1 ± 2.8	3.5 ± 0.5	3.5 ± 0.5	3.5 ± 0.7
HAPE	80.3 ± 5.4	2.1 ± 0.3	3.4 ± 0.5	2.7 ± 0.2
CALL	115.4 ± 10.2	3.4 ± 0.2	4.6 ± 0.2	3.9 ± 0.2
CYDA	100.7 ± 2.2	3.8 ± 0.2	3.2 ± 0.1	3.5 ± 0.2
AEPE	116.8 ± 6.3	3.7 ± 0.6	4.3 ± 0.3	4.0 ± 0.6
CRCR	118.7 ± 1.2	4.7 ± 0.6	4.1 ± 0.2	4.3 ± 0.6
PASP	105.6 ± 18.9	2.9 ± 0.6	4.5 ± 0.8	3.6 ± 0.9
SPRU	104.3 ± 6.7	3.0 ± 0.4	3.9 ± 0.3	3.4 ± 0.4
SPSP	96.0 ± 12.9	2.3 ± 0.8	4.2 ± 1.2	3.1 ± 0.8
TRNU	104.2 ± 8.2	2.9 ± 0.7	3.8 ± 0.4	3.3 ± 0.7

Activation energies ranged from 80.3 ± 5.4 kJ mol⁻¹ for HAPE up to 118.7 ± 1.2 kJ mol⁻¹ for CRCR. For all investigated plant species, the activation energies were higher than 50 kJ mol⁻¹, which also indicates that the emissions were not due to enzymatic activity (Schönknecht et al., 2008). Q₁₀ values for the emissions from halophyte leaf litter varied between 2.7 ± 0.2 and 4.4 ± 0.4 based on measurements at 30 and

50°C. Comparison of the slopes (proportional to the activation energy) of the Arrhenius plots for all halophyte species using ANCOVA revealed that the slopes were not significantly different ($F = 1.465$, $P > 0.25$, $n = 12$). Therefore, a common slope was calculated corresponding to an average observed activation energy of 103 kJ mol^{-1} (Zar, 2007). This indicates that even though emissions vary largely between leaf litter of different halophyte species, their response to changing temperatures is similar for all investigated species. This may be used to estimate the importance of leaf litter for the CH₃Cl budget when global temperatures are changing.

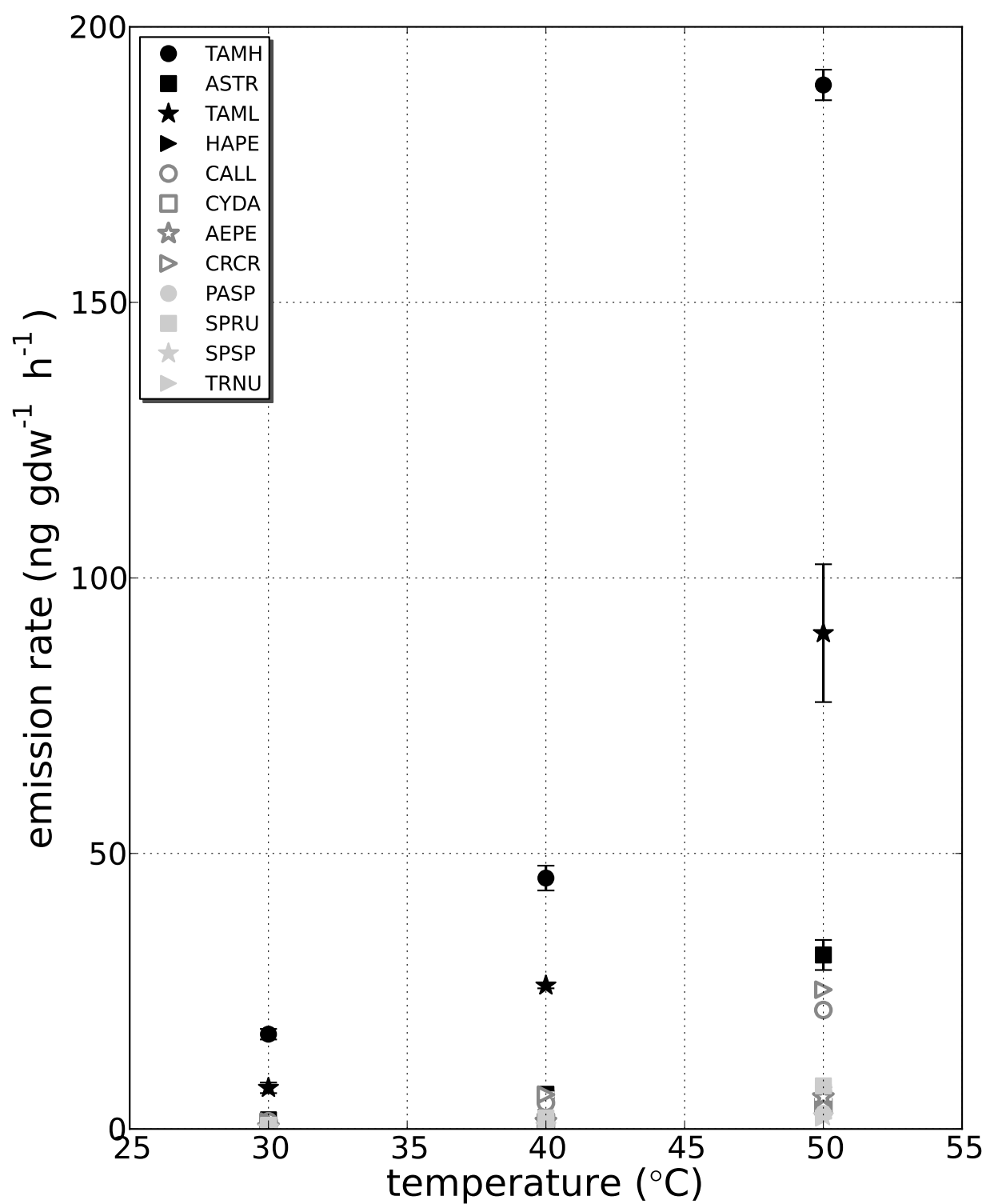


Figure 4.6: Emission rate of CH_3Cl as a function of temperature for halophyte leaf litter of twelve species.

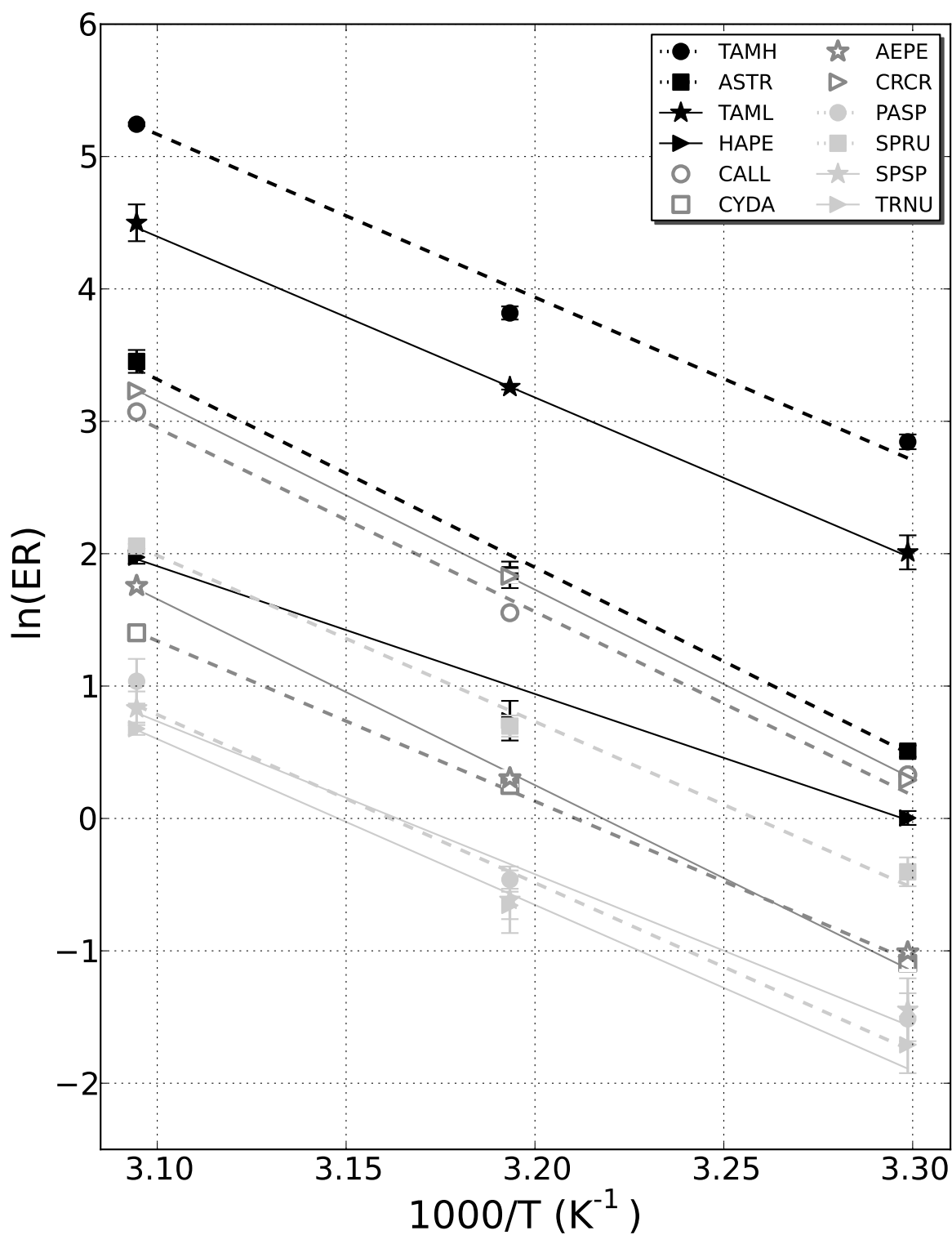


Figure 4.7: Arrhenius plot for CH₃Cl emissions from leaf litter of twelve halophyte species.

4.3.5 The temporal evolution of the CH₃Cl emission rates from leaf litter

In the initial experiments with the dynamic plant system a decrease of the CH₃Cl emission rate was observed during measurements at high temperatures. As for the C₂–C₅ hydrocarbons (Chapter 2), this was investigated in an experiment where the CH₃Cl emission rates were measured for maize leaves at high temperature (80 and 100 °C) over the course of several days (Fig. 4.8).

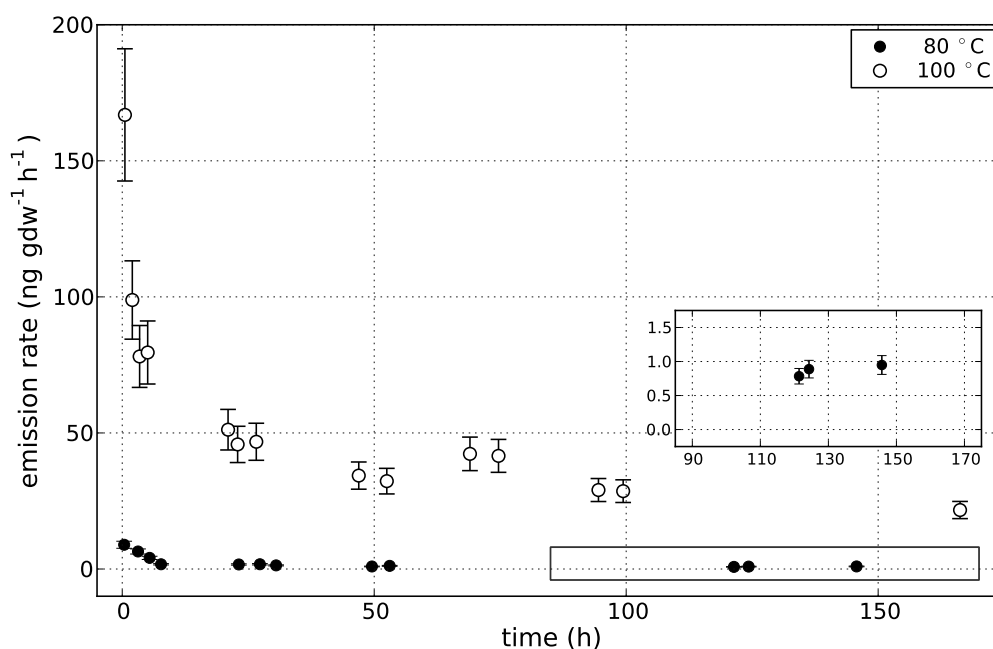


Figure 4.8: Emission rates of CH₃Cl as a function of time for whole maize leaves at 80 and 100 °C. The inset illustrates the low emission rates between 85 and 170 h, which are still above our detection limit.

The CH₃Cl emission rates showed an initial peak, then a sharp decrease to lower values within several hours, followed by a much slower decay in the following hours. However, decline of the emission rates below our detection limit was not observed within the 170 h duration of the experiment. To determine whether the emission rate would eventually decrease below the detection limit, or stay at an asymptotic value, the experiment should be repeated for a longer period.

Depletion of the pool of chloride ions may have been the cause of the decline of the CH₃Cl emission rate. At 100 °C the emission rates were more than one order of magnitude higher than at 80 °C during the entire experiment period. Consequently, the integrated amount of CH₃Cl released during the 170 h experiment was much larger

at 100 °C, indicating that at 100 °C additional methoxyl groups or chloride ions were accessible compared to 80 °C. This was in contrast to our initial expectation that the total releasable CH₃Cl amount of a leaf should be independent of temperature, and that depletion of a pool of precursor is only faster at high temperature, as was observed for the emission of oxygenated volatile organic compounds by Warneke et al. (1999). As the total releasable CH₃Cl amount of a leaf appeared to be temperature dependent, at least at high temperatures, this quantity is unsuitable for estimates of the global source of CH₃Cl from leaf litter.

Like for the C₂–C₅ hydrocarbon emissions from leaf litter (Chapter 2) the effect of long term storage of the leaf litter on the CH₃Cl emissions was assessed. Measurements of the emission rate as a function of temperature were performed for whole leaf litter of sequoia directly after drying of the batch, and 10 months later (data not shown). Similar results were obtained as for the C₂–C₅ hydrocarbons: after 10 months the CH₃Cl emission rates still increased exponentially with temperature, but the values were lower than directly after drying the batch of leaf litter. In the low temperature regions, the emission rates were of comparable magnitude, but at high temperatures the emission rates were approximately 60–90% lower than directly after collection of the leaf batch.

4.4 Implications for atmospheric chemistry and climate change

Climate change models predict temperature increases of several degrees in the following decades, and more frequent occurrence of heat waves and droughts (IPCC, 2007). Therefore, CH₃Cl emissions from leaf litter will potentially become more important in the future. In addition, climate change scenarios predict less rain fall and higher evaporation rates in particular in semi-arid areas, which are characterized by a negative water budget. Some of these semi-arid areas are also characterized by salt lakes or salty soils. In a changing climate, the quantity and scale of hyper saline lakes and salty soils is therefore likely to increase (IPCC, 2007). Halophytes, the dominant vegetation living in these salty areas, will therefore be exposed to increasing temperatures and soil salinity and are expected to play an increasing role in the future as climate is changing. In addition, the continuing negative impact of climate change and anthropogenic pressure on the ecosystems alter the plant growth conditions, which can result in favorable conditions for halophyte plant communities as occurred in semi-arid Mediterranean climate (Salinas et al., 2000). Moreover, these alterations increase the possibility of invasive species, among them *Tamarix* species (Natale et al., 2010).

In order to assess the significance of CH₃Cl emissions from leaf litter for its global

budget, a simple upscaling similar to the one described in Sect. 2.4 is performed. The CH_3Cl emissions measured at 30 °C (Table 4.4) during the initial study were assumed to continue over one year at a constant rate. This estimate should be seen as upper limit for the source of CH_3Cl from leaf litter, because a) 30 °C is much higher than the annual global mean temperature, b) timing of litter fall and the availability of leaf litter throughout the year was not taken into account, c) by performing the experiments in synthetic air the emission rates were possibly optimized by maximizing the air-to-leaf gradient of CH_3Cl , and d) the emission rates at 30 °C were assumed to be constant throughout the year. Additional details on this upscaling method can be found in Sect. 2.4. Using this method the global annual source of CH_3Cl from leaf litter was estimated at 0.11–1.5 Tg yr^{-1} based on measurements using ground leaves, and 0.02–5.5 Tg yr^{-1} when based on whole leaf litter. For comparison, the total global annual sink of CH_3Cl is estimated between 3.9 and 5.4 Tg yr^{-1} (Keppler et al., 2005; Yoshida et al., 2006; Xiao et al., 2010) This indicates that our upper estimate for emissions from leaf litter is similar to the estimated global sink strength and suggests that leaf litter is a potentially important source of CH_3Cl .

This method only gives a rough upper limit for actual global CH_3Cl emissions. However, our results corroborate the findings from an earlier study where contributions up to 2.5 Tg yr^{-1} were estimated from senescent plant material (Hamilton et al., 2003). In this study, the global CH_3Cl emission estimated from leaf litter can be as high as the total global estimated source. This warrants further research, especially field measurements are required to verify whether the emissions measured in our laboratory setting are comparable to emissions in nature.

4.5 Conclusions

Methyl chloride was emitted from dry leaf litter at ambient temperatures, and for all investigated plant species the emission rate increased with temperature. The emission rates varied largely between different plant species. Emission rates of CH_3Cl were not significantly correlated to the chloride content of the plant material, or the methoxyl group content. Thus, the correlation between the CH_3Cl emission rate and the chloride content of leaf litter that was observed by Hamilton et al. (2003) for leaf litter of Northern Ireland trees should not be generalized. Methyl chloride emissions may depend on vegetation type, are limited by other factors, or could be influenced by litter decomposition stage.

The emissions were not due enzymatic activity, as indicated by the continuous increase of the emission rate with increasing temperature, and activation energies that were

higher than 50 kJ mol⁻¹. Continuous heating of the leaf litter at high temperature caused a substantial decline of the CH₃Cl emission rate within hours. At ambient temperature, the decline of the emission rate was only visible on a timescale of months to years.

For leaf litter of all plant species, the Arrhenius relation describes the increase of the CH₃Cl emission rate with temperature. For the halophyte plant species, the temperature dependence of the emissions was similar, and an average observed activation energy of 103 kJ mol⁻¹ was found. The Q₁₀ temperature coefficients varied between 2.7 and 4.4 for the different halophyte species. This indicates that for a temperature increase of 5°C, the emissions of CH₃Cl from leaf litter are likely to increase by a factor 1.4 - 2.2. Thus, because of the strong temperature dependence of the emission rates, CH₃Cl emissions from leaf litter will likely increase in a changing climate with elevated temperatures. A simple upscaling showed that leaf litter may be a globally significant source of CH₃Cl. However, the estimated range is large and should be considered as an upper limit. Field measurements are required for better constraining the global source of CH₃Cl from leaf litter.

Acknowledgements

This work was supported by the Netherlands Organization of Scientific Research (NWO) under Grant No. 016.071.605 and by the DFG research unit 763 'Natural Halogenation Processes in the Environment - Atmosphere and Soil'. Karsten Kotte and Stefan Huber are acknowledged for collecting the halophyte samples.

CHAPTER 5

METHYL CHLORIDE FIELD EXPERIMENTS: CH₃CL EMISSIONS FROM LEAF LITTER AND CH₃CL SOIL FLUXES

The laboratory experiments have shown that the emission of CH₃Cl from leaf litter may be substantial. Additional field measurements are required to determine the environmental significance of leaf litter as a source of CH₃Cl. This field study was carried out at the end of the PhD project and consists of a limited set of experiments. The CH₃Cl fluxes from leaf litter were measured in a field experiment and the fluxes were compared to measurements in the laboratory. In addition, the soil fluxes of CH₃Cl were determined. Leaf litter emitted CH₃Cl, but only in periods with fresh leaf litter fall. Outside these period, the flux from leaf litter was zero or even negative. The CH₃Cl emission rate increased with temperature, but the temperature increase did not follow the Arrhenius relation as was observed in the laboratory experiments. Large differences were found between the laboratory and field measurements, which may be caused by differences the moisture content of the leaf material. The soil flux of CH₃Cl was measured at four location. At each location, the soil was a net sink of CH₃Cl. At one location, the soil flux was regularly measured, and the flux was correlated to the soil temperature.

5.1 Introduction

Laboratory experiments have shown that leaf litter is a potentially important source of CH₃Cl (e.g. Chapter 4). However, the global estimate of leaf litter as a source of CH₃Cl is uncertain. Especially field experiments are required to investigate the leaf litter source under natural conditions.

In addition, the soil has been identified as a net sink of CH₃Cl, although both production and consumption of CH₃Cl by soils are reported. Estimates for the global sink strength are uncertain and highly variable due to the limited amount of measurements. Khalil and Rasmussen (2000) measured the CH₃Cl soil fluxes in forests in Brazil and grass fields in Greenland and estimated a global soil sink of 0.5 Tg yr⁻¹. This is in the range of 0.3 - 0.6 Tg yr⁻¹ suggested by Graedel and Keene (1995). A larger soil sink of 1 Tg yr⁻¹ was estimated by Rhew et al. (2003).

Bacteria are responsible for the degradation of CH₃Cl in soils. Several bacteria that use CH₃Cl as a sole source of carbon have been identified from a variety of terrestrial environments (McDonald et al., 2002; McAnulla et al., 2001; Miller et al., 2004), which indicates that the soil can be a widespread sink of CH₃Cl. The production of CH₃Cl in the soil is an abiotic process (Keppler et al., 2000). During the oxidation of organic matter, chloride ions are methylated without sunlight or microbial activity.

Using a stable isotope tracer technique, Rhew et al. (2003) measured the simultaneous production and consumption of CH₃Cl for a boreal forest soil in Alaska. They found that the uptake of CH₃Cl was larger than the CH₃Cl production and consequently the boreal soil was identified as a net sink. Rhew and Abel (2007) measured the gross soil flux of CH₃Cl for Californian temperate annual grasslands in 2004 and 2005 with the same technique. Net emission dominated the dry season, whereas net uptake was dominant in the wet season. Gross production of CH₃Cl was strongly depending on the plant species covering the soil, whereas gross consumption was strongly affected by soil moisture. However, in saturated soils the uptake rates show a significant decline, probably due to the limited diffusive transport of air into the soil. The Arctic coastal plain and continental interior are net CH₃Cl sinks (Teh et al., 2009). Hydrology was the dominant factor regulating the CH₃Cl flux. The highest gross uptake was observed in drier areas, whereas gross uptake in flooded areas was low. Temperature played a secondary role in the uptake of CH₃Cl, and is likely more important in drier ecosystems.

In this study the emission of CH₃Cl from leaf litter was investigated in field experiments. Laboratory experiments (Chapter 4) showed that emissions from leaf litter can be substantial, and that they strongly increase with temperature. Therefore, the

influence of air- and soil temperature on the CH_3Cl emissions from leaf litter was investigated in field experiments. To investigate the agreement between laboratory and field experiments, CH_3Cl emissions were measured in the laboratory for leaf litter that was collected during the field experiments, and compared to the emissions measured in the field experiments. In addition, the soil flux of CH_3Cl was measured at different locations, and the influence of soil temperature on this flux was determined.

5.2 Experimental methods

5.2.1 Location of the field experiments

Two series of field experiments were performed in which CH_3Cl fluxes were measured at four different locations. The first experiment series was performed between September 2010 and January 2011 in a garden in Moordrecht (The Netherlands). The goal was to study the emission of CH_3Cl from leaf litter. In addition, the uptake of CH_3Cl by the soil was investigated. The second experiment series was performed between April and June 2011. No fresh leaf litter was available in that period, and only the size and variability of the soil fluxes was investigated. These experiments were performed in a greenhouse in the Botanic garden of Utrecht University (Utrecht, The Netherlands), on a sandy soil in the grasslands of Sandwijck (De Bilt, The Netherlands), and on a clay soil next to the river the Kromme Rijn (Bunnik, The Netherlands).

5.2.2 Chamber and flux measurements

Methyl chloride fluxes were determined by measuring the change of the mixing ratio as a function of time in a closed chamber placed on soil. The chamber was closed for a pre-determined sampling time (0–60 min). Afterwards an air sample was extracted from the chamber. After extraction, the chamber was opened to equilibrate the soil with the atmosphere. This procedure was repeated for all sampling times. The chamber consists of two parts. A metal ring (diameter = 30 cm) was pushed into the ground for a depth of 5 to 10 cm. A plexiglass chamber (diameter = 30 cm, height = 27.5 cm) was placed on top of this metal ring. A ventilator was placed inside the chamber to mix the air. At the top of the chamber, a 1/4 inch PFA teflon line was attached that could be connected to a sampling flask. Via a septum in the chamber, a temperature sensor was inserted to monitor the air temperature during the sample collection period. A photo the setup is shown in Fig. 5.1 (left).

Air samples were collected in 1 L glass flasks (Normag Labor- and Prozesstechnik

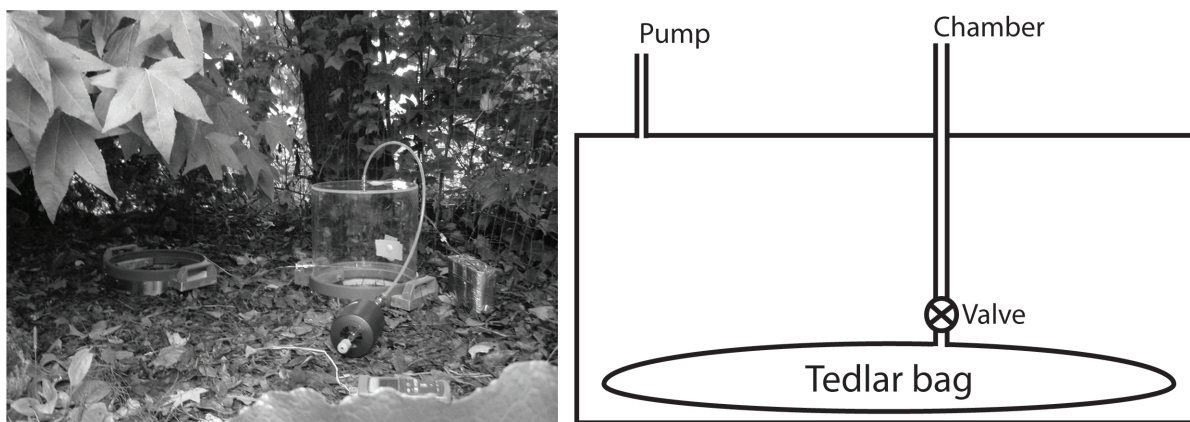


Figure 5.1: Left: Photo of the metal rings in the soil and the chamber that was connected to a sampling flask. Right: schematic picture of the lung sampler. A pump is connected at the location indicated in the picture. When the air is pumped away from the closed box, the Tedlar bag is filled with air from the chamber.

GmbH, Ilmenau, Germany) during the 1st experiment series or 2 L Tedlar bags (Supelco analytical, Bellefonte, PA, USA) during the 2nd experiment series. The glass flasks were evacuated before use, and filled during the field experiment by opening the flask. Disadvantage of sampling with the glass flasks was that, to avoid a too low pressure in glass flask during the mixing ratio measurement, only 250 mL of each sample could be used for analysis of the CH_3Cl mixing ratio. The Tedlar bags were five times flushed with synthetic air before use and then emptied. They were filled by using a 'lung sampler' (www.caslab.com/Forms-Downloads/Flyers/Lung_Sampler_Instructions.pdf). A schematic picture of the lung sampler is shown in Fig. 5.1 (right). From the Tedlar bags at least 1 L of air could be used for measurement of the CH_3Cl mixing ratio, which reduced the uncertainty of the measurement compared to the glass flask samples.

In the first experiment series the soil uptake and the effect of leaf litter on the soil flux were investigated. Therefore, two metal rings were placed next to each other. From one of the rings, all plant material was removed (soil ring), whereas from the other ring no plant material was removed (leaf litter ring). Methyl chloride mixing ratios were measured as a function of sampling time for both rings. From the difference between the two, the effect of leaf litter on the net CH_3Cl flux was determined. No fresh leaf litter was available during the second field experiment (April-June), and only the soil flux was measured.

In all experiments, the soil temperature was measured at 1, 5 and 10 cm depth with a thermocouple. The litter fall was determined by measuring the mass of the leaf litter that has fallen in the soil ring since the previous experiment day. This freshly

fallen leaf litter was removed from the soil ring and dried at room temperature. Afterwards, the mass of the dried litter was determined. In the period with fresh litter fall, measurements were performed approximately once per week. During the second experiment also the volumetric water content of the soil was determined by using a moisture sensor (5TM, Decagon device, WA, USA).

5.2.3 Laboratory measurements

Methyl chloride emission rates from leaf litter measured during the first field experiment series were compared with emission rates measured in laboratory experiments on leaf litter of the same trees. On the first day of the field experiment (9 September 2010), leaf litter was collected that was already decaying since the previous winter. On 7 October 2010, freshly fallen leaf litter was collected from the same location. Both leaf litter fractions were air-dried at room temperature for two months and stored in plastic zip bags until they were measured in the laboratory. The CH_3Cl emission rates as a function of temperature were measured as described in Sect. 2.2.

5.2.4 Measurement of the CH_3Cl mixing ratio

A gas chromatograph with flame ionization detector was used for measurement of the CH_3Cl mixing ratio. Details of the instrument can be found in Sect. 2.2.3.

5.2.5 Calculations and statistics

The uptake of CH_3Cl by the soil has been identified as a first order process by Rhew et al. (2003). Here, the soil uptake flux was also calculated by assuming that the uptake of CH_3Cl is a first-order process that could be described by

$$mr(t) = mr(0) \exp(-k_{soil}t) + C \quad (5.1)$$

with $mr(0)$ the initial mixing ratio, $mr(t)$ the mixing ratio at sampling time t , and k_{soil} the uptake rate coefficient that was derived by applying a least-squares fit to the mixing ratios at different sampling times.

The soil flux (F_{soil}) was then calculated using

$$F_{soil} = \frac{k_{soil} mr_{amb} h M}{V_m} \quad (5.2)$$

with mr_{amb} the average ambient mixing ratio (540 ppt, Khalil and Rasmussen (1999)), h the height of the chamber (27.5 cm), M the molar mass of CH₃Cl (50.49 g mol⁻¹), and V_m the molar volume (24.5 L mol⁻¹). The soil flux is reported in units of $\mu\text{g m}^{-2}\text{h}^{-1}$.

Production of CH₃Cl by leaf litter was assumed to be a zero-order process. At each sampling time, the mixing ratio in the chamber without plant litter was subtracted from the mixing ratio in the chamber with plant litter. The emission rate coefficient k_{leaf} and its uncertainty were derived from a linear least-squares fit through difference in these mixing ratios as function of sampling time. The emission rate ER was then calculated according to

$$ER = \frac{k_{leaf} M V_{chamber}}{A V_m} \quad (5.3)$$

with $V_{chamber}$ the volume of the chamber (78 L). A is either the surface area of the chamber, or the dry weight of the leaf litter. For experiments in which the leaf litter flux was compared to the soil flux, the emission rate was scaled to the surface area of the chamber, which was fully covered with leaf litter, and A is the chamber surface area (0.28 m²). For those experiments, the emission rate is reported in units of $\mu\text{g m}^{-2}\text{h}^{-1}$. However, if a different amount of leaf litter would have been present in the ring, a different flux would be expected. To compare the leaf litter emissions in field and laboratory experiments, the emissions were normalized to the mass of the leaves, and A was the dry mass of the freshly fallen leaf litter. The emission rate is then reported in units of $\text{ng gdw}^{-1}\text{h}^{-1}$. The temperature dependence of the CH₃Cl rate coefficients was quantified by the activation energy (Eq. 2.2)

5.3 Results and discussion

5.3.1 Soil uptake at different locations

The uptake of CH₃Cl was determined by measuring the mixing ratio as a function of sampling time for the different locations (Fig. 5.2). In Moordrecht several experiments were performed, but only one is shown. For the other locations only one experiment was performed. At each location, the soil was a net sink of CH₃Cl. The uptake was indeed a first order process, which is indicated by the good agreement between the measurements and the exponential fit using Eq. 5.1.

Table 5.1 gives an overview of the calculated values for k_{soil} and the other parameters measured at the different locations. The volumetric water content was only deter-

mined during the measurements in the second field experiment and varied between 13.8% at Kromme Rijn and 27.7% in the Botanic garden. The soil temperatures at different depths were variable and depended on the time of year and the location. The largest uptake rate coefficient, and consequently the largest flux ($4.5 \mu\text{g m}^{-2}\text{h}^{-1}$), was observed at the Kromme Rijn. Smaller fluxes were observed during all measurements at the other locations. In Moordrecht the flux varied between 0.5 and $2.2 \mu\text{g m}^{-2}\text{h}^{-1}$ on the different experiment days. The fluxes measured in the Botanic garden and Sandwijck, 1.8 and $1.2 \mu\text{g m}^{-2}\text{h}^{-1}$, respectively, were in the range that was observed in Moordrecht.

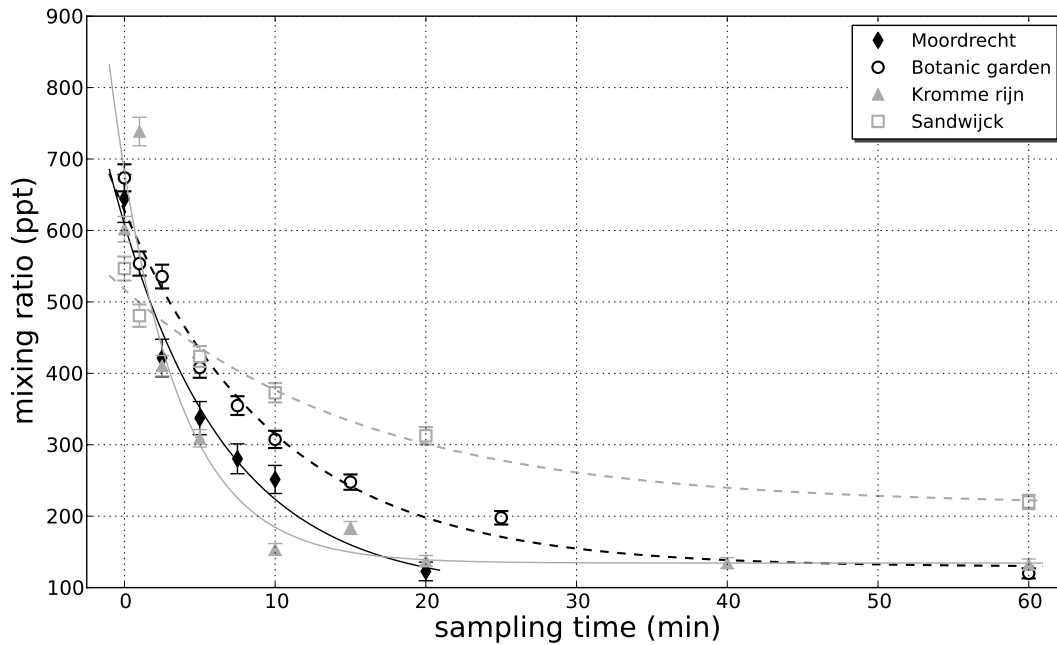


Figure 5.2: Methyl chloride mixing ratio as a function of sampling time at different locations. Markers indicate the measurements, whereas the lines indicate the fit using Eq. 5.1. Note that for Moordrecht several measurement series were performed, but only one is shown in this figure.

Soil fluxes of CH_3Cl have been reported in previous studies. Teh et al. (2009) reported an average CH_3Cl uptake rate of $590 \pm 107 \text{ nmol m}^{-2}\text{d}^{-1}$ for the Arctic region, corresponding to $1.24 \pm 0.23 \mu\text{g m}^{-2}\text{h}^{-1}$. Although their experiments were performed in a colder region, their average flux is in the range of fluxes measured in this study. Rhew and Abel (2007) measured the gross CH_3Cl fluxes for an annual grassland in California using an isotope tracer method. The net fluxes were largely influenced by plant communities. However, since our measurements were performed on bare soil, our fluxes can be compared to their measurements of the gross CH_3Cl uptake. Rhew

Table 5.1: Overview of the measured parameters at the different locations. In the Botanic garden, Kromme Rijn and Sandwijck only one experiment was performed. Uncertainties in k_{soil} and the flux were derived from the uncertainty in the least-squares fit. For Moordrecht more experiments were performed and the range of measured values is reported.

parameter	Moordrecht	Botanic garden	Kromme Rijn	Sandwijck
k_{soil} (min ⁻¹)	0.02 - 0.12	0.10 ± 0.01	0.24 ± 0.6	0.06 ± 0.01
flux (μg m ⁻² h ⁻¹)	0.5 - 2.2	1.8 ± 0.2	4.5 ± 1.0	1.2 ± 0.2
soil moisture (%)	n.d.	27.7	13.8	20.6
T _{soil} (1 cm) (°C)	-1.0 - 17.8	22.7	15.4	18.2
T _{soil} (5 cm) (°C)	-0.2 - 16.6	21.9	14.6	18.1
T _{soil} (10 cm) (°C)	1.2 - 15.9	21.2	14.0	17.8

and Abel (2007) measured gross uptake fluxes up to 617 nmol m⁻²d⁻¹, corresponding to 1.30 μg m⁻²h⁻¹. This is also comparable to our measured fluxes. Methyl chloride fluxes measured by Khalil and Rasmussen (2000) were at the low end of the range observed in our experiments. Based on measurements in Greenland and Brazilian forests, they reported a net uptake of 0.27 – 0.65 μg m⁻²h⁻¹. Only some of the fluxes measured during the experiments in Moordrecht fall within this range. The uptake of CH₃Br by the soil has been measured by Shorter et al. (1995). Since the uptake fluxes of CH₃Cl and CH₃Br for the same soil are often highly correlated (Rhew and Abel, 2007), their CH₃Br measurements have been used to estimate the global soil sink of CH₃Cl in atmospheric models (Lee-Taylor et al., 2001; Yoshida et al., 2004, 2006). The uptake rate coefficients reported by Shorter et al. (1995) vary between 0.042 min⁻¹ for tropical forests and savanna and 0.25 min⁻¹ for temperate forests, woodlands and shrublands. This corresponds well to the range of k_{soil} 's observed in our study (0.02 – 0.24 min⁻¹). In general, our measured fluxes and rate coefficients are in agreement with the published values.

5.3.1.1 The dependence of the CH₃Cl uptake on soil temperature

The uptake of CH₃Cl by soils has been identified as a biological process (Rhew et al., 2003). Because many biological processes are temperature dependent, the uptake rate coefficients were plotted as a function of soil temperature in Fig. 5.3a for all experiments performed in Moordrecht, the Botanic garden, Kromme Rijn, and Sandwijck. The corresponding Arrhenius plot is shown in Fig. 5.3b.

Although this is a limited dataset, there was a general trend towards higher uptake at higher temperatures. The correlation coefficient between k_{soil} and the soil temperature

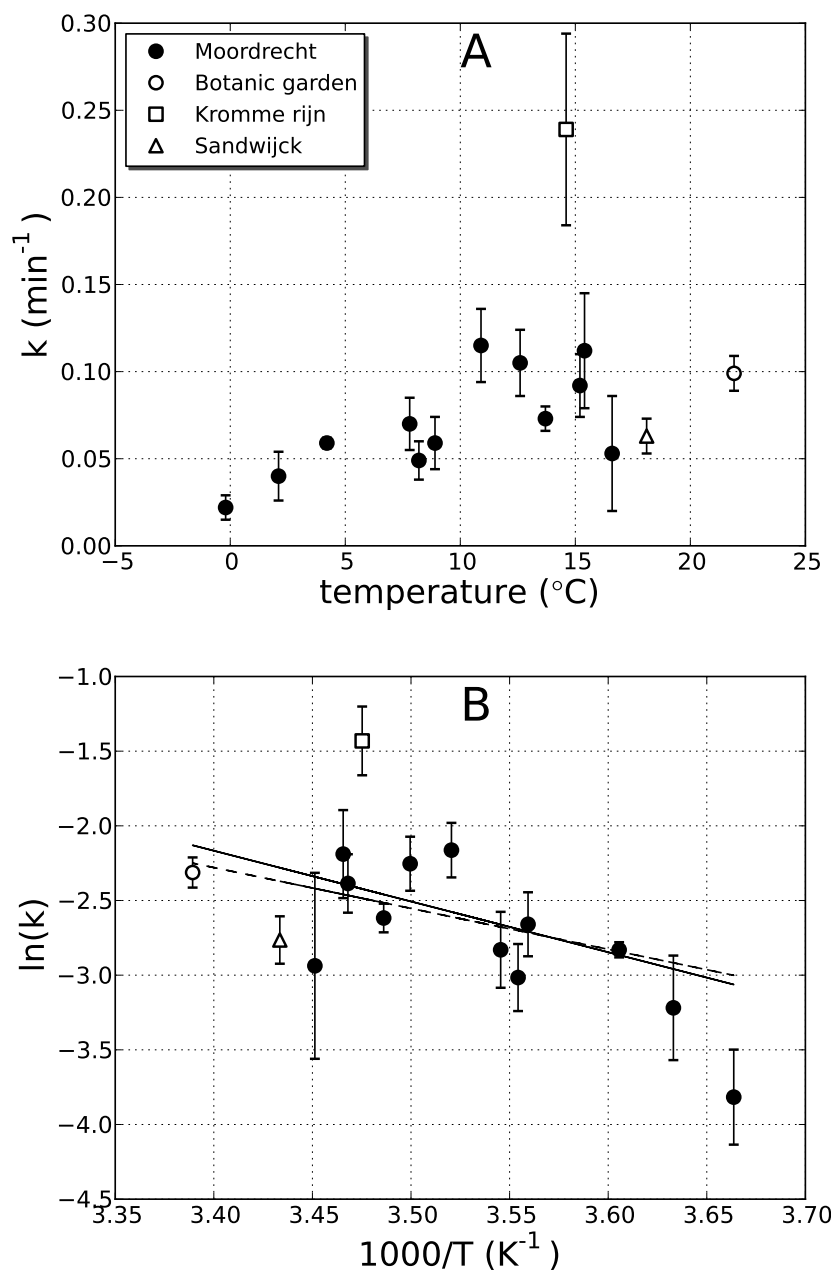


Figure 5.3: (A) Rate coefficients for CH_3Cl uptake by the soil as a function of soil temperature at 5 cm depth for all experiments and (B) the corresponding Arrhenius plot the linear fit through all measurements. Measurements at different locations are indicated by different markers. The dashed line indicates the fit through all data, whereas the solid line is the fit through the measurements performed in Moordrecht

at 5 cm was 0.46. However, this correlation was not statistically significant ($n=15$, $p > 0.05$). The correlation between k_{soil} and the soil temperature at 1 or 10 cm depth was comparable (not shown). However, when only the measurements in Moordrecht were taken into account, the correlation increased to 0.68 ($n=12$, $p < 0.05$), which is statistically significant. The relation between k_{soil} and the soil temperature at 5 cm was described by

$$k_{soil} = (0.0032 \pm 0.0009)T_{5cm} + (0.040 \pm 0.006) \quad (5.4)$$

The activation energy derived from the Arrhenius plot was $22.8 \pm 7.0 \text{ kJ mol}^{-1}$ when all measurements were taken into account, and $28.3 \pm 8.3 \text{ kJ mol}^{-1}$ when only the measurements from Moordrecht were used.

Although larger uptake is observed at higher soil temperatures, temperature is probably not the only factor that determines the uptake rate of CH₃Cl. Teh et al. (2009) concluded that the hydrology of the soil is the main factor that controls the soil flux, whereas temperature only plays a key role in drier ecosystems. They found that the uptake of CH₃Cl was higher when the soil moisture content increased. However, when the soil moisture content was too high, diffusion of air into the soil was limited, and therefore also the uptake of CH₃Cl. A parabolic relation between CH₃Cl uptake and soil moisture was also observed by Rhew et al. (2010). Unfortunately, in our experiments the volumetric water content was only measured during the second experiment series. Since this series consists of only one measurement at each of the locations, no dependence of the uptake on soil moisture could be determined. However, the significant correlation between the CH₃Cl flux and the soil temperature in Moordrecht indicates that for this specific soil the temperature is an important factor.

5.3.2 Methyl chloride emissions from leaf litter

The fluxes of CH₃Cl measured in Moordrecht between September 2010 and January 2011 on bare soil and soil covered with leaf litter are shown in Fig. 5.4 (top). In addition, the CH₃Cl flux from leaf litter, which was derived from the difference between the two soil fluxes, is shown in this figure. Figure 5.4 (middle) shows the soil- and air temperature during the experiment period, whereas the amount of fresh litter fall is shown in the bottom panel. During the whole period of the experiment, the soil flux of CH₃Cl was negative and ranged between -0.5 and $-2.2 \text{ } \mu\text{g m}^{-2}\text{h}^{-1}$. In October, leaf litter emitted CH₃Cl in small amounts. The highest flux of CH₃Cl from leaf litter was $0.6 \pm 0.4 \text{ } \mu\text{g m}^{-2}\text{h}^{-1}$. As a consequence, the net flux was reduced in this period, but remained negative. In the remaining period of the experiment, the flux from leaf litter

was small, or even negative.

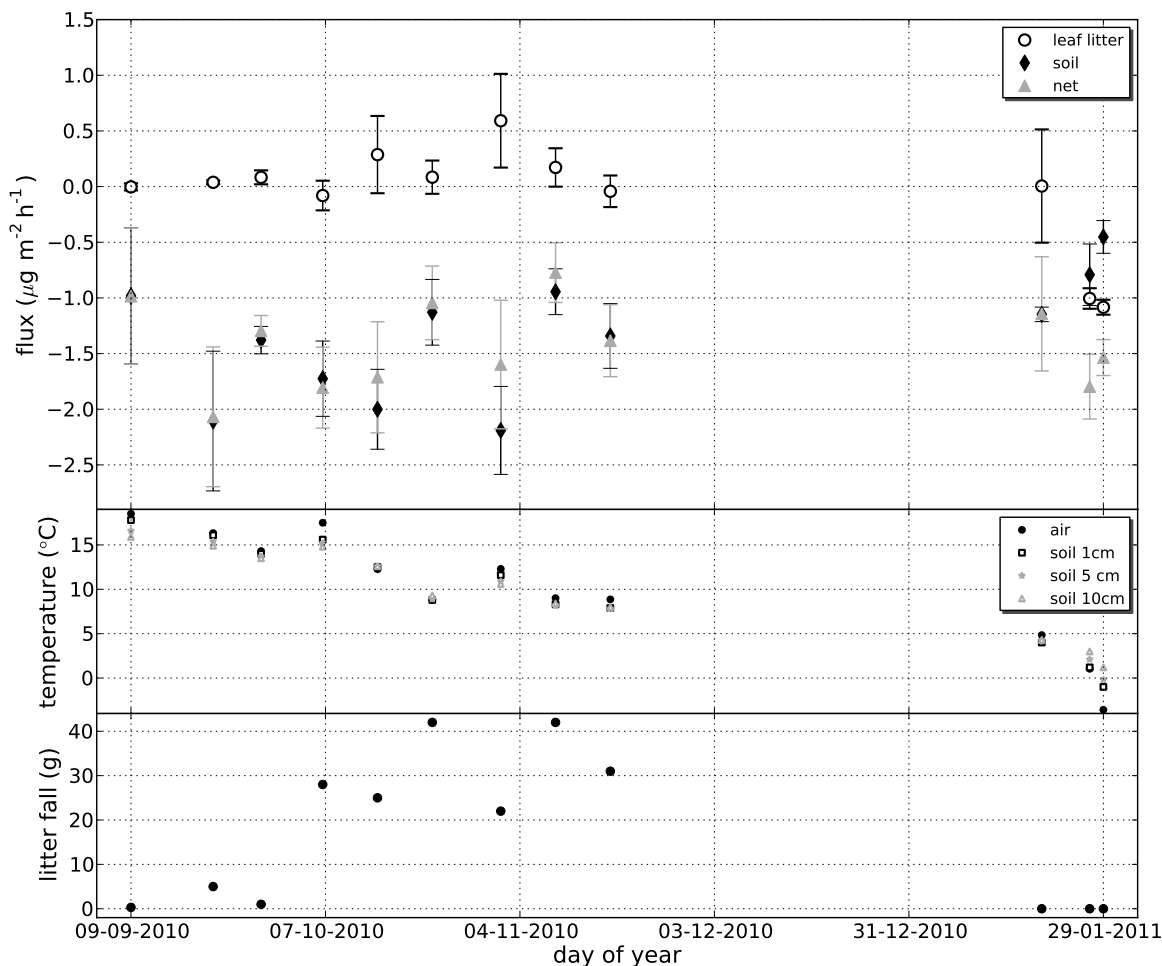


Figure 5.4: Top: net, soil and leaf litter flux of CH_3Cl at different times of the year in Moordrecht. Middle: Air temperature and the soil temperature at different depths. Bottom: The amount of freshly fallen leaf material since the previous experiment day.

Possibly leaf litter is not emitting CH_3Cl , but only reducing the soil uptake by limiting the transport of CH_3Cl towards the soil. Between 15 October and 18 November, the largest amount of fresh leaf litter had fallen. In this period, the litter fall was correlated to the soil uptake flux, but not to the leaf litter flux. This suggests that leaf litter is not emitting CH_3Cl , but only reducing the uptake. However, in September no fresh leaf litter fell, but the soil was covered by a layer of leaf litter from the previous year. This layer did not effect the uptake of CH_3Cl by the soil, and suggests that the fresh leaf litter fallen in October is actually emitting CH_3Cl . In addition, laboratory experiments

(see Sect. 5.3.2.1) indicate that fresh leaf litter collected from the field site has the potential to emit CH₃Cl. To determine whether the leaf litter flux is actually an emission of CH₃Cl by the leaf litter, or only a reduction of the soil uptake due to reduced transport of CH₃Cl into the soil, an isotope tracer technique should be used (Rhew and Abel, 2007; Rhew et al., 2010).

The results of these experiments are similar to the results found by Blei and Heal (2011). For a deciduous forest in Scotland they observed that the flux of CH₃Cl from leaf litter was slightly negative most of the year, except for a period in which the fall of fresh litter was high. In this period a large positive CH₃Cl flux from leaf litter was observed. Averaged over a year, the flux of CH₃Cl from leaf litter was positive in their study. During the period of fresh leaf litter fall, Blei and Heal (2011) observed a CH₃Cl flux of $\sim 10 \mu\text{g kg}^{-1}\text{h}^{-1}$. On a mass basis, the highest CH₃Cl flux from leaf litter in our study was $15 \mu\text{g kg}^{-1}\text{h}^{-1}$ (see Fig. 5.5).

5.3.2.1 Comparison of leaf litter emissions measured in field and laboratory experiments

For a comparison between laboratory and field experiments, CH₃Cl emission rates were measured in the laboratory from leaf litter that was collected during the field experiments. The measurements were performed on both fresh and decayed leaf litter. The emission rates as a function of air temperature are shown in Fig. 5.5. For comparison with the laboratory measurements, the CH₃Cl emissions from leaf litter measured during the field experiments were normalized to the mass of the freshly fallen leaf litter, and are also shown in Fig. 5.5. Only data from experiment days at which fresh leaf litter was fallen were included, because old leaf litter did not emit CH₃Cl in the field.

The laboratory experiments show that fresh leaf litter emits CH₃Cl at much higher rates than decayed leaf litter. At temperatures between 20 and 70°C, the emission rates varied between 0.02 and 0.65 ng gdw⁻¹h⁻¹ for decayed leaf litter, whereas fresh leaf litter emitted 0.17 – 6.1 ng gdw⁻¹h⁻¹. The difference can be explained as follows: during the decomposition of leaf litter, inorganic chlorine is converted to organochlorine (Myneni, 2002; Leri and Myneni, 2010). For the formation of CH₃Cl, inorganic chlorine is required. This may not be available in decayed leaf litter and can explain the decrease in emission rate from fresh to decayed leaf litter. In addition, chloride ions may have leached from the decayed litter, which can also explain the low emissions from decayed leaf litter. The laboratory experiments on fresh and decayed leaf litter are in agreement with our field study, where leaf litter emissions were only observed in periods with fresh litter fall (Fig. 5.4).

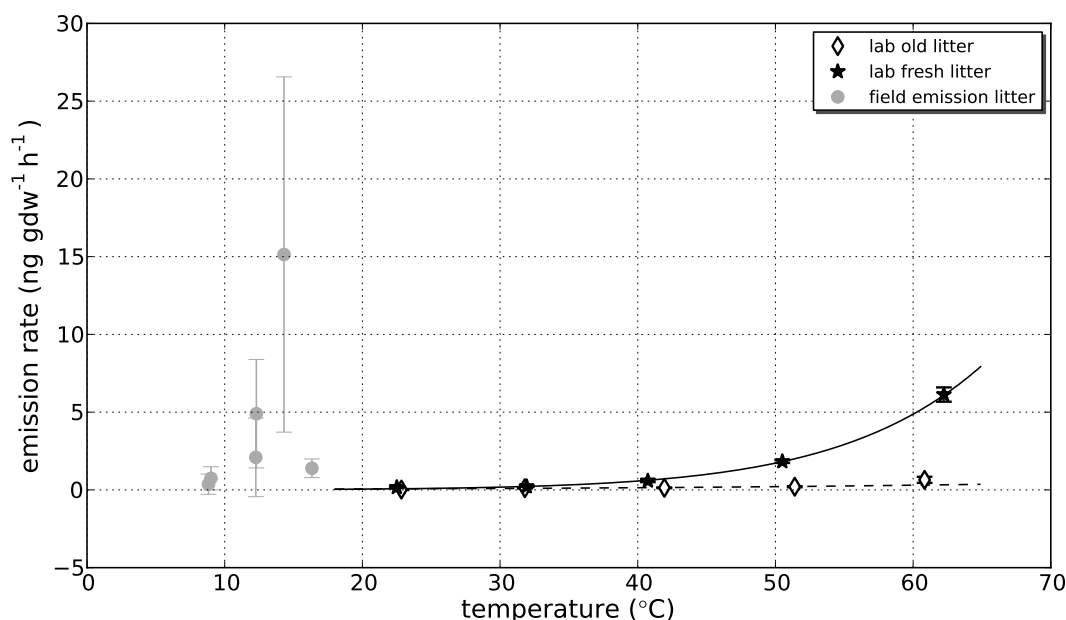


Figure 5.5: Methyl chloride emission rates from leaf litter in laboratory experiments. The lines indicate the fit with the Arrhenius equation (Eq. 2.2). The emission rates measured during the field experiment in Moordrecht on leaf litter of the same plant are also shown.

In the field experiments the CH_3Cl emission rate varied from close to zero up to $15 \pm 11 \text{ ng gdw}^{-1} \text{ h}^{-1}$ for freshly fallen leaf litter. Although the temperature during the field experiments was much lower than in the laboratory experiments, the emission rates measured in the field were higher than for the laboratory experiments where decayed or fresh leaf litter was used. The CH_3Cl emission rates measured in both field and laboratory experiments were normalized to the dry mass of the leaf litter. However, differences in the moisture content of the leaf litter at the time of measurement are expected (for laboratory experiments the leaf litter was first air-dried). This may explain the differences between the field and the laboratory experiments. It should also be kept in mind that the field study consisted of only a limited set of measurements. In addition, the uncertainties of the fluxes were large. Therefore, the experimental method should be improved to reduce these uncertainties and more measurements should be performed to accurately determine the fluxes of CH_3Cl from leaf litter in the field.

In the laboratory experiments the temperature dependence of the emission rates was described by the Arrhenius relation, whereas for the field experiments higher emission rates were observed at higher temperature, but without a clear relation. The labora-

tory experiments also show that fresh leaf litter has the capability to emit CH₃Cl, and suggests that the emissions measured from leaf litter in the field in October are real emissions, and not just a reduction of the uptake of CH₃Cl by the soil (Sect. 5.3.2). Activation energies were derived for the measurements in the laboratory. The activation energy of the CH₃Cl emissions from decayed leaf litter was $42 \pm 12 \text{ kJ mol}^{-1}$, whereas for fresh leaf litter this was $90 \pm 6 \text{ kJ mol}^{-1}$. For the fresh litter the Arrhenius relation better fitted the measurements than for the decayed leaf litter. This was reflected in the relatively high uncertainty in the activation energy for decayed leaf litter compared to fresh leaf litter. The activation energies observed in the laboratory experiments for both fresh and decayed leaf litter are in the low range of the previously observed activation energies (Sect. 4.3.4).

5.4 Conclusions

In this study the deposition flux of CH₃Cl to the soil and the potential emissions from leaf litter have been measured in field experiments. For comparison, the CH₃Cl flux from leaf litter was measured in laboratory experiments. The soil CH₃Cl flux was always negative, indicating that the soil was a net sink of CH₃Cl. The uptake rates of CH₃Cl by the soil varied between 0.5 and $4.5 \mu\text{g m}^{-2}\text{h}^{-1}$, which compared well with previously reported values even though they were measured in different ecosystems. The uptake rate coefficients were positively correlated to temperature, although other factors, e.g. the volumetric water content of the soil, are also expected to influence the uptake rate. Leaf litter emissions were derived from the difference of the CH₃Cl flux between a litter-covered and a litter-free soil. Differences between the two fluxes were observed in autumn during a period with fresh leaf litter fall, which suggests that leaf litter emitted CH₃Cl. However, this flux from leaf litter is small compared to the uptake by the soil, and the net flux is negative during the whole experiment period. Also the flux from leaf litter has a large uncertainty. In periods without fresh leaf litter fall, no emissions of CH₃Cl from leaf litter were observed, i.e. there were no detectable differences between the CH₃Cl fluxes for a soil covered with or without leaf litter. The laboratory experiments showed that there are large differences between CH₃Cl emissions from fresh and decayed leaf litter. In addition, large differences were found between measurements in the laboratory and the field for the same leaf litter. The emission rates of CH₃Cl from leaf litter derived indirectly during field experiments were higher than the directly measured emissions during the laboratory experiments on both fresh and decayed leaf litter. The experiments thus imply that plant litter also emits CH₃Cl in natural environments. To further assess the environmental importance of CH₃Cl emissions from leaf litter, more experiments

are needed to explain the differences between field and laboratory experiments and to determine the factors that cause the variations in the CH_3Cl emission rates. In addition, the experimental method should be improved to reduce the uncertainty of field measurement and to more accurately measure the CH_3Cl fluxes.

CHAPTER 6

METHYL CHLORIDE MODELING: THE IMPORTANCE OF LEAF LITTER EMISSIONS

Emissions of methyl chloride (CH_3Cl) contribute significantly to the destruction of stratospheric ozone and understanding the global budget of CH_3Cl is therefore of great importance. There are several indications that leaf litter emits substantial amounts of CH_3Cl , but global models have not yet taken these emissions into account. In this study, the emission of CH_3Cl from leaf litter was investigated using the global chemistry transport model TM5. Forward simulations with different emission scenarios were performed based on recent findings from the literature concerning leaf litter emissions. These simulations showed that at station Trinidad Head (mid latitudes of North America), a substantial seasonal emission from leaf litter was required to match the measured CH_3Cl mixing ratios at this station. The TM5-4D-Var system was subsequently used to perform several inversions to optimize the CH_3Cl emission estimate using the measurements from surface stations. In the Tropics, both leaf litter and living vegetation emit CH_3Cl and emissions from these sources could not be optimized separately. However, the inversions indicated that the main CH_3Cl sources were located in the Tropics, whereas the mid- and high latitudes were only a minor source. This is in agreement with earlier studies. Sensitivity studies performed to investigate the robustness of the optimized emissions indicated that the net emissions from the tropical regions varied between 3.0 and 3.3 Tg yr^{-1} , which is more than 90% of the global net emissions.

This chapter is based on:

- L. Derendorp, M. C. Krol, T. Röckmann, J. W. Elkins, R. Wang, and M. Maione, *Modeling methyl chloride: the importance of leaf litter emissions*, in preparation.

6.1 Introduction

Although the number of studies that measured CH₃Cl emissions from leaf litter is limited, a simple up-scaling of laboratory experiments indicated that leaf litter may be an important CH₃Cl source (Hamilton et al. (2003); Keppler et al. (2004) and Chapter 4). These experiments also showed that the CH₃Cl emission rate is strongly temperature dependent. Hamilton et al. (2003) also found a strong correlation between the CH₃Cl emission rate and the chloride content of the leaf litter, but this could not be confirmed in the laboratory experiment described in this thesis. In addition, large variations in the CH₃Cl emission rate between different plant species were observed. Methyl chloride emissions from leaf litter have also been detected during field experiments in the tropical rain forests of Borneo (Blei et al., 2010) and in a temperate deciduous forest in Scotland (Blei and Heal, 2011). Because of the large variations between plant species and because the factors that control the emissions are uncertain, the global estimates of leaf litter as a source of CH₃Cl vary largely. For example, Hamilton et al. (2003) estimated the global leaf litter source between 30 and 2500 Gg yr⁻¹, which is a contribution up to 60% of the estimated sink strength.

The potential importance of leaf litter as a source of CH₃Cl is confirmed by isotope studies. Leaf litter is the most depleted known source of CH₃Cl ($\delta^{13}\text{C} = -135\text{‰}$, Keppler et al. (2004)). In order to balance the strong ¹³C kinetic isotope effect in the removal of CH₃Cl (Gola et al., 2005), a significant fraction of CH₃Cl from the depleted leaf litter source is required to balance the isotope budget (Keppler et al., 2005; Saito and Yokouchi, 2008). Yet, recent global CH₃Cl modeling studies performed by Lee-Taylor et al. (2001), Yoshida et al. (2004, 2006) and Xiao et al. (2010) have not taken into account the emissions from leaf litter. However, these model studies showed that the Tropics are a strong source of CH₃Cl. Lee-Taylor et al. (2001) used a three-dimensional model and found that the observed CH₃Cl mixing ratios and latitudinal distribution were best reproduced when a tropical terrestrial source of 2330-2430 Gg yr⁻¹ was included in the model. They also noted that the mixing ratios at remote sites where most measurements are carried out were relatively insensitive to the precise parametrization of the tropical source. Yoshida et al. (2004) concluded that an even larger tropical source was required to match the observations, and estimated a biogenic tropical emission of 2900 Gg yr⁻¹. Inverse modeling studies were performed by Yoshida et al. (2006) and Xiao et al. (2010) in which methyl chloride emission estimates were optimized using the available surface and aircraft measurements of the CH₃Cl mixing ratios. These studies confirmed the importance of the tropical regions and estimated terrestrial biogenic CH₃Cl emissions of 2500 and 2200 Gg yr⁻¹, respectively, for the Tropics.

To date, there are still substantial uncertainties in the understanding of the atmospheric

CH₃Cl budget. Until a few years ago only half to two-thirds of the estimated CH₃Cl sinks ($\sim 4000 \text{ Gg yr}^{-1}$) could be balanced by known sources of CH₃Cl (Butler, 2000; Graedel and Keene, 1995; Keene et al., 1999). In recent years, additional sources, mainly natural, have been identified that can balance or even outweigh the total global sink strength (Keppler et al., 2005; Saito and Yokouchi, 2008; World Meteorological Organization, 2010). However, it remains uncertain which sources are most important for the atmospheric budget and which parameters control the emissions. The main sink for CH₃Cl is oxidation by the hydroxyl (OH) radical in the troposphere, but also the soil may be a significant sink of CH₃Cl (Khalil and Rasmussen, 2000; Keppler et al., 2005; Rhew et al., 2010). Known sources of CH₃Cl include tropical plants (Yokouchi et al., 2002, 2007), biomass burning (Lobert et al., 1999), industry (McCulloch et al., 1999), wood rotting fungi (Harper, 1985; Anke and Weber, 2006), oceans (Moore, 2000; Ooki et al., 2010), salt marshes (Rhew et al., 2000; Rhew and Mazéas, 2010), soil (Keppler et al., 2000), rice paddies (Khan et al., 2011; Redeker et al., 2000) and leaf litter (Hamilton et al. (2003); Keppler et al. (2004) and Chapter 4). The leaf litter source and the soil sink are already described in Chapter 4 and 5. The other sources and sinks of CH₃Cl are described below.

6.1.1 Biomass burning

Methyl chloride is formed during the smoldering phase of biomass burning, which is characterized by the insufficient availability of oxygen (Blake et al., 1996). Carbon monoxide is formed during the same combustion phase, and consequently high correlations between CH₃Cl and CO emissions are observed during biomass burning. Because CO emissions from biomass burning are more often measured and better quantified, global estimates for CH₃Cl emissions from biomass burning are often based on a measured CH₃Cl/CO ratio, and emission estimates for CO. Alternatively, global CH₃Cl emission estimates are based on the chlorine content of plant material, but the disadvantage of this method is that the burning efficiency is not taken into account. In addition, the amount of studies that measured the chlorine content is limited, and therefore the chlorine content of plant material is uncertain (Lobert et al., 1999). The emission of CH₃Cl from biomass burning contributes significantly to the global CH₃Cl budget. Estimates for the global source of CH₃Cl from biomass burning range between 550 and 900 Gg yr⁻¹ (Lobert et al., 1999; Yoshida et al., 2006; Xiao et al., 2010).

6.1.2 Tropical vegetation

For many years the known sources of CH₃Cl were smaller than the identified sinks. The missing source was expected to be in the Tropics, because this would explain the uniform distribution of CH₃Cl between the northern and southern hemisphere, despite their differences ocean and land area. In 2000, Yokouchi et al. (2000) investigated the seasonality of CH₃Cl sources and sinks in Japan, Canada, the Arctic, and the northwest Pacific Ocean and found evidence that there are significant CH₃Cl emissions from warm coastal lands, particularly tropical islands. During calm nights, mixing ratios were enhanced up to 1500 ppt, which is ~ 3 times the average ambient mixing ratio. In addition, the CH₃Cl concentrations were closely correlated to those biogenic compounds that were emitted by terrestrial plants (e.g. α -pinene). In 2002 several plant species that are able to release CH₃Cl have been identified. Plants belonging to the *Dipterocarpaceae*, *Marattiaceae*, *Cyatheaceae* and *Dicksoniaceae*, common tropical plant families, are responsible for significant CH₃Cl emissions (Yokouchi et al., 2002). Five years later, more CH₃Cl emitting families were identified. Yokouchi et al. (2007) investigated 187 tropical and subtropical plant species on Iriomote Island (Japan) and found 33 species that were able to emit CH₃Cl.

Several studies estimated the annual emission of CH₃Cl from tropical forests. Scheeren et al. (2003) performed measurements of the CH₃Cl mixing ratio during an aircraft campaign above the Surinam tropical rainforest in 1998 and reported mixing ratios between 550 and 700 ppt close to the surface. Gebhardt et al. (2008) measured CH₃Cl mixing ratios during an aircraft campaign in the same region in October 2005. High mixing ratios (>700 ppt) were observed near the ground which decreased with altitude. In addition, a high CH₃Cl/CO ratio was observed, indicating that biomass burning was not the main source. Gebhardt et al. (2008) found a positive correlation between the CH₃Cl mixing ratio and the time spent over land. A global net flux of $1.5 \pm 0.6 \text{ Tg yr}^{-1}$ was estimated for the tropical regions based on their measurements. This is low compared to tropical emissions estimated in modeling studies (2.2 and 2.9 Tg yr^{-1} , Yoshida et al. (2004, 2006); Xiao et al. (2010)).

Isotopes may be used to constrain the tropical source of CH₃Cl, because the isotopic ratio of CH₃Cl emitted by tropical vegetation is lower than that of CH₃Cl produced by the other known sources, with the exception of dead leaves. For CH₃Cl emitted by two tropical ferns, $\delta^{13}\text{C}$ values of -72.4 ± 1.4 and -69.3 ± 0.9 ‰ have been measured, which is a depletion of 42.3 and 43.4 ‰ compared to bulk biomass (Harper et al., 2003). In addition, the stable carbon isotope ratios of CH₃Cl were measured in foliar emissions from 14 tropical plant species by Saito and Yokouchi (2008) and an average $\delta^{13}\text{C}$ value of -83 ‰ was found.

Although tropical rain forests contribute significantly to the global emission of CH_3Cl , the factors controlling the emission rate of CH_3Cl are largely unknown (Saito and Yokouchi, 2006). Large intraspecies variability is observed, in addition to differences between young and mature plants (Yokouchi et al., 2002, 2007). Methyl halides are likely synthesized in plant cells through enzymatic transfer of a methyl group from S-adenosyl-L-methionine (SAM) to halides (Saito and Yokouchi (2006) and the references therein) by methyl transferases. Methyl transferase activity is considered to be temperature dependent. Methyl chloride fluxes have been measured by Blei et al. (2010) in a lowland tropical rain forest in Malaysian Borneo. The plants were mainly from the *Dipterocarpaceae* and the dominant factor determining the CH_3Cl flux from live plants was plant species. The emission of CH_3Cl represents only a small proportion of the halogen content, so it is likely that variation in the expression of the methyl transferase enzyme in a particular plant species will drive the variation in CH_3Cl flux, at least as much as intrinsic variation of tissue halogen content (Blei et al., 2010).

6.1.3 Ocean

The oceans play a significant role in the natural cycle of CH_3Cl and can present both a source and a sink. In case the CH_3Cl partial pressure in the atmosphere is larger than the saturation pressure in seawater, there is a net flux of CH_3Cl from the atmosphere to the ocean, and vice versa. In cold waters at high latitudes, CH_3Cl is taken up by the oceans, whereas in warm tropical waters the CH_3Cl flux is directed from the ocean towards the atmosphere (Moore, 2000; Khalil et al., 1999). Based on measurements of the CH_3Cl concentration in the atmosphere and the ocean and the solubility of CH_3Cl in seawater, Moore (2000) estimated the net flux of CH_3Cl from the ocean to the atmosphere at $300 - 400 \text{ Gg yr}^{-1}$, whereas Khalil et al. (1999) estimated the net flux at 655 Gg yr^{-1} .

Ooki et al. (2010) performed a study on the CH_3Cl flux between the ocean and the atmosphere in the subarctic and subtropical regions of the Pacific Ocean. In the northern transition waters, which have high biological activity, the levels of CH_3Cl were high. Biological production of CH_3Cl is caused by macroalgae, cyanobacteria or phytoplankton (Brownell et al., 2010; Smythe-Wright et al., 2010). CH_3Cl can also be produced in seawater through abiotic pathways. Nucleophilic substitution of CH_3Br or CH_3I by the chloride ion results in the formation of CH_3Cl . In addition, methyl chloride can be photochemically produced from colored dissolved organic compounds (Elliott and Rowland (1993); Moore (2008); Butler (1994)).

6.1.4 Fungi

The main structural components of wood are cellulose, hemi-cellulose and lignin. Especially the lignin fraction of the wood is hard to decompose due to its complex chemical structure. White rot fungi are the only fungi that are able to decompose this lignin fraction into water and CO₂, because they possess special enzymes. The activity of those enzymes depends on the presence of certain small molecules, of which the synthesis depends on the presence of CH₃Cl. White rot fungi are able to produce this CH₃Cl. During the initial fungal growth phase, CH₃Cl that is synthesized by the fungi is directly utilized, but in later growth phases, certain genera of white rots (*Phellinus* and *Inonotus*) release excess quantities of CH₃Cl into the atmosphere (Watling and Harper, 1998; Harper, 1985; Anke and Weber, 2006).

The global emission of CH₃Cl by fungi depends on (1) the amount of woody tissue that is annually decomposed by white rot fungi, (2) the chloride content of wood, (3) the global abundance of CH₃Cl releasing fungal species and (4) the mean percentage conversion of Cl⁻ to CH₃Cl by each group of CH₃Cl producing fungi. Although highly uncertain, the global emission of CH₃Cl by fungi is estimated at 160 Gg yr⁻¹ (Watling and Harper, 1998). Khalil et al. (1999) also estimated the uncertainty and found a range of 42 - 470 Gg yr⁻¹.

6.1.5 Salt marshes

Coastal salt marshes are a potentially significant source of CH₃Cl to the atmosphere due to the significant abundance of organic matter and free halides in these areas. However, a wide range of emission rates has been reported for different geographic locations. Outside the Tropics, salt marshes may be the largest natural terrestrial source of CH₃Cl (Rhew and Mazéas, 2010).

Rhew et al. (2000) estimated the global flux of CH₃Cl from salt marshes at 170 Gg yr⁻¹, whereas Manley et al. (2006) estimated this flux between 49 and 160 Gg yr⁻¹. Uncertainty in the global emission estimate for salt marshes is partly caused by an uncertainty of ~50% in the estimated global salt marsh area.

6.1.6 Wetlands, peatlands and rice paddies

Temperate wetlands and peatlands are among the established natural sources of CH₃Cl (Dimmer et al., 2001; Hardacre et al., 2009). Also rice paddies, inland wetlands covering ~ 1% of the global land area, are emitters of CH₃Cl (Redeker et al., 2000; Khan et al.,

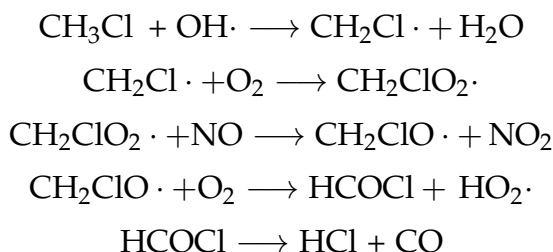
2011). The global annual CH_3Cl flux from peatland ecosystems was estimated at 5.5 (0.9–43.4) Gg yr^{-1} (Dimmer et al., 2001). Whether tundras are a net source or sink of CH_3Cl is unclear. Rhew and Abel (2007) estimated a net global uptake of 11.2 Gg yr^{-1} by all tundras, whereas Hardacre et al. (2009) observed a small net production of CH_3Cl for the Swedish arctic region.

6.1.7 Anthropogenic sources

Methyl chloride emissions due to anthropogenic activity only have a small contribution in the global CH_3Cl budget. Methyl chloride is released during the incineration of municipal and industrial waste. The source of chlorine for these emissions is combustible plastics, mainly polyvinyl chloride (PVC) (Graedel and Keene, 1995). In addition, CH_3Cl is released during the combustion of coal for industrial processes or power and heat generation. The global emission of CH_3Cl due to anthropogenic activities is estimated at 162 Gg yr^{-1} (McCulloch et al., 1999).

6.1.8 Oxidation by the OH radical

The main atmospheric sink of CH_3Cl is oxidation by the OH radical (3.2 Tg yr^{-1} , Kepler et al. (2005)). The oxidation of CH_3Cl results in the formation of formyl chloride (HCOCl), which subsequently decomposes to CO and HCl (Graedel and Keene, 1995):



The reaction between OH and CH_3Cl has a large ^{13}C kinetic isotope effect of 1.059 ± 0.008 (Gola et al., 2005). Because of this large isotope effect, a highly depleted source of CH_3Cl , like leaf litter, is required to balance the atmospheric CH_3Cl isotope budget.

6.1.9 Goal

The goal of this study was to investigate the environmental importance of leaf litter as a source of CH_3Cl using a global chemistry transport model. First, different CH_3Cl

emission scenarios were constructed and the impact of changing individual source and sink contributions on the modeled CH₃Cl mixing ratio distribution was studied. The modeled mixing ratios were then compared to measurements of the CH₃Cl mixing ratio at different surface stations. Based on these simulations, a prior estimate of the global CH₃Cl emissions was derived. This prior emission estimate was further optimized in an inverse modeling framework to obtain a global CH₃Cl emission estimate that was in optimal agreement with the available CH₃Cl surface measurements.

6.2 Methods

6.2.1 The model

The global chemistry transport model TM5 as described by Krol et al. (2005) was adjusted to include CH₃Cl emissions and removal processes. Forward simulations with monthly varying estimates of CH₃Cl emissions were used to simulate mixing ratios for the year 2005. The model has a 6x4° horizontal resolution, 25 vertical layers and a time step of 1 h was used. Meteorological fields from the European Centre for Medium-Range Weather Forecasts (ECMWF) were used to drive the model.

To optimize the monthly CH₃Cl emission estimates, the four dimensional variational data assimilation system (TM5-4D-Var) first described by Meirink et al. (2008) was used and adjusted for CH₃Cl. The emissions were optimized between December 2004 and February 2006, but only the results for 2005 were analyzed. Observations from January and February 2006 were used to constrain the emissions at the end of 2005. A spin-up month (December 2004) was used, because the initial mixing ratio field was not optimized in the inversion. This initial mixing ratio field was derived from a forward simulation with the prior emission estimate. The net emissions were optimized on the model grid and then aggregated over larger geographical regions. A prior grid scale uncertainty of 100% of the emission was used. The horizontal spatial correlation length of the emissions was set at 1000 km, whereas temporal correlation lengths of 1 and 9.5 months were used for different source categories (see Sect. 6.2.4). These correlation lengths lead to a correlation coefficient of 0.37 and 0.90, respectively, from month to month. These correlations were used to reduce the effective number of emission parameters in the optimization (Meirink et al., 2008). Without these correlations, the number of free parameters (15x2700x2) would largely exceed the number observations (2700 for the whole period).

The main atmospheric sink of CH₃Cl is oxidation by the OH radical. The temperature dependence of the rate coefficient as described by Sander et al. (2003) was used in the

model. The reaction between CH_3Cl and OH is a first order reaction and depends on the CH_3Cl mixing ratio. Therefore, the removal of CH_3Cl was calculated each model time step using a monthly OH climatology (Spivakovsky et al., 2000), which was scaled by a factor 0.92 based on methyl chloroform simulations (Huijnen et al., 2010). In the inversions, the OH field was not optimized to keep the model linear. To test the sensitivity of the optimized emissions to the OH climatology, inversions were performed with an OH field derived from a full chemistry simulation with the TM5 model (Huijnen et al., 2010). This TM5 OH field has a lower OH concentration above the terrestrial tropical areas, especially over South America.

The uptake of CH_3Cl by the soil is a potentially important sink of CH_3Cl (e.g. Khalil and Rasmussen (2000) and Rhew et al. (2003)). Soil uptake of CH_3Cl is also a first order process and therefore depends on the local atmospheric mixing ratio. In the forward simulations, the uptake of CH_3Cl by the soil was calculated at each model time step using the deposition module as described by Ganzeveld et al. (1998). This module calculates the deposition of CH_3Cl as a function of several resistances (Wesely, 1989). The total uptake of CH_3Cl by the soil could be varied by changing the soil resistance parameter. For the inversions, the soil uptake was optimized as a negative emission of which the monthly distribution was derived from a forward simulation with the deposition module. Although this procedure is different from a first order loss process, it was verified that the difference between a simulation with the deposition module or a simulation with the soil as a negative emission was less than 1% in the modeled mixing ratios. Production of CH_3Cl in the soil as reported by Keppler et al. (2000) was not included in the model. The global annual uptake of CH_3Cl by the soil is shown in Fig. 6.3.

6.2.2 Sources

For each CH_3Cl source, a global distribution was constructed based on literature and available databases, as detailed in the following subsections. A scaling factor was then used to vary the strength of each source in different model simulations. The total emission of CH_3Cl was set to 4000 Gg yr^{-1} . Estimates of the CH_3Cl emission from biomass burning, ocean, fungi, salt marshes, wetlands and anthropogenic sources, 1772 Gg yr^{-1} in total, are shown in Table 6.1. The remaining CH_3Cl emissions (2228 Gg yr^{-1}) were divided between the leaf litter and the tropical living vegetation source. Saito and Yokouchi (2008) estimated, based on the isotopic signature of both sources, that living vegetation contributes 50 - 70% of the total tropical emissions, whereas leaf litter contributes the other 30 - 50%. In our initial emission scenario the ratio of the emissions from leaf litter and living tropical vegetation was chosen at 40:60, but the sensitivity

of the modeled mixing ratios to this ratio was investigated (see Sect. 6.2.4). Details of the global distribution of the sources are described below. For some large sources the global distribution of the annual CH₃Cl emission is shown in Fig 6.3.

Table 6.1: Overview of the strength (Gg yr⁻¹) of the sources used in the model for the initial emission scenario.

source	strength
Leaf litter	891
Tropical vegetation	1337
Biomass burning	560 ^a
Fungi	163 ^b
Salt marshes	170 ^c
Wetlands	49 ^d
Anthropogenic sources	162 ^e
Ocean	668 ^f
Total emission	4000

^a for 2005, see Sect. 6.2.2.3

^b Watling and Harper (1998)

^c Rhew et al. (2000)

^d Keppler et al. (2005)

^e McCulloch et al. (1999)

^f Khalil and Rasmussen (1999)

6.2.2.1 Leaf litter

Laboratory studies have shown that CH₃Cl emissions from leaf litter depend on temperature and the amount of available leaf litter (Hamilton et al. (2003); Keppler et al. (2004) and Chapter 4). In addition, strong variations of the emission rates between plant species have been observed, but the cause of these variations is not well understood. In the model, the leaf litter emissions depend on temperature according to the Arrhenius relation, in which an activation energy of 100 kJ mol⁻¹ was used (Chapter 4). In absence of systematic information on the differences in emissions between plant species, the emissions were equally distributed over all plant species, i.e. a uniform pre-exponential factor in the Arrhenius relation was used. Monthly leaf litter emissions were then calculated using monthly mean surface temperature fields (ECMWF). The emissions were scaled with the plant litter production rates for different vegetation types as reported by Matthews (1997). Estimates of the fine litter production were

used to estimate the leaf litter production for each vegetation type. For the Tropics the litter production was assumed to be constant throughout the year. For the mid- and high latitudes it was assumed that the production of leaf litter is maximum in October and March for the Northern- and Southern Hemisphere, respectively, and exponentially decaying in time. Exponential decay timescales of 1 and 4.5 months were used in different simulations. It should be noted that the division between the mid latitudes and Tropics locally leads to large gradients in the modeled plant litter emissions in October. The timing of the CH_3Cl emissions from leaf litter for the mid latitudes is in agreement with a field experiment of Blei and Heal (2011), who observed in a forest in Scotland a large emission peak in autumn, whereas during the rest of the year the emissions were small or small uptake was observed. At high latitudes, the leaf litter emissions were very small compared to the mid latitudes due to the low temperatures and low litter production rates.

6.2.2.2 Living tropical vegetation

Estimates of the global annual emission of CH_3Cl from tropical vegetation vary between 910 and 2900 Gg yr^{-1} (Keppler et al., 2005; Yoshida et al., 2004), but similar to the emissions from leaf litter, the factors that control the CH_3Cl emissions from living vegetation are uncertain. Two distributions for the emission of CH_3Cl from living tropical vegetation were investigated. First, the emissions were uniformly distributed over the tropical evergreen rainforest, mangroves, (sub)tropical evergreen seasonal broadleaved forest and the subtropical evergreen forests (vegetation classes 1, 2 and 3 from Matthews (1997)). In the second distribution, the living vegetation emissions were scaled with the leaf area index (LAI, ECMWF) of the ecosystems. In addition, the emissions from living vegetation were distributed over a larger area by including the vegetation classes 4, 9, 13 and 15 from Matthews (1997), which are mainly located in the Tropics. Consequently, the area on which living vegetation emits CH_3Cl was increased from $17 \times 10^{12} \text{ m}^2$ for the uniform distribution to $29 \times 10^{12} \text{ m}^2$ for the distribution scaled with LAI. No seasonal cycle in the CH_3Cl emission from living tropical vegetation was applied.

6.2.2.3 Biomass burning

Methyl chloride and carbon monoxide (CO) are formed during the same combustion phase and a high correlation between CO and CH_3Cl emissions from biomass burning has been observed (Lobert et al., 1999). Lobert et al. (1999) also noted that because CO emissions are more often measured and better quantified, estimates for CH_3Cl emis-

sions from biomass burning can be based on a measured CH₃Cl:CO ratio, and emission estimates for CO. In addition, methyl chloride emissions depend on the chlorine content of the burnt plant material.

In the model, the emission of CH₃Cl was estimated based on the monthly emission estimate for CO from biomass burning from the GFED3.1 database for 2005 (Van der Werf et al., 2010). To account for variations in the chlorine content of vegetation in different geographical regions, different scaling factors (CH₃Cl:CO ratios) were used for different regions (Table 6.2). When applying these scaling factors to the GFED3.1 database, the global emission of CH₃Cl from biomass burning was scaled to 560 Gg yr⁻¹, which is within the range 545 - 611 Gg yr⁻¹ estimated by Yoshida et al. (2004, 2006).

Table 6.2: *Scaling factors (ppb/ppb) for the conversion of CO emissions from biomass burning to CH₃Cl emissions for different geographical regions.*

region	factor ($\times 10^{-3}$)
South America ^a	0.85
Africa ^b	0.67
India and South East Asia ^c	1.74
Australia ^d	1.74
North America and other regions ^b	0.20

^a Blake et al. (1996)

^b Lobert et al. (1999)

^c Scheeren et al. (2002)

^d Australia is dominated by Eucalyptus trees, which have a high chlorine content (Watling and Harper, 1998). Therefore, the same factor as for India and South East Asia is used.

6.2.2.4 Other sources of CH₃Cl

White rot fungi release CH₃Cl during the decomposition of wood. The global emission depends on the amount of wood that is decomposed, the chlorine content of the wood, and the availability of fungi that are able to decompose the wood. The fungal emissions were calculated as outlined by Watling and Harper (1998) and Khalil et al. (1999). Salt marshes are a source of CH₃Cl to the atmosphere due to the high abundance of organic matter and free halides in these areas. The emission of CH₃Cl from the salt marshes was uniformly distributed over all salt marsh areas (GGHYDRO hydrological database (Cogley, 2003)). The ocean is both a source and a sink of CH₃Cl. In cold waters CH₃Cl is taken up by the ocean, whereas warm waters are a net source

of CH_3Cl . The oceanic flux of CH_3Cl as reported by the Reactive Chlorine Emission Inventory (RCEI) was used in the model (Khalil et al., 1999). The anthropogenic emission of CH_3Cl due to industrial processes and waste incineration was also taken from the RCEI (McCulloch et al., 1999). Wetlands are a minor source of CH_3Cl (Keppler et al., 2005) and the emissions from wetlands were uniformly distributed over all wetland areas. The wetland area was derived from the NASA-GISS wetland ecosystem dataset in combination with the fractional inundation dataset (Matthews and Fung, 1987; Matthews, 1989). No seasonality was applied to the emissions from fungi, salt marshes, ocean, wetlands and the anthropogenic sources.

6.2.3 Observations

6.2.3.1 Surface stations

Flask measurements were performed by the National Oceanic and Atmospheric Administration, Earth System Research Laboratory (NOAA/ESRL) with a frequency varying from a few times per year up to once a week. In addition, continuous high frequency measurements of the atmospheric CH_3Cl mixing ratio have been performed by NOAA/ESRL and the Advanced Global Atmospheric Gases Experiment (AGAGE) network at several stations. At each station, the high frequency measurements that were performed between 12 and 15 h local time were averaged to calculate daily CH_3Cl mixing ratios during relatively well mixed afternoon conditions. Averaging of the continuous measurements also created a balance between the amount of flask and continuous measurements. Three hourly CH_3Cl mixing ratio were measured at Mount Cimone (Italy), an AGAGE affiliated station, by the University of Urbino (Urbino), and monthly mean mixing ratios were reported by the National Institute for Environmental Studies (NIES) for Hateruma Island (Japan). The measurements from Mount Cimone and Hateruma Island were not used in the base inversion, but used for validation or sensitivity studies. Different measurement scales were used by the networks and the calibration factors as reported by Xiao et al. (2010) were applied to the measurements. An overview of the measurement stations is given in Table 6.3 and the location of the stations is plotted in Fig. 6.4.

6.2.3.2 Aircraft and ship measurements

The number of station measurements is limited, especially in the tropical regions, where the largest emissions are located. Therefore, measurements from aircraft and ship campaigns that were performed in this region have been used to validate the

CHAPTER 6. MODELING THE CH₃CL BUDGET

Table 6.3: Overview of the surface stations where CH₃Cl was measured in 2005 and that were used in this study.

station	ID	latitude (°N)	longitude (°E)	altitude (m)	network	flask/continuous
Barrow, Alaska, USA	BRW	71.32	-156.60	11	NOAA/ESRL	continuous
Cape Grim, Tasmania, Australia	CGO	-40.68	144.69	94	AGAGE	continuous
Jungfraujoch, Switzerland	JFJ	46.55	7.99	3580	AGAGE	continuous
Mace Head, Ireland	MHD	53.33	-9.90	5	AGAGE	continuous
Mauna Loa, USA	MLO	19.54	-155.58	3397	NOAA/ESRL	continuous
Niwot Ridge, Colorado, USA	NWR	40.04	-105.54	3523	NOAA/ESRL	continuous
Ragged Point, Barbados	RPB	13.17	-59.43	45	AGAGE	continuous
Tutuila, American Samoa, USA	SMO	-14.24	-170.57	42	NOAA/ESRL	continuous
South Pole, Antarctica, USA	SPO	-89.98	-24.80	2810	NOAA/ESRL	continuous
Trinidad Head, USA	THD	41.05	-124.15	107	AGAGE	continuous
Ny-Alesund, Svalbard	ZEP	78.91	11.88	474	AGAGE	continuous
Mount Cimone, Italy	MTE	44.12	10.42	2165	Urbino	continuous
Alert, Nunavut, Canada	ALT	82.45	-62.52	210	NOAA/ESRL	flask
Harvard Forest, (USA)	HFM	42.90	-72.30	340	NOAA/ESRL	flask
Cape Kumukahi, Hawaii	KUM	19.52	-154.82	3	NOAA/ESRL	flask
Park falls, USA	LEF	45.92	-90.27	868	NOAA/ESRL	flask
Palmer station, USA	PSA	-64.92	-64.00	10	NOAA/ESRL	flask
Summit, Denmark	SUM	72.58	-38.48	3238	NOAA/ESRL	flask
Tierra del Fuego	TDF	-54.87	-68.48	20	NOAA/ESRL	flask
Hateruma Island, Japan	HAT	24.05	123.82	10	NIES	flask

optimized emission estimate from the inversion. Aircraft measurements performed by the National Aeronautics and Space Administration's (NASA) Global Tropospheric Experiment (GTE) and ship cruise measurements from NOAA/ESRL were used. An overview of the campaigns is shown in Table 6.4. These campaigns were not performed in 2005 and a direct comparison with the measurements is difficult due to e.g. varying meteorological conditions in different years. Also antropogenic emissions may have increased throughout the years, but this is only a small (162 Gg yr^{-1}) CH₃Cl source (Table 6.1). The measurements were compared to the modeled mixing ratios at the same location (longitude, latitude, altitude) and time of year and then averaged per altitude and geographical region.

6.2.4 Emission scenarios for the forward simulations

Forward simulations with different CH₃Cl emission scenarios were performed to investigate the influence on the simulated mixing ratios. First, the spatial distribution of the emissions from living tropical vegetation was varied. Instead of a uniform distribution of the emissions over the tropical rainforest, the emissions were scaled with the

Table 6.4: Overview of the aircraft and ship campaigns that were used for the validation of the inversion results.

aircraft			cruise		
campaign	region	year	campaign	region	year
PEM-Tropics A	tropical Pacific	1996	BLAST-I	Pacific Ocean	1994
PEM-Tropics B	tropical Pacific	1999	BLAST-II	Atlantic Ocean	1994
TRACE-A	tropical Atlantic	1992	GasEx 98	Atlantic/east Pacific Ocean	1998
TRACE-P	western Pacific	2001			
PEM-West A	western Pacific	1991			
PEM-West B	western Pacific	1994			
ABLE-2A	South America	1985			

LAI and distributed over a larger vegetated area (Sect. 6.2.2.2). Second, the strength of the soil sink was increased from $\sim 650 \text{ Gg yr}^{-1}$ to $\sim 1350 \text{ Gg yr}^{-1}$, based on estimates by Keppler et al. (2005). To keep the net emissions comparable to the other simulations, the increase of the soil sink was compensated by an increase of the emissions from leaf litter and living tropical vegetation. Third, the ratio of the emissions from leaf litter and living tropical vegetation was changed from 40:60 to 0:100 (no leaf litter) and 80:20. Last, the timing of the CH_3Cl emissions from the leaf litter source on the mid- and high latitudes was varied by using leaf litter decay timescales of 4.5 and 1 month (Sect. 6.2.2.1). An overview of the emission scenarios is given in Table 6.5.

Table 6.5: Overview of the emission scenarios for the forward simulations. Decay timescale is the exponential timescale at which leaf litter production at mid- and high latitudes decreases in time. Tropical distribution indicates whether the emissions from living tropical vegetation were uniformly distributed or scaled with the leaf area index.

simulation	soil sink (Gg yr^{-1})	ratio leaf litter:living vegetation	decay timescale (month)	tropical distribution
1	-650	40:60	4.5	uniform
2	-650	40:60	4.5	LAI scaled
3	-1350	40:60	4.5	LAI scaled
4	-650	80:20	4.5	LAI scaled
5	-650	0:100	4.5	LAI scaled
6	-650	40:60	1.0	LAI scaled

6.2.5 Setup for the inversions

Based on the forward simulations with different emission scenarios, a set of emissions was chosen that was used as the prior estimate for the inversions. Because of the limited amount of station measurements, it was necessary to restrict the number of parameters in the inversion. Therefore, the emissions from the different sources and the soil sink, which was optimized as a negative emission, were divided in two categories. The first category consisted of the emissions that varied on relatively short timescales (biomass burning and leaf litter at the mid- and high latitudes, 620 Gg yr⁻¹) and a temporal correlation length of 1 month was used. The other sources and the soil sink, 2730 Gg yr⁻¹ in total, were not expected to vary strongly throughout the year and were grouped in the second category with a temporal correlation length of 9.5 month.

Additional inversions were performed to investigate the sensitivity of the optimized emissions. First, the temporal correlation length of the two emission categories was varied (sens1). Second, to investigate the influence of OH, the scaled Spivakovsky OH field was replaced by the TM5 OH field (sens2, Sect. 6.2.1). For the base inversion it was observed that emissions in South America strongly decreased. To investigate whether a specific set of measurements was responsible for this decrease, stations that are potentially influenced by South American emissions were excluded from the inversion and replaced by Mount Cimone. In Sens3 the measurements from Ragged Point Barbabos (north east of South America) were replaced by Mount Cimone and in Sens4, American Samoa, Cape Kumukahi, and Mauno Loa (west of South America) were replaced by Mount Cimone. Last, the influence of the prior emission estimate on the optimized emissions was investigated. In Sens5, the prior emissions in the Tropics were reduced, whereas for the mid- and high latitude no changes were made. An overview of the performed sensitivity studies is shown in Table 6.6.

Table 6.6: Overview of the inversions that were performed to estimate the net emissions of CH₃Cl. τ_{short} and τ_{long} are the temporal correlation lengths (months) for the sources that vary on short and long timescales, respectively. When stations were excluded from the inversion, the data from Mount Cimone was used.

inversion	OH field	τ_{short}	τ_{long}	excluded stations	note
Base	Spivakovsky	1	9.5		
Sens1	Spivakovsky	9.5	9.5		
Sens2	TM5	1	9.5		
Sens3	TM5	1	9.5	RPB	
Sens4	TM5	1	9.5	SMO, KUM, MLO	
Sens5	Spivakovsky	1	9.5		Lower prior emissions in Tropics.

6.3 Results and discussion

6.3.1 Forward simulations using emission scenarios

For simulations 1, 2 and 3 (Table 6.5) the measured and modeled mixing ratios are shown in Fig. 6.1 for stations Barrow, Mace Head, Tutuila, South Pole, Trinidad Head and Jungfraujoch. In these simulations the strength of the soil sink and the distribution of the emissions from living vegetation were varied. At mountain stations, represented by Jungfraujoch, a strong seasonal cycle was present in the modeled CH_3Cl mixing ratio for all simulations, but this strong seasonality was not present in the measurements. At South Pole station the seasonal cycle was shifted. The modeled maximum and minimum mixing ratios occurred later in the year than in the measurements. At the other stations, a comparable seasonal cycle was observed in the modeled and measured mixing ratios. The distribution of the emissions from living tropical vegetation (simulation 2) only had a minor influence on the modeled mixing ratios at the stations. However, most of the measurement stations are not located in the Tropics. Lee-Taylor et al. (2001) also found that the mixing ratios at the remote mid- and high latitude stations were relatively insensitive to the distribution of the emissions in the tropical regions.

A stronger soil sink strength (simulation 3) had a pronounced effect on the modeled mixing ratios. The increase of the soil sink was compensated by an increase of the emissions from living vegetation and leaf litter, which were mostly located in the Tropics (Sect. 6.2.4). Increasing both the soil sink and the emissions in tropical regions lead to lower CH_3Cl mixing ratios at the northern high latitudes and higher mixing ratios in the tropical regions. For Barrow, lower mixing ratios due to the large soil sink were in better agreement with the measurements than the other simulations. In contrast, for Trinidad Head the simulations with the smaller soil sink agreed better with the measurements, especially in the second half of the year. At station Mace Head, pollution events were observed throughout the year. Simulations with the small soil sink were in better agreement with the measured pollution peaks, whereas the simulation with the large soil sink better agreed with the low mixing ratios between the pollution events at Mace Head. At the southern high latitudes the soil uptake is negligible due to small fraction of land. Consequently, at South Pole station higher mixing ratios were observed when the larger soil sink and tropical emission were used, because of the increased transport from the Tropics to the South Pole. In the following emission scenarios, the smaller soil sink was used.

Strong indications for the importance of CH_3Cl emissions from leaf litter were observed at station Trinidad Head. Each year, elevated CH_3Cl mixing ratios were ob-

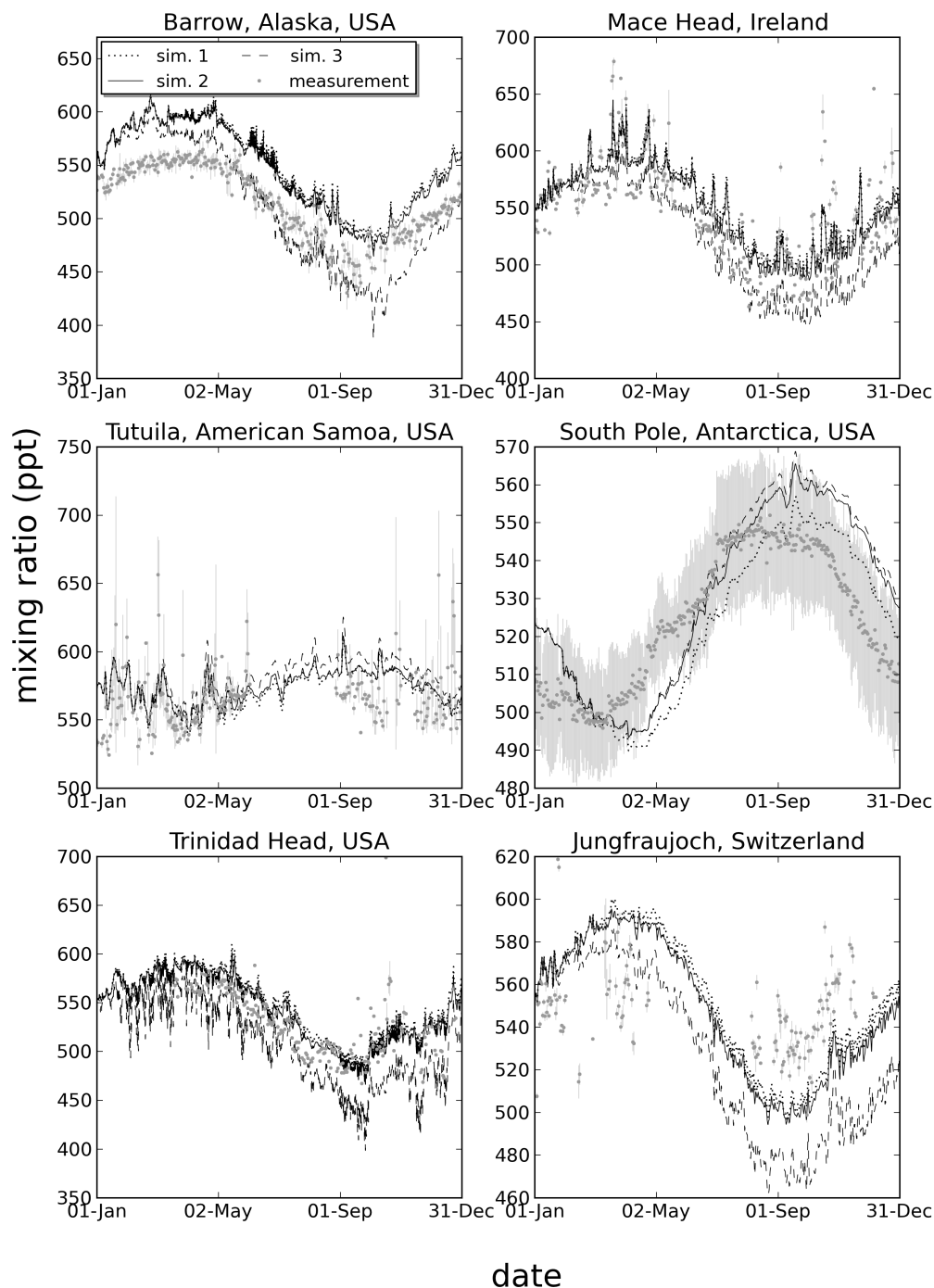


Figure 6.1: Modeled and measured CH_3Cl mixing ratios at six stations for simulations in which the soil sink strength and the distribution of the emissions from living vegetation was varied.

served in autumn at this station. Figure 6.2 shows the measured and modeled mixing ratios for simulations 2, 4, 5 and 6 in which the ratio of the emissions from leaf litter and living vegetation and the leaf litter decay time scale were varied. For simulation 5 (no leaf litter), the high mixing ratios measured in October and the beginning of November were not reproduced by the model. The absence of the leaf litter source reduced the emissions at mid- and high latitudes, whereas the emissions from living vegetation in the Tropics were increased in this simulation. Those tropical emissions did not reach station Trinidad Head and resulted in relatively low mixing ratios throughout the year. With a leaf litter:living vegetation ratio of 80:20 (simulation 4), relatively high mixing ratios were simulated in summer, which were not measured at this station. The high mixing ratios in autumn were best reproduced in simulation 6, the only simulation in which a leaf litter decay time scale of 1 month was used. In this simulation, high CH_3Cl mixing ratios were observed in autumn, whereas in the rest of the year the mixing ratios were relatively low. This was in agreement with the measurements at this station. Apparently, a leaf litter source was required to match the CH_3Cl observations at Trinidad Head, but the timing of the leaf litter emissions was important.

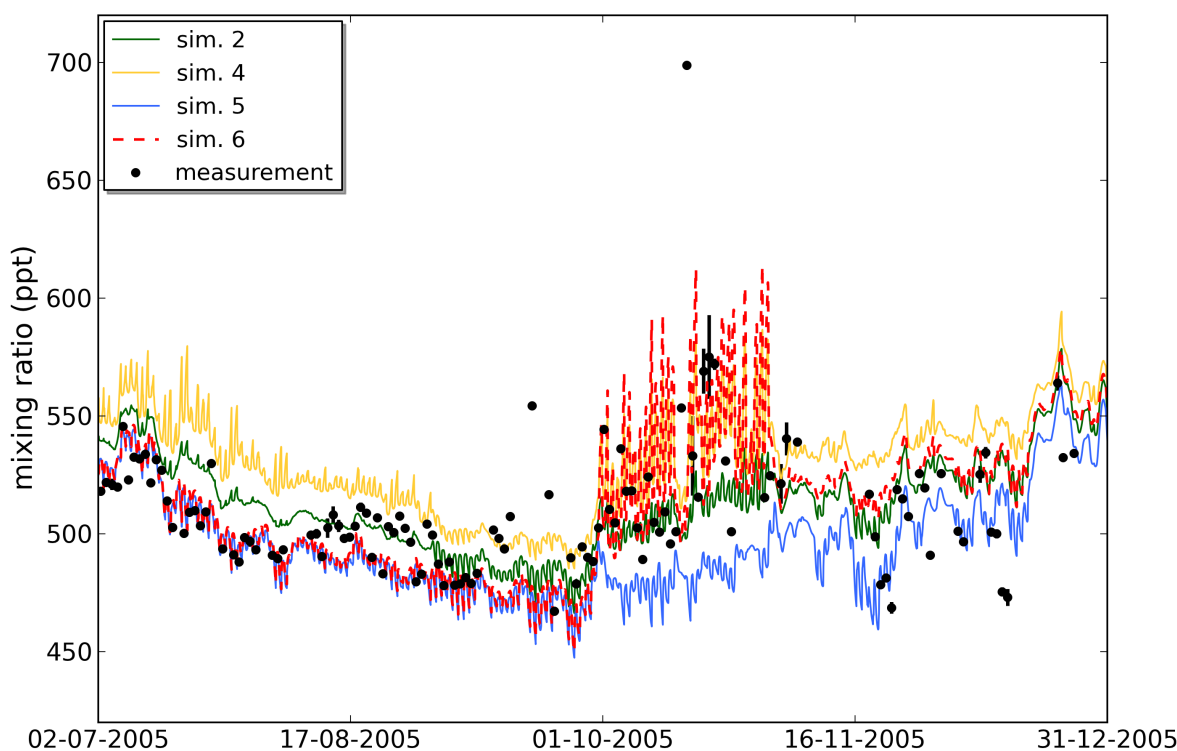


Figure 6.2: Modeled and measured CH_3Cl mixing ratios at station Trinidad Head for simulations in which the ratio of the emissions from leaf litter and living vegetation and the leaf litter decay time scale was varied.

Based on the simulations described above, the emission scenario of simulation 6 (Table 6.5) was chosen as the prior emission estimate for optimization in a mathematical framework. Simulation 6 was comparable to simulation 2 at most stations except at Trinidad Head, where simulation 6 better reproduced the high mixing ratios in autumn. The annual emission maps for CH₃Cl from leaf litter, tropical living vegetation and biomass burning and the uptake of CH₃Cl by the soil are shown in Fig. 6.3 for illustration. The net emission from all sources and the soil sink is shown in Fig. 6.7 (upper left). These figures indicate that, although substantial emissions from leaf litter were required to match the observations at Trinidad Head (North America) in autumn, the total emission in that region was small compared to the emissions in the Tropics.

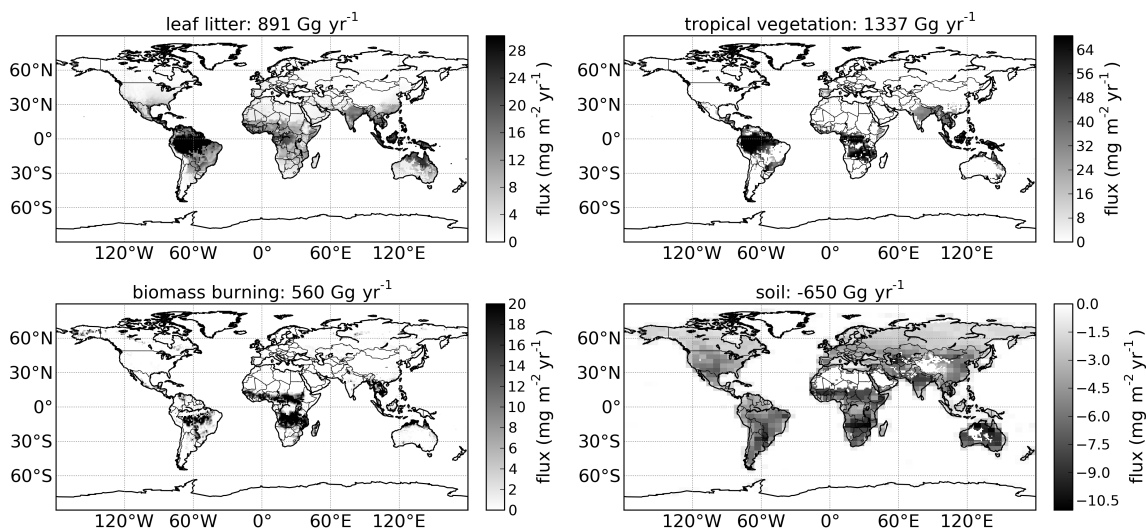


Figure 6.3: Annual emissions of CH₃Cl from leaf litter, living tropical vegetation and biomass burning and the uptake of CH₃Cl by the soil. These emissions were used in the prior emission estimate for the inversions.

For simulation 6, which was used as the prior emission estimate for further optimization, the yearly average CH₃Cl mixing ratios at the surface are shown in Fig. 6.4. High mixing ratios were modeled above the tropical land surfaces. For example, above the forests in South America yearly average mixing ratios above 1000 ppt were simulated. Also for the other simulations the modeled mixing ratios were high in this region. However, field campaigns in South America did not report these high mixing ratios. Scheeren et al. (2003) performed measurements of the CH₃Cl mixing ratio during an aircraft campaign above the Surinam tropical rainforest in 1998 and reported mixing ratios between 550 and 700 ppt close to the surface. Comparable mixing ratios were measured by Gebhardt et al. (2008) during a campaign in the same region. This hints to an overestimate of the emissions in South America. At the mid- and high latitudes,

mixing ratios between 500 and 600 ppt were modeled, which compared well with the study of Khalil and Rasmussen (1999). Instead of further modifying the emissions to match the available observations, we employed inverse modeling to obtain the best estimate of the emissions in the next section.

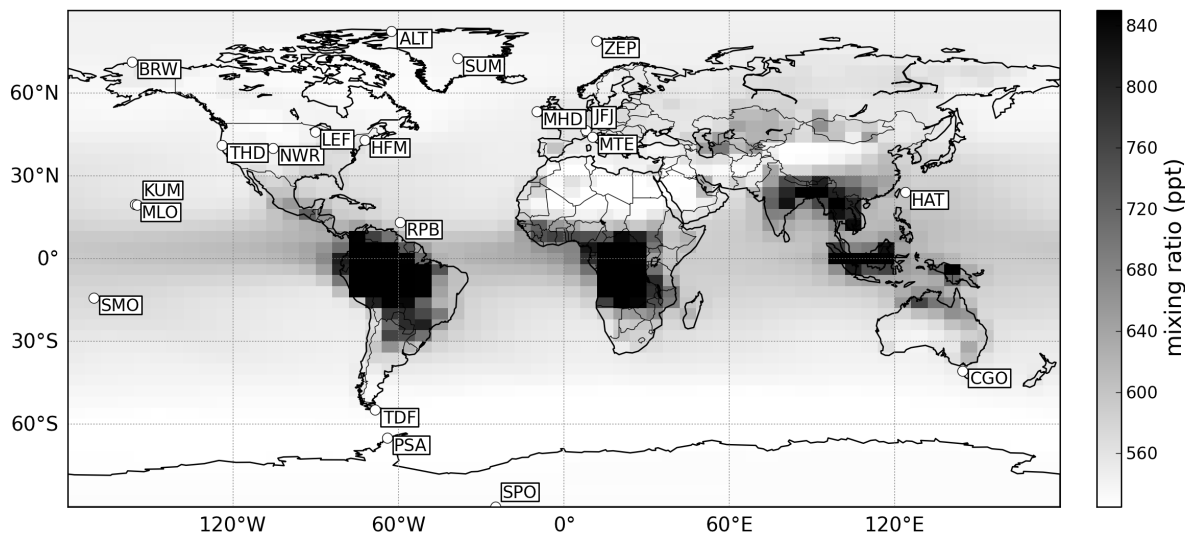


Figure 6.4: Yearly average surface CH_3Cl mixing ratios for a simulation with the emissions that were used as prior estimate for the inversions. The Spivakovsky OH field was used in this simulation. The location of the measurement stations is also indicated.

6.3.2 Inversions

For the base inversion, the mixing ratios modeled with the prior and posterior, i.e. optimized, emissions are shown in Fig. 6.5, together with the measured mixing ratios for the stations Barrow, Jungfraujoch, Mace Head, Tutuila, South Pole and Trinidad Head. In addition, a scatter plot of the modeled and measured mixing ratios at all stations is shown in Fig. 6.6 for the simulations with the prior and the posterior emissions.

Both figures show that, by design, the inversion was able to adjust the emissions such that the modeled mixing ratios were in much better agreement with the measurements than when the prior emissions were used. Overall, the mean bias of the modeled mixing ratios with respect to the measurements reduced from a small underestimate of 7.3 ppt to a negligible overestimate of 0.6 ppt. The χ^2 for all measurements, defined as the square of the difference between the measured and modeled mixing ratios divided

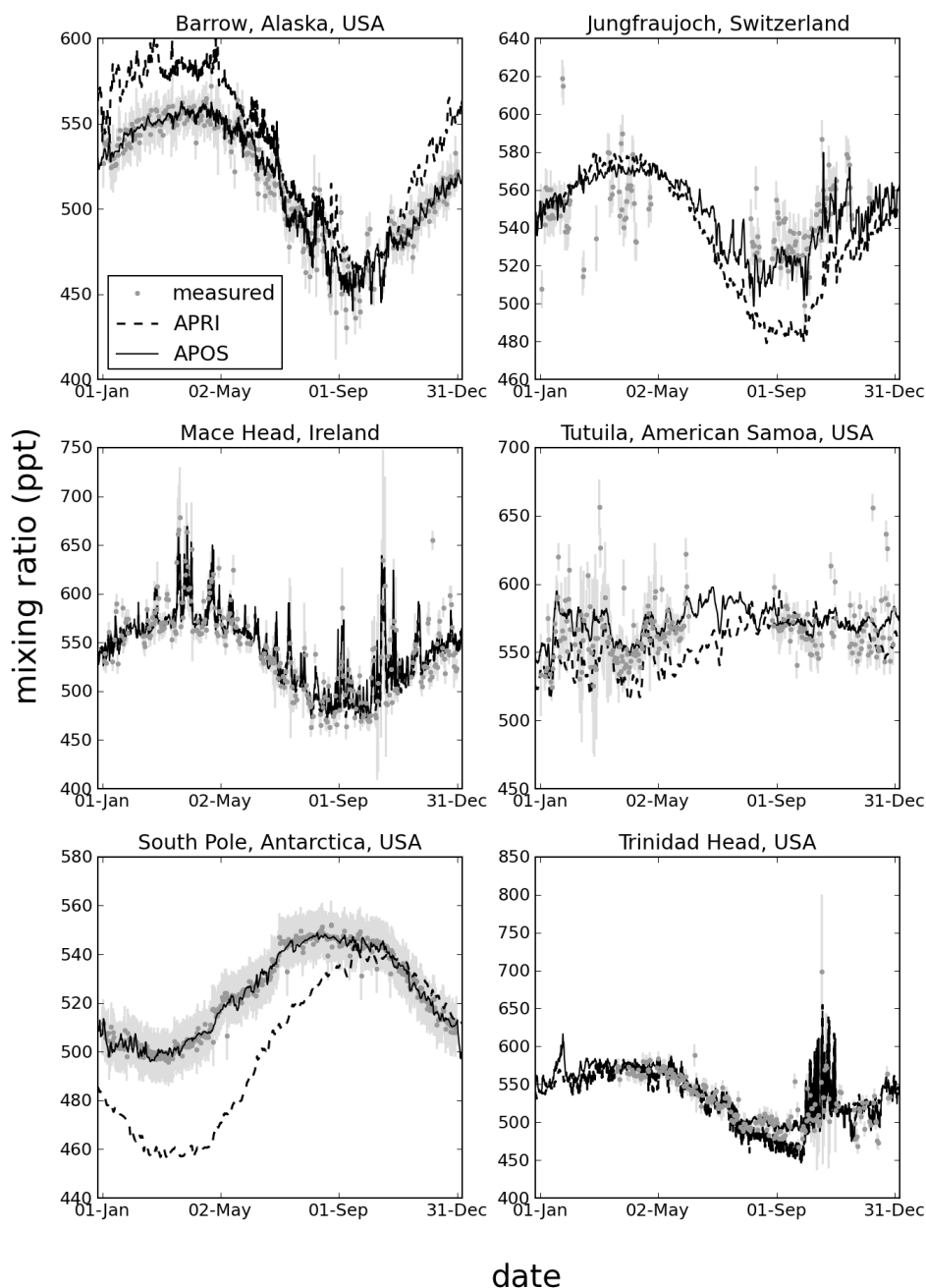


Figure 6.5: Measured and modeled CH_3Cl mixing ratios simulated with the prior (APRI) and posterior (APOS) emissions at six stations used in the inversion. Especially at South Pole station differences in the prior simulation and the forward simulations in Fig. 6.1 were observed, which was due to the use of a slightly different initial mixing ratio field in the simulations.

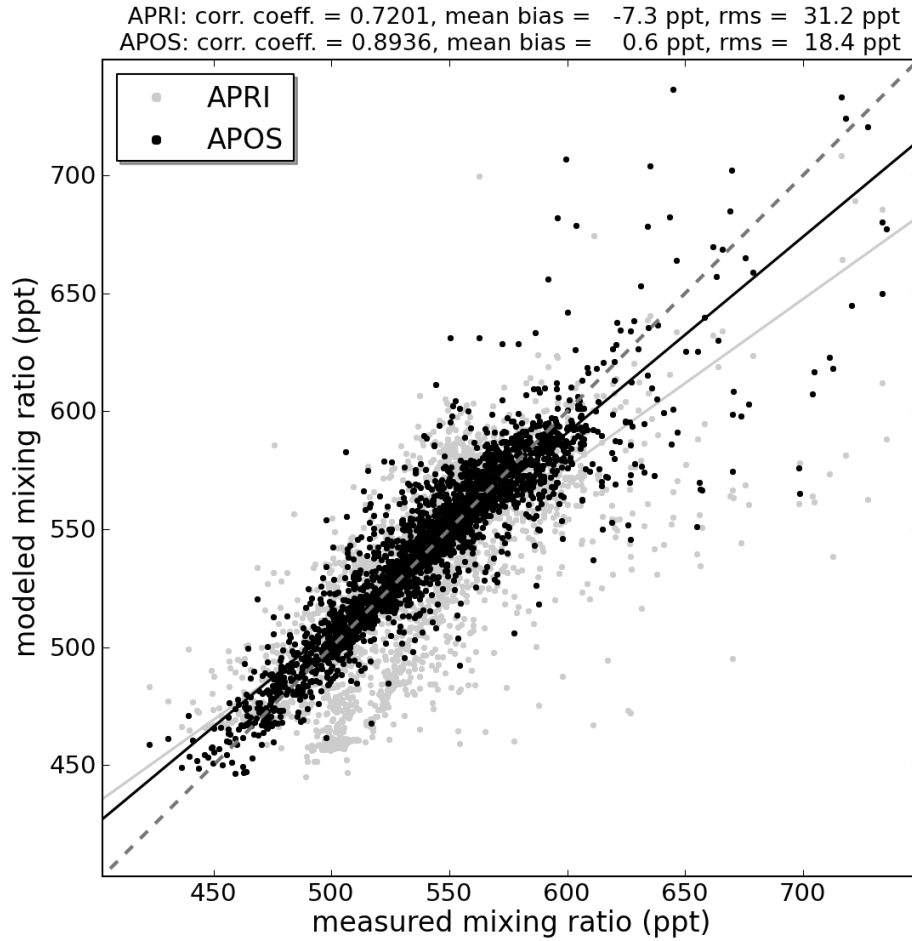


Figure 6.6: Measured and modeled daily mixing ratios for the prior (APRI) and posterior (APOS) emissions at all stations. The bias is defined as model - measurement.

by the uncertainty of the measurement, reduced from 6.2 in the prior simulation to 1.6 in the posterior simulation. In addition, the root mean square difference between the modeled and measured mixing ratios decreased, whereas the correlation coefficient increased in the posterior simulation. Also for each individual station, the fit between the modeled and measured mixing ratios improved. For most stations the number of outliers, defined as a measurement that deviates more than two standard deviations from its modeled values, was below 5% when the posterior emissions were used. However, at stations where many pollution events were observed (e.g. Cape Grim, due to local emissions from coastal areas (Cox et al., 2003)), the number of outliers was higher. This was due to the limitations of a coarse resolution model to represent small scale pollution events.

For the base inversion, the annual prior and posterior emissions are shown in Fig. 6.7. In addition, the difference between the prior and posterior emissions, and the uncertainty reduction on the grid are shown. In the prior simulations the uncertainty in each grid box was proportional to the emission in that box. In the posterior simulation, the uncertainty was reduced in regions where the stations are located and the measurements constrained the emissions. The high emissions from the tropical forest in South America were reduced by more than 50% in the posterior estimate, whereas the emissions from Africa strongly increased. The robustness of these changes will be examined in the sensitivity studies in Sect. 6.3.3. The northern high latitudes were a small net sink of CH₃Cl, which was also observed by Teh et al. (2009) for field measurements around Barrow station. Also the Southern Ocean remained a small net sink of CH₃Cl in the posterior emission estimate.

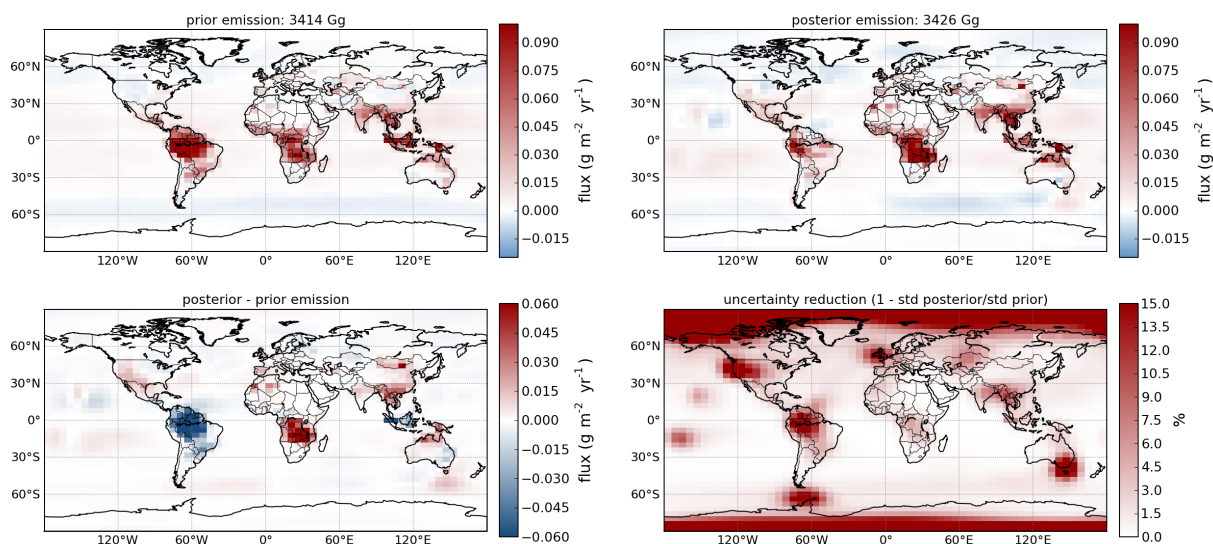


Figure 6.7: Prior and posterior emissions for the base inversion. Also the emission increment (posterior - prior emission) and the uncertainty reduction of the posterior emission estimate with respect to the prior emission estimate are shown.

6.3.2.1 Seasonality

At South Pole station, the seasonal cycle of the mixing ratios was in agreement with the observations when the posterior emission estimate was used (Fig. 6.5). In contrast, for a simulation with the prior emissions the seasonal cycle was shifted. Beyersdorf et al. (2010) also observed for methyl iodide mixing ratios measured at the South Pole that the seasonal cycle was different than expected based on sea surface temperature and

biological activity. Both parameters have a significant effect on the uptake and emission of CH_3Cl by the ocean. At mountain stations, represented by Jungfraujoch, the amplitude of the seasonal cycle was too large in the prior simulation. In the posterior simulation, the amplitude was in much better agreement with the measurements.

Changes in the seasonality from the prior to the posterior simulation are expected to be caused by changes in the seasonal cycle of the emissions. In Fig. 6.8 the net CH_3Cl emissions from the Tropics, South America, Africa and Oceania are shown for three-month periods in 2005. Emissions from these regions are transported to the South Pole (see next section and Fig. 6.9).

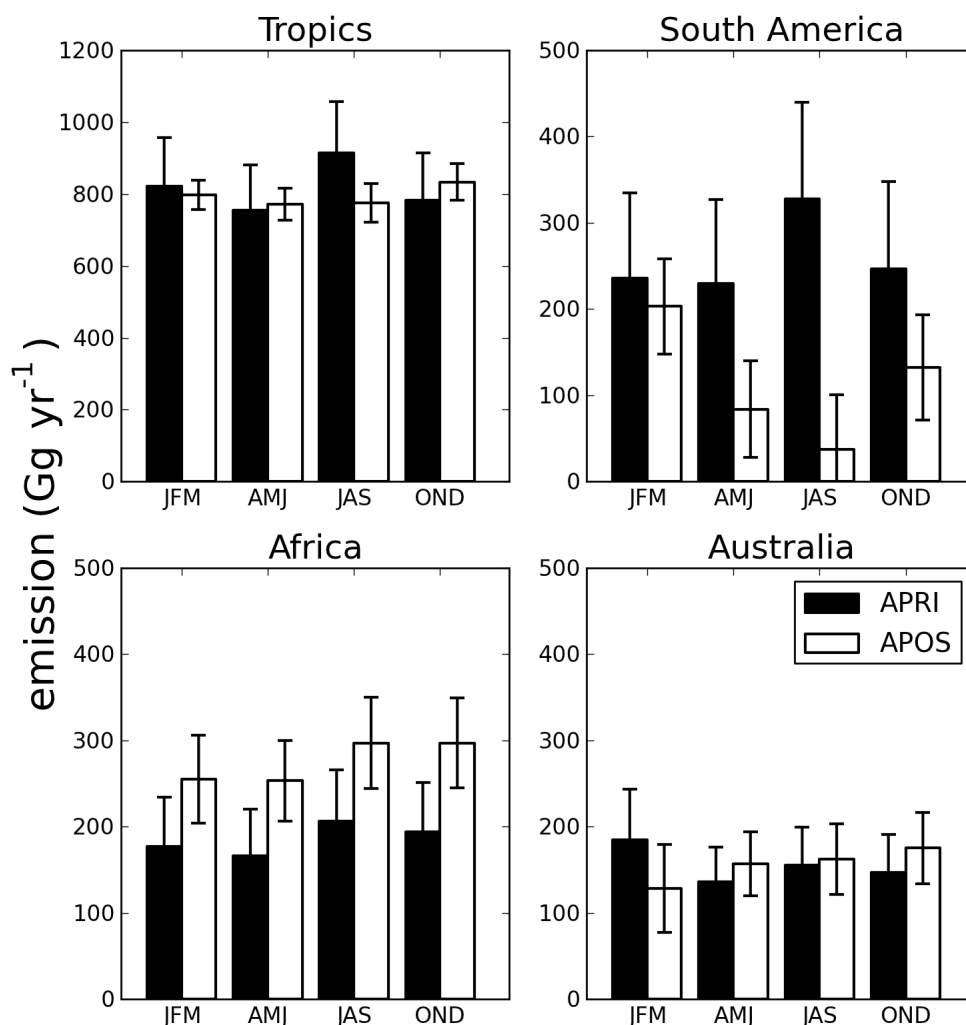


Figure 6.8: Prior (APRI) and posterior (APOS) emissions for three month periods in 2005 for different geographical regions.

The most pronounced changes were observed for South America. In the prior simulation the emissions were maximum in July-September, whereas in the posterior simulation they were minimum in this period. However, throughout the year the South American emissions decreased, whereas at South Pole station the mixing ratios increased from the prior to the posterior simulation. It is therefore not likely that the emission changes in South America were responsible for the improved fit at the South Pole. For Australia the emissions were maximum in January-March in the prior simulation, whereas in the posterior simulation maximum emissions were found in October-December. However, the Australian emission changes were small compared to changes in the other regions and possibly only had a minor influence on the changes at the South Pole. For Africa the emissions increased throughout the year which likely caused the increase of the mixing ratios at South Pole station. The increase of the emissions from the prior to posterior simulation was comparable in each period, and is therefore not expected to cause the shift the minimum and maximum mixing ratio from prior to posterior simulation. Changes in the net uptake of CH₃Cl by the Southern Ocean from the prior to the posterior simulation (not shown) were minor and therefore not expected to have a significant effect on the modeled mixing ratios. In the inversion, december 2004 was used as a spin up month, but not analyzed. The emissions from Africa and South America in this spin up month were strongly increased in the posterior compared to the prior simulation, which may have contributed to the change shift in the seasonal cycle.

The emissions from Africa were detected at station Jungfraujoch (see next section and Fig. 6.9). The increase of the African emissions may therefore have been responsible for the improved fit in the second half of the year at this station.

6.3.3 Sensitivity study

For different geographical regions, the annual net emissions are shown in Table 6.7 for different sensitivity inversions. As the number of CH₃Cl measurements is limited, the emissions were aggregated over the whole year and over continental scale areas. Although there were clearly differences between the sensitivity inversions, some general patterns were observed. In all inversions the global net emission, all sources and the soil sink, was estimated at $\sim 3400 \text{ Gg yr}^{-1}$ with only a small uncertainty ($\pm 60 \text{ Gg}$). In the prior emission estimate of the base scenario and sens1 - sens4, more than 90% of the emissions was located in the Tropics. After optimizing the emissions in the inversions, the emissions remained in the tropical regions. In Sens 5 the prior emissions in the tropical regions were reduced from 3272 to 2454 Gg yr^{-1} . After optimization, the emissions in the Tropics increased again to 3061 Gg yr^{-1} , which was

only slightly lower compared to the other inversions. This indicates that the tropical emissions are well observed by the measurement network. In all inversions, more than 90% of the optimized net CH_3Cl emissions was assigned to the Tropics and the emission estimates ranged between 3061 and 3323 Gg yr^{-1} . This is slightly higher than the estimate of 2900 Gg yr^{-1} from tropical biogenic sources by Yoshida et al. (2004) and much higher than the 2200 and 2500 Gg yr^{-1} estimated by Xiao et al. (2010) and Yoshida et al. (2006), respectively. There are several reasons for the differences between the studies. First, their estimates only consider biogenic emissions from terrestrial tropical areas and do not include emission from e.g. biomass burning and the ocean between 30°S and 30°N that are included in our estimate. Second, our higher emission estimate for the Tropics may have been caused by too slow transport in TM5 of tropical emissions to the poles that was recently identified by Patra et al. (2011). Higher emissions are then required to match the observed mixing ratios at the high latitudes. Last, the differences between the studies may be caused by the different approaches to optimize the emissions. Yoshida et al. (2006) and Xiao et al. (2010) optimized the emissions for large geographical regions with a prescribed geographical distribution of the emissions. In contrast, in this study the emissions were optimized on the model grid to avoid aggregation errors and then aggregated over larger regions. This more sophisticated approach leads, at least in the TM5 model, to a robust emission estimate ($>3000 \text{ Gg yr}^{-1}$) in the Tropics. In addition, different OH fields and transport models were used in the studies, which can lead to different results.

Increasing the temporal correlation length of the source that varied on small time scales (biomass burning and leaf litter on the mid- and high latitudes) from 1 to 9.5 months only had a minor effect on the total optimized emissions (Base vs Sens1). This is likely because the variable sources were small ($\sim 22\%$) compared to the sources that varied on longer time scales, whereas the largest differences between the prior and posterior emission estimate were found for the sources that varied on the longer timescale (not shown). Changing the OH field from Spivakovsky to TM5 (Sens2) caused a further decrease of the emissions in South America compared to the base inversion, compensated by increasing emissions in Africa, Oceania and Asia. This decrease in South America was expected, because in the TM5 OH field the OH concentration above South America was lower than in the Spivakovsky OH field. Consequently, there was less removal of CH_3Cl in this region and less emissions were required to match the observations.

The spatial pattern of the tropical emissions changed substantially from the prior to the posterior emission estimate. The emissions from South America strongly decreased and this was compensated by an increase of the emissions from Africa and Asia. However, the reduction of the uncertainty from the prior to the posterior estimate was only minor for Africa. This indicates that the African emissions were poorly constrained

by the measurements and were likely adjusted to compensate for changes in other regions. More measurements around Africa, e.g. at station Ascension Island, are required to better constrain the emissions. A much stronger decrease of the uncertainty was observed for South America, which indicates that the emissions were better constrained by the measurements. Studies sens3 and sens4 were performed to examine which stations were responsible for the decreasing emissions in South America.

Table 6.7: Prior and posterior CH₃Cl emission estimates (Gg yr⁻¹) for the sensitivity inversions for different geographical regions. Note that these are net emission estimates and include all sources and the soil sink.

	base		sens1	sens2	sens3	sens4	sens5	
region	prior	posterior	posterior	posterior	posterior	posterior	prior	posterior
Nam	181 ± 59	168 ± 48	168 ± 50	220 ± 49	228 ± 49	211 ± 50	136 ± 48	182 ± 40
Sam	1041 ± 345	455 ± 176	436 ± 181	328 ± 176	234 ± 170	602 ± 211	771 ± 247	600 ± 131
Europe	40 ± 22	47 ± 18	46 ± 17	50 ± 18	72 ± 16	60 ± 17	40 ± 22	59 ± 18
Africa	743 ± 185	1102 ± 160	1118 ± 165	1097 ± 160	1255 ± 165	943 ± 163	584 ± 136	1013 ± 122
Oceania	623 ± 147	622 ± 131	619 ± 135	671 ± 131	656 ± 128	617 ± 135	487 ± 111	660 ± 99
Asia	563 ± 138	716 ± 85	717 ± 81	681 ± 86	620 ± 81	762 ± 96	439 ± 105	649 ± 71
Tropics	3273 ± 447	3178 ± 81	3173 ± 80	3086 ± 78	3106 ± 85	3323 ± 121	2454 ± 323	3061 ± 71
Globe	3414 ± 457	3426 ± 57	3423 ± 57	3346 ± 55	3365 ± 60	3439 ± 88	2595 ± 335	3381 ± 48

In sens3 the measurements from Ragged Point Barbados, north-east of South America, were not used in the inversion and replaced by measurements from Mount Cimone (Italy). The South American emissions decreased even further than in the base inversion to almost 20% of the prior estimate, indicating that the measurements at Ragged Point Barbados avoided a stronger decrease of the posterior emissions. In sens4 the measurements from Mauno Loa, Cape Kumukahi and American Samoa, located west of South America, were excluded from the inversion. The posterior emissions from South America decreased, but much less than in the base inversion. This shows that the measurements from the stations at Hawaii and Samoa were responsible for part of the decrease of the South American emissions. It appears that the measurements on the stations west of South America have a contrasting effect to the measurements at Ragged Point Barbados. As for the other inversions, the decrease of the emissions in South America was compensated by increasing emissions in Africa and Asia. Thus, in sens4 African emissions were enhanced less than in the base inversion.

To further investigate which stations are sensitive to emissions from different regions, three additional forward simulations were performed. Methyl chloride was emitted throughout 2005 from either South America, Africa or Australia, while at the rest of the globe the emissions were set to zero. The initial mixing ratio was zero everywhere. For each emission region, the modeled monthly mean mixing ratios and their standard deviations are shown in Fig. 6.9 for different stations. For stations that are sensitive

to emissions from a certain region, the increase of the modeled mixing ratio in time was highly variable, which was indicated by the large standard deviation. In contrast, when emissions are detected at a station only after long range transport or diffusion processes, the increase of the mixing ratio in time was rather smooth. This was the case at for example South Pole station.

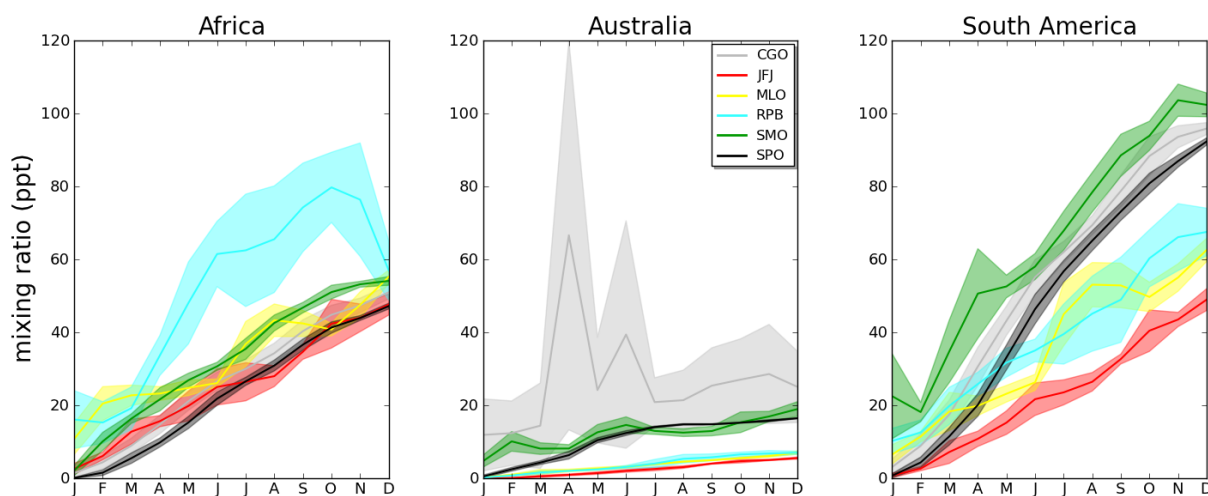


Figure 6.9: Modeled CH_3Cl mixing ratios at selected stations when CH_3Cl is only emitted from Africa, Australia or South America for 2005.

Ragged Point Barbabos was very sensitive for emissions from Africa. Mauna Loa and Jungfraujoch also detected some of the African emissions. Those stations were likely responsible for the small uncertainty reduction of the emission estimate that was observed for Africa. The emissions from Australia were mainly detected by station Cape Grim, although some of the emissions were also transported to American Samoa and the South Pole. The sensitivity inversions sens3 and sens4 already showed that Ragged Point Barbados and the measurement stations west of South America put constraints on the emissions in this region. Figure 6.9 shows that Samoa is the main station at which South American emissions were detected, whereas Ragged Point Barbados and the stations at Hawaii were less sensitive to these emissions. A significant fraction of the CH_3Cl emissions from South America also reached Cape Grim and the South Pole and those stations likely contributed to the adjustment of the prior emission estimate in this region.

6.3.4 Validation

6.3.4.1 Aircraft and ship measurements

A comparison between the simulated CH₃Cl mixing ratios using prior and posterior emission estimates (base inversion) and the measurements made during aircraft campaigns and ship cruises is shown in Fig. 6.10. Because the measurements were performed in different years than the model simulation, they were averaged per altitude for different geographical regions. For South America, high mixing ratios were found near the surface in the prior simulation. However, the posterior emissions were much lower, which resulted in lower mixing ratios above South America. The bias of the modeled mixing ratio with respect to the aircraft- and ship measurements for this region reduced for simulations with the posterior compared to the prior emissions, indicating that the emission estimate improved. For Africa, the prior simulation was in reasonable agreement with the measurements in the lower troposphere, but posterior modeled mixing ratios tend to overestimate the measurements. In the upper troposphere, both the prior and the posterior simulation underestimated the measurements. For South East Asia the prior and posterior simulation were comparable and both overestimated the measurements.

The comparison with the aircraft and ship measurements confirms that the reduction of the emissions from South America was an improvement of the emission estimate, whereas the increase of the emissions from Africa lead to a poorer fit with the aircraft and ship measurements, especially between 2-5 km. This is in agreement with the pattern of uncertainty reduction observed in Fig. 6.7. The uncertainty of the emission estimate for South America reduced substantially, indicating that the emission adjustment was driven by the observations. For Africa only a small uncertainty reduction was observed due to constraints from Ragged Point Barbabos and to a lesser extend due to constraints from Mauna Loa and Jungfrauoch. Part of emission adjustment was likely to compensate for emission changes in South America.

6.3.4.2 Comparison with independent station observations

For the base inversion the measurements performed at Hateruma Island and Mount Cimone were compared to the modeled mixing ratios using the prior and posterior emission estimates (Fig. 6.11). For Hateruma Island, monthly mean mixing ratios were available and the error bars indicate the standard deviation of the measurements in that month. The error bars are relatively large indicating that the mixing ratios are highly variable. The difference between simulations with the prior and posterior emissions was small at this station and both simulations also show the high variability in mixing

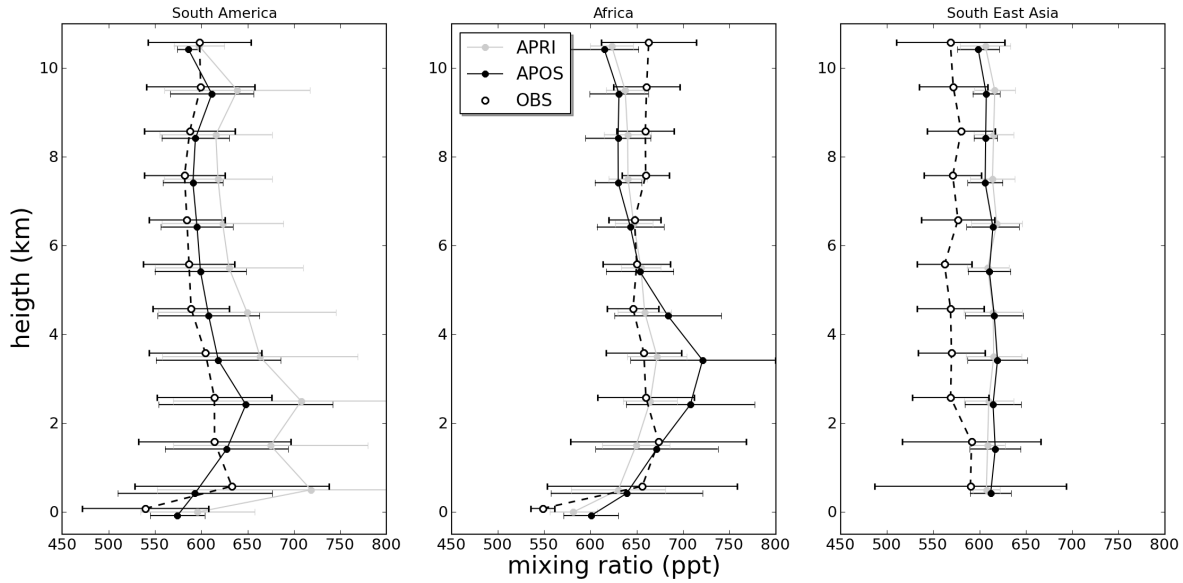


Figure 6.10: Comparison between the modeled mixing ratios using the prior (APRI) and posterior (APOS) emission estimates and the mixing ratios measured during aircraft campaigns and ship cruises (OBS) in different geographical regions. The measurements at 0 m altitude are the ship measurements. The aircraft measurements are averaged over 1000 m intervals.

ratios. Although direct comparison between the modeled and monthly mean mixing ratios is difficult, they are of comparable magnitude.

For Mount Cimone, the amplitude of the seasonal cycle was smaller in the posterior than in the prior simulation, which was in better agreement with the measurements. This improvement was expected, because at station Jungfraujoch, another mountain station located nearby that was used in the inversion, the amplitude of the seasonal cycle also improved. However, the pollution events measured in April were not reproduced by the model, possibly due to the coarse spatial resolution of the model. The pollution events were not measured at Jungfraujoch, indicating that they might have been caused by local pollution that was not included in the model. The measurements in August and September were in better agreement with the posterior than the prior simulation, indicating that the emission estimate improved at the mid latitudes.

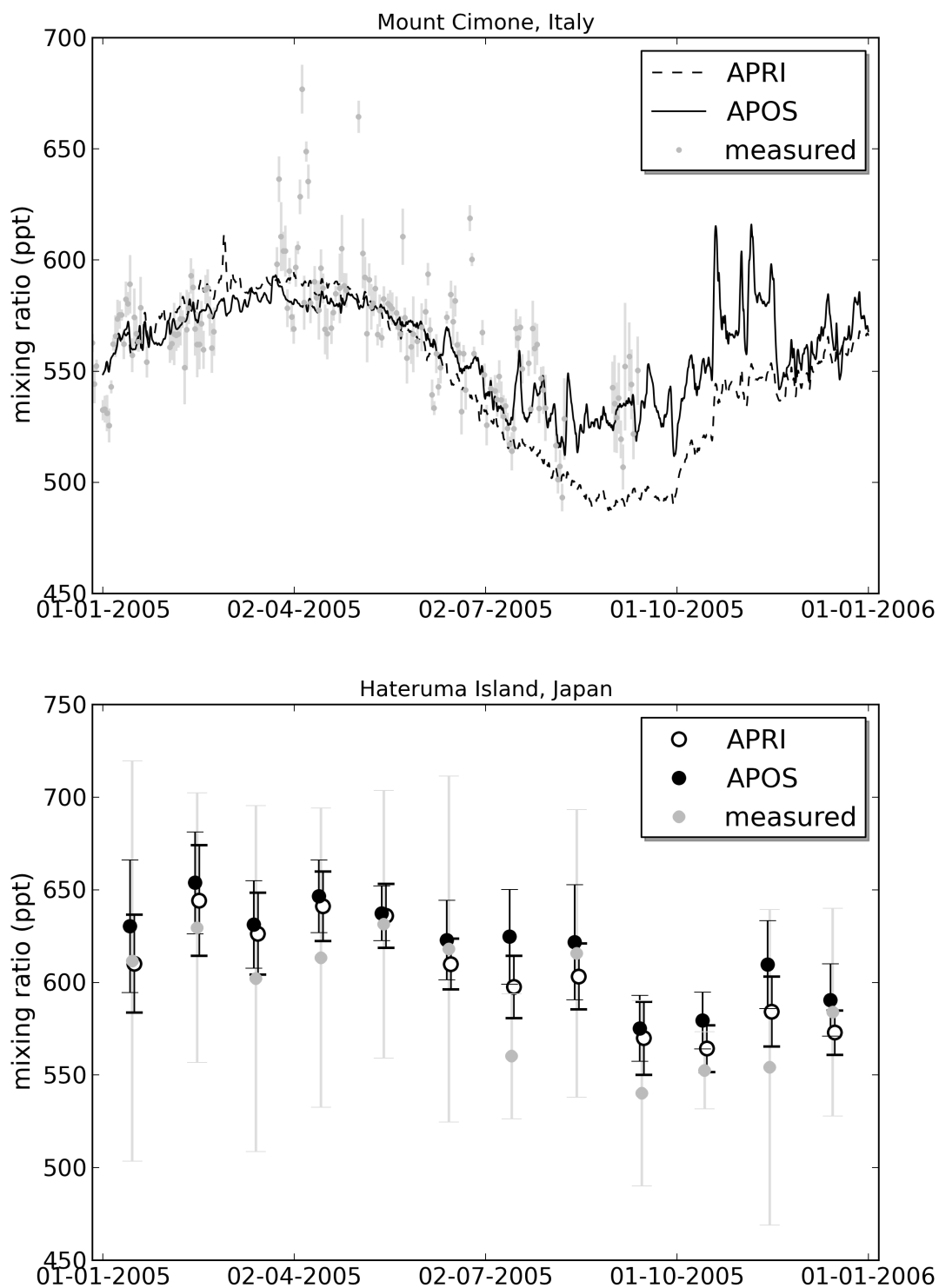


Figure 6.11: Comparison between the measurements at stations that were not used in the inversion with modeled mixing ratios using the prior (APRI) and posterior (APOS) emission estimates. For Hateruma Island the measurements are monthly means, whereas for mount Cimone daily average mixing ratios are plotted.

6.4 Summary and conclusion

The goal of this study was to investigate the environmental importance of leaf litter as a source of CH_3Cl with a global model and to infer emission estimates at continental scales using the available measurements. Estimating the strength of the leaf litter source turned out to be difficult. The amount of stations that measured CH_3Cl was limited and most stations were not located in the regions with the largest sources. In addition, a substantial fraction of the leaf litter source is likely located in the Tropics, where also the living vegetation contributes significantly to the CH_3Cl emissions. Only the forward simulation at Trinidad Head (North America) indicated that a leaf litter source is required to match the observations at this station in autumn. More measurement stations are required to investigate with higher confidence whether there are other mid- and high latitude locations where leaf litter is an important source of CH_3Cl in autumn.

Even though the number of CH_3Cl measurements was limited, inversions could be used to estimate the net emission of CH_3Cl from different geographical regions. The most important findings are:

- In all inversions, the emissions from tropical South America decreased. This was supported by independent aircraft and ship measurements.
- The emissions from Africa and Asia increased in the posterior compared to the prior estimate. However, there were only a few measurements to constrain the emissions from Africa and emission increments in this region were likely partly due to compensate for emission changes in other tropical regions.
- The largest emissions from CH_3Cl were located in the Tropics ($> 90\%$), whereas the mid- and high latitudes were only a minor source or even a net sink of CH_3Cl .
- A denser monitoring network in the Tropics would be required to better constrain the CH_3Cl emissions from the tropical regions. For example, CH_3Cl measurements from Ascension Island, located between South America and Africa, would be useful to constrain the emissions from both continents.

Acknowledgements

This work was supported by the Netherlands Organization of Scientific Research (NWO) under Grant No. 016.071.605. James Elkins (NOAA), Stephen Montzka (NOAA), Geoff Dutton (NOAA), Ray Wang (AGAGE), Yoko Yokouchi (NIES) and Michela Maione

(University of Urbino) are acknowledged for supplying the CH₃Cl measurements from the different stations.

The goal of this thesis was to investigate leaf litter as a source of volatile compounds to the atmosphere. Leaf litter is available at the Earth's surface in large quantities and has the capability to emit many different volatile compounds. Several hydrocarbons, terpenes and oxygenated compounds that are emitted from leaf litter are already identified in previous studies (e.g. Isidorov and Jdanova (2002)), but there are still substantial uncertainties in the quantities that are emitted and the factors that control the emissions. In this project the focus was on C₂–C₅ hydrocarbons, CO, H₂ and CH₃Cl. The emission of these compounds was measured for different plant species in the laboratory and experiments were performed to identify factors that influence the emission rates. In addition, for CH₃Cl a small field study and a modeling study were performed.

The first compounds investigated in this study were hydrocarbons. Methane emissions from decaying plant material were already detected in several earlier studies (e.g. Kepler et al. (2009) and the references therein) and the methane emission rate depended on both temperature and UV radiation. In addition, the emission of ethane and ethene from detached tobacco leaves was strongly influenced by UV radiation (McLeod et al., 2008). The emission of larger hydrocarbons (monoterpenes and C₄–C₁₀ hydrocarbons) was reported by Isidorov and Jdanova (2002), but the fluxes were not quantified. The experiments described in this thesis focussed on C₂–C₅ hydrocarbon emissions from leaf litter and the influence of temperature and UV radiation on the emissions. Several C₂–C₅ hydrocarbons were emitted from leaf litter of different plant species at temperatures that occur under natural conditions. The emissions strongly increased when leaf litter was heated or irradiated with UV light. Both the wavelength and the intensity of the UV radiation had a strong influence on the emission rate. In addition, UV in-

duced hydrocarbon emissions were enhanced when leaf litter was placed in humid air, whereas no emissions were observed for leaf litter in a N₂ atmosphere. This implies that the emission of C₂–C₅ hydrocarbons from leaf litter depends on the presence of oxygen. Not all C₂–C₅ hydrocarbons were emitted from leaf litter. For example, no emissions of *i*-butane and *i*-pentane have been detected. A study on the underlying production process in the leaf litter should be performed to understand why not all hydrocarbons are emitted by the leaf litter. For the investigation on C₂–C₅ hydrocarbon emissions from leaf litter, only laboratory experiments have been performed. A simple up-scaling of the experiments clearly showed that the amount of C₂–C₅ hydrocarbons that was emitted from leaf litter was insignificant for the global budgets of those compounds. Therefore, no field experiments were performed to further investigate C₂–C₅ hydrocarbon emissions from leaf litter.

A small study was performed in which the emission of H₂ and CO from leaf litter of *Sequoiadendron giganteum* was measured. Previous studies by Schade et al. (1999) and Tarr et al. (1995) already showed that CO can be emitted from leaf litter upon heating or irradiation of the leaf litter with UV light. The experiments described in this thesis confirmed these findings, and the emission of CO from sequoia leaf litter indeed increased with temperature and UV radiation intensity. Emissions of H₂ from leaf litter were not measured before. For *Sequoiadendron giganteum* leaf litter, H₂ emissions were observed when the leaf litter was heated to at least 50 °C or irradiated with UV light in an atmosphere without oxygen. Although such high air temperatures are rarely reached, they are more easily observed at the soil surface. Field experiments should be performed to investigate whether leaf litter emission occur under natural conditions with these high soil surface temperatures. In addition, these experiments were only performed on one plant species. Experiments on more plants, especially species growing under high temperature conditions, should be performed to investigate whether the findings for this plant species can be generalized.

The last compound investigated in this study was CH₃Cl. Previous studies already showed that leaf litter has the capability to emit substantial amounts of methyl halides into the atmosphere. Methyl bromide emissions from leaf litter were measured by Wishkerman et al. (2008) and the emission rates depended on temperature and the bromide content of the plant material. Similar results were found in studies on CH₃Cl and the emission rates depended on temperature and the chloride content of the leaf litter (Hamilton et al., 2003; Keppler et al., 2004; Yassah et al., 2009). In this study CH₃Cl emissions were measured from leaf litter of different plant species. A simple upscaling of laboratory experiments indicated that leaf litter can be a globally important source of CH₃Cl, but there are substantial uncertainties in the global estimate. Part of this uncertainty is because the factors that control CH₃Cl emissions from leaf

litter are unclear. The laboratory experiments showed that for each investigated plant species, the emission rates increased with temperature following the Arrhenius relation. Besides the increase of the emission rate with temperature, there were large differences between plant species that could not be explained. A series of experiments on leaf litter of halophytes with a varying chloride content showed that there was no significant correlation between the CH_3Cl emission rate and the chloride or methoxyl group content of the plant material, which is in contrast to the findings by Hamilton et al. (2003). This suggests other factors strongly influence the emission of CH_3Cl from leaf litter. Possibly the emissions depend on plant species, vegetation form or decomposition stage. In addition, the moisture content of the plant material or the humidity of the surrounding atmosphere influence the CH_3Cl emission rate. The effect of these factors on the emission should be investigated to understand the variations between plant species and to obtain more accurate global estimates.

A limited set of field experiments showed that leaf litter under natural conditions also emitted CH_3Cl . However, the uncertainties in the emission rate measurements were large. A comparison between laboratory and field experiments on leaf litter of the same plant also showed large differences. To improve the estimate of CH_3Cl emissions from leaf litter, more field experiments are required. First, the method to measure the CH_3Cl fluxes in the field should be improved to reduce the uncertainty of the flux measurements. The method used in this study measures the net fluxes of CH_3Cl , whereas simultaneous production of CH_3Cl by the leaf litter and uptake of CH_3Cl by the soil occur. Therefore, an isotope tracer method as described by e.g. Rhew and Abel (2007) can be used to simultaneously measure the uptake and emission in one experiment. Second, the difference between the field and laboratory experiments should be understood and the factors that control the CH_3Cl emission rate should be identified.

A global chemistry transport model was used to investigate the global budget of CH_3Cl including the emissions from leaf litter. The only surface station where leaf litter likely has a strong influence on the measured mixing ratios was Trinidad Head (North America). At this station, very high CH_3Cl mixing ratios were observed in autumn that were only reproduced by the forward model simulations when a substantial leaf litter source was included. If leaf litter is indeed the main source of this variability, then it must be important also at many other locations, but the present network is not really designed to detect these emissions. In the Tropics both leaf litter and living vegetation are expected to emit significant amounts of CH_3Cl . Due to the comparable spatial and temporal pattern of these emissions, it was not possible to determine the contribution of both sources individually. Inversions were performed to estimate the net CH_3Cl emission for different geographical regions. Because of the limited amount of CH_3Cl

measurements and comparable temporal and spatial pattern of the emissions, only the net emission of CH_3Cl was optimized for different geographical regions. The inversions indicated that the Tropics were the main source of CH_3Cl , with more than 90% of the global net emissions. Several sensitivity studies indicated that this was a robust estimate. In all inversions, the optimized, posterior emissions from South America were smaller than in the initial, prior emission estimate, whereas the emissions from Africa were larger. However, analysis of the results shows that this result, although it is robust in different sensitivity tests, may not be well constrained by measurements. The number of stations that measures CH_3Cl , especially in the Tropics where most sources are located, is limited. To obtain a more accurate and more detailed estimate of the CH_3Cl emissions, a denser measurement network is needed. For example, measurements from station Ascension Island would be useful to constrain the emissions from both South America and Africa.

Dit proefschrift beschrijft de emissie van vluchtige stoffen door blad materiaal. Het gaat hierbij dan specifiek over bladeren die bomen en struiken gedurende een bepaalde periode van het jaar laten vallen. Dit kan gebeuren in een winter periode als gevolg van kou of gedurende droge periodes in een klimaat met veel variatie in regenval. Levende planten emitteren grote hoeveelheden vluchtige stoffen in de atmosfeer, maar ook de uitstoot van dit gevallen bladmateriaal kan substantieel zijn. Honderden chemische stoffen die uit bladmateriaal vrijkomen zijn al geïdentificeerd, maar er zijn nog steeds grote onzekerheden over de grootte van de uitstoot en de factoren die daarop van invloed zijn. De hoeveelheid bladmateriaal die jaarlijks geproduceerd wordt, is enorm ($44 - 49 \times 10^{12}$ kg) en de emissie van vluchtige stoffen is mogelijk dan ook groot. De uitgestoten stoffen kunnen een belangrijke invloed op de atmosfeer hebben. Sommige stoffen zijn voorlopers van de productie van ozon in de troposfeer (de onderste laag van de atmosfeer) wat bijdraagt aan smog vorming. Andere stoffen worden juist naar de stratosfeer (11-50 km) getransporteerd waar ze bijdragen aan de vorming van het ozongat boven Antarctica.

Het doel van dit project was het meten van de emissie van vluchtige stoffen uit plant materiaal en het identificeren van factoren die deze emissies beïnvloeden. Het project heeft zich gericht op C_2 – C_5 koolwaterstoffen, methyl chloride (CH_3Cl), waterstof (H_2) en koolstofmonoxide (CO) en onderzocht is hoe de uitstoot van deze stoffen beïnvloed wordt door temperatuur, UV straling en vocht. Vervolgens is de invloed van de gemeten emissies op de atmosfeer bepaald. Voor de koolwaterstoffen is dit gedaan met behulp van een eenvoudige opschaling van de emissie, terwijl er voor CH_3Cl ook gebruik is gemaakt van een atmosferisch chemie-transport model.

Hoofdstuk 2 richt zich op de uitstoot C_2 – C_5 koolwaterstoffen en het effect van temperatuur en UV straling hierop. Emissies van ethaan, etheen, propaan, propen en n-pentane zijn waargenomen, maar verschillen per plant soort. Tussen 20 en 100°C namen de emissies toe met temperatuur. De afhankelijkheid van de emissies van temperatuur wordt beschreven door de Arrhenius vergelijking. Deze vergelijking kan ook gebruikt worden om een activeringsenergie te bepalen en voor alle onderzochte planten was deze groter dan 50 kJ mol^{-1} . Deze relatief hoge activeringsenergie is, samen met de toename van de emissie met temperatuur tot 100°C, een indicatie dat de uitstoot is veroorzaakt door een chemisch proces en niet door biologische activiteit. Op constante temperatuur nemen de emissies van C_2 – C_5 koolwaterstoffen af in de tijd. Op hoge temperatuur (80-100 °C) is de afname al merkbaar op een tijdschaal van uren, terwijl op omgevingstemperatuur ($\sim 20^\circ\text{C}$) hier maanden voor nodig zijn. C_2 – C_5 koolwaterstoffen worden ook door plant materiaal uitgestoten wanneer dit wordt bestraald met UV straling. De emissies nemen lineair toe met de intensiteit van de UV straling. Ook blijkt dat UV straling met korte golflengte (UVB) effectiever is in het generen van koolwaterstoffen dan UV straling met langere golflengte (UVA). De vochtigheid van de lucht blijkt ook van invloed te zijn op de emissies. Voor bladmateriaal in vochtige lucht zijn emissies waargenomen die drie keer hoger zijn dan in droge lucht. Hoewel duidelijk is dat C_2 – C_5 koolwaterstoffen door bladmateriaal uitgestoten worden en dat de uitstoot beïnvloed wordt door temperatuur, UV straling en vocht, heeft een simpele opschaling ook laten zien de emissie geen significante invloed heeft op de globale budgetten van deze stoffen.

De emissie van H_2 en CO door plant materiaal wordt beschreven in hoofdstuk 3. Het was al langer bekend dat CO wordt geëmitteerd door dood en ontbindend plantmateriaal, maar emissies van H_2 zijn niet eerder gemeten. Wel was bekend dat er H_2 kan vrijkomen als bepaalde componenten waaruit planten bestaan worden bestraald met UV straling. Deze experimenten zijn uitgevoerd met slechts één plantensoort en hebben laten zien wanneer deze plant wordt verhit tot minimaal 50°C er ook H_2 vrijkomt. Wanneer bladmateriaal in een atmosfeer zonder zuurstof wordt geplaatst en vervolgens bestraald wordt met UV straling, wordt er ook H_2 waargenomen. Deze onderzochte plantensoort emitteerde ook CO. De gemeten CO emissie was afhankelijk van temperatuur, UV straling en de aanwezigheid van zuurstof en kwam goed overeen met eerder uitgevoerde studies.

De hoofdstukken 4-6 gaan over CH_3Cl . Voor deze stof zijn zowel laboratorium- als veldmetingen gedaan. Deze worden beschreven in respectievelijk hoofdstuk 4 and 5. Hoofdstuk 6 beschrijft een studie waarin CH_3Cl wordt gemodelleerd.

De resultaten van de laboratorium experimenten over CH_3Cl zijn gepubliceerd in twee artikelen. In het eerste artikel zijn CH_3Cl emissies gemeten van verschillende

plant soorten. Het bleek dat er grote verschillen zijn in de hoeveelheid CH_3Cl die door verschillende planten wordt uitgestoten. Wel nam voor iedere onderzochte plant de emissie toe met toenemende temperatuur. Net als voor de koolwaterstoffen, kon de toename van de emissie met temperatuur worden beschreven door de Arrhenius vergelijking en werden de emissies veroorzaakt door een abiotisch proces. Het tweede artikel heeft zich gericht op de variatie in de emissies tussen de verschillende plant soorten. Voor deze tweede studie zijn halofyten gebruikt. Dit zijn plantensoorten die kunnen groeien in bodems met een hoog zoutgehalte. Als gevolg is het zoutgehalte, en dus het chloorgehalte, van de plant ook hoog. Voor twaalf soorten halofyten zijn de emissies van CH_3Cl gemeten op verschillende temperaturen. De verwachting was dat de CH_3Cl emissie hoger zou zijn voor plant met een hoger chloorgehalte, aangezien dit al eerder was gevonden in een studie door Hamilton et al. (2003). Echter, deze experimenten lieten zien dat de correlatie tussen de CH_3Cl emissie en het chloorgehalte van het blad niet significant is. Het chloorgehalte is dus niet de bepalende factor voor de emissies. Er moeten dus andere factoren zijn die de emissie sterk beïnvloeden. De toename van de emissie met temperatuur was wel vergelijkbaar voor de onderzochte halofyten.

Hoofdstuk 5 beschrijft een beperkte, maar interessante set veldexperimenten die niet zijn gepubliceerd. Tijdens deze experimenten is de uitstoot van CH_3Cl door het plantmateriaal gemeten. Het bleek dat er alleen emissies waarneembaar waren in perioden waarin vers blad gevallen was. Om de metingen te vergelijken met laboratoriummetingen is tijdens de veldmetingen blad verzameld. De emissies van dit blad zijn vervolgens gemeten in het laboratorium. Deze vergelijking liet zien dat er grote verschillen waren tussen de emissies gemeten tijdens de veld- en laboratoriumexperimenten voor blad van dezelfde boom. De uitstoot die gemeten was in het veld was veel groter dan tijdens de laboratoriummetingen. Dit kan te maken hebben met verschillen in het vochtgehalte van de plant ten tijde van de meting. Een nadeel van de veldmetingen is dat de onzekerheid in de meting erg groot is. Het is dan ook belangrijk om de meetmethode te verbeteren om nauwkeuriger de emissies te kunnen meten. Tijdens de veldexperimenten is ook de opname van CH_3Cl door de bodem gemeten. Tijdens alle metingen was deze opname groter dan de emissie van CH_3Cl door het aanwezige plantmateriaal. Ook bleek dat de opname gerelateerd was aan bodemtemperatuur: voor een hogere bodemtemperatuur was de opname groter. Echter, er was geen perfecte correlatie tussen bodemtemperatuur en emissie gevonden, wat suggereert dat ook andere factoren van invloed zijn op de opname. Een van de mogelijke factoren is bodemwater en dit zou onderzocht kunnen worden in vervolg experimenten.

De studie waarin CH_3Cl in de atmosfeer gemodelleerd is, is beschreven in hoofdstuk 6. Met behulp van een chemisch transport model is onderzocht hoe de emissies

van CH_3Cl door de atmosfeer verspreid worden. Verschillende emissiescenario's zijn gebruikt om CH_3Cl mixing ratios op verschillende meetstations te simuleren. Deze gesimuleerde mixing ratios zijn vervolgens vergeleken met metingen die op stations. Uit deze simulaties kwam naar voren alleen op een meetstation in Noord Amerika het plant materiaal een belangrijke bron was. Echter, het aantal stations dat de mixing ratios van CH_3Cl meet is beperkt en het is mogelijk dat er meer locaties zijn waar ontbindend plant materiaal een belangrijke bron is. Dit zal verder onderzocht moeten worden. In de tropen wordt CH_3Cl ook in grote hoeveelheden geëmitteerd door levende vegetatie. In deze gebieden is het dan ook lastig om te bepalen welk deel van de emissies door levende planten en welk deel door ontbindend plant materiaal veroorzaakt wordt. Naast simulaties met verschillende emissiescenario's zijn er ook inversies uitgevoerd. In een inversie wordt een emissie schatting met behulp van een wiskundige methode zo aangepast dat de gesimuleerde mixing ratios optimaal overeenkomen met de gemeten mixing ratios. Omdat er weining CH_3Cl metingen zijn, is alleen het totaal van alle emissies voor verschillende gebieden geschat. De inversies laten zien dat meer dan 90% van alle CH_3Cl emissies in de tropen plaatsvindt. Daarnaast bleek dat de emissies in Zuid Amerika lager waren dan in de initiële emissie schatting, terwijl de emissies in Afrika juist hoger waren. Om een nauwkeurigere en meer gedetailleerde emissie schatting te krijgen, zijn meer stations nodig waar CH_3Cl gemeten wordt.

BEDANKT!

Het onderzoek dat vooraf is gegaan aan het schrijven van dit proefschrift, heb ik natuurlijk niet helemaal alleen gedaan. Daarom wil ik graag een aantal mensen bedanken.

Allereerst Thomas en Rupert voor alle hulp bij het opzetten van de experimenten en de discussies over de resultaten. Natuurlijk waren Carina en Michel onmisbaar voor het uitvoeren van de experimenten in het lab. Zonder jullie praktische oplossingen en ideeën was het niet mogelijk geweest om al het werk in de afgelopen vier jaar te doen. Het model project heb ik alleen kunnen uitvoeren met de hulp van Maarten. Werken met een model was iets nieuws voor mij, maar ik heb er veel van kunnen leren en er ook veel plezier in gehad.

Next, I want to thank Frank, Asher and Colin. The project on the halophytes would not have been possible without you. I really enjoyed working on this project. The (mail) discussions we had on the interpretation of the results were very useful and motivating and have resulted in a nice paper.

Joralf wil ik graag bedanken voor alle experimenten die je in het lab hebt uitgevoerd. Omdat je ze zo goed uitgevoerd hebt, hebben we de resultaten uiteindelijk ook nog kunnen publiceren. Natuurlijk ben ik ook blij dat je mijn paranimf wilt zijn.

Het veld project heb ik niet uit kunnen voeren zonder de hulp van Vincent, en daar wil ik je hartelijk voor bedanken. Helaas ging de GC kapot en hebben we het project nooit helemaal af kunnen maken. Gelukkig zijn er wel interessante resultaten uit jou metingen gekomen en die zijn dan ook terecht gekomen in dit proefschrift.

Ook mijn ouders hebben meegewerkt aan het veld project. Jullie hebben een groot deel van de monsters verzameld in de tuin, ondanks kou en regenbuien op sommige dagen. Deze monsters hebben ook weer geleid tot interessante metingen en daar ben

ik natuurlijk erg blij mee.

Als laatste, maar zeker niet onbelangrijk, wil ik Pim bedanken. Eindeloos hebben wij over onze projecten gediscussieerd, zowel op het IMAU als thuis. Ik heb dit altijd erg nuttig gevonden en denk dat het ook goed is geweest voor dit project. Gelukkig hoefde het niet altijd over onderzoek te gaan en zijn we er ook regelmatig even tussenuit gegaan naar bergachtig gebied om daar heerlijk te fietsen.

CURRICULUM VITAE

Leonie Derendorp is geboren op 16 september 1984 in Moordrecht waar ze ook opgroeiëde. In 2002 behaalde ze haar VWO diploma op de Goudse Waarden te Gouda. Vervolgens volgde ze tussen 2002 en 2006 de bachelor opleiding Scheikunde aan de Universiteit Utrecht. Tijdens deze opleiding volgde Leonie ook een aantal vakken over meteorologie en luchtkwaliteit aan de universiteit van Wageningen. Na deze bachelor opleiding begon ze aan de master opleiding 'Meteorologie, fysische oceanografie en klimaat' bij het 'Instituut voor Marien en Atmosferisch onderzoek Utrecht'. Haar afstudeeronderzoek voerde ze uit in groep atmosferische fysica en chemie van prof. dr. Thomas Röckman. Het onderzoek bestond uit het ontwikkeling van systeem waarmee de organische en elementaire fractie van aerosol deeltjes gescheiden kon worden. Na het afronden van de master opleiding in 2007 is Leonie direct begonnen met een promotie onderzoek in dezelfde onderzoeksgroep. Dit onderzoek richtte zich op het meten van vluchtige stoffen die uitgestoten worden door ontbindende boombladeren.

BIBLIOGRAPHY

- Anke, H. and Weber, R. W. S. (2006). White rots, chlorine and the environment - a tale of many twists. *Mycologist*, 20:83–89.
- Atkins, P. and de Paula, J. (2002). *Physical chemistry*. Oxford university press, seventh edition.
- Austin, A. T. and Vivanco, L. (2006). Plant litter decomposition in a semi-arid ecosystem controlled by photodegradation. *Nature*, 442:555–558.
- Ayres, E., Steltzer, H., Simmons, B. L., Simpson, R. T., Steinweg, J. M., Wallenstein, M. D., Melior, N., Parton, W. J., Moore, J. C., and Wall, D. H. (2009). Home-field advantage accelerates leaf litter decomposition in forests. *Soil Biol. Biochem.*, 41:606–610.
- Bauer, K., Conrad, R., and Seiler, W. (1980). Photooxidative production of carbon monoxide by phototrophic microorganisms. *Biochim. et Biophys. Acta*, 589:46–55.
- Bernhard, G., Mayer, B., Seckmeyer, G., and Moise, A. (1997). Measurements of spectral solar UV irradiance in tropical Australia. *J. Geophys. Res.*, 102:8719–8730.
- Beyersdorf, A. J., Blake, D. R., Swanson, A., Meinardi, S., Rowland, F. S., and Davis, D. (2010). Abundances and variability of tropospheric volatile organic compounds at the South Pole and other Antarctic locations. *Atmos. Environ.*, 44:4565 – 4574.
- Blake, N. J., Blake, D. R., Sive, D. C., Chen, T.-Y., and Rowland, F. S. (1996). Biomass burning emissions and vertical distribution of atmospheric methyl halides and other reduced carbon gases in the South Atlantic region. *J. Geophys. Res.*, 101(D19):24151–24164.
- Blei, E., Hardacre, C. J., Mills, G. P., Heal, K. V., and Heal, M. R. (2010). Identification and quantification of methyl halide sources in a lowland tropical rainforest. *Atmos. Environ.*, 44:1005–1010.

BIBLIOGRAPHY

- Blei, E. and Heal, M. R. (2011). Methyl bromide and methyl chloride fluxes from temperate forest litter. *Atmos. Environ.*, 45:1543–1547.
- Brady, N. C. and Weil, R. R. (1999). *The nature and properties of soils*. Prentice Hall, twelfth edition.
- Brandt, L. A., Bohnet, C., and King, J. Y. (2009). Photochemically induced carbon dioxide production as a mechanism for carbon loss from plant litter in arid ecosystems. *J. Geophys. Res.*, 114. G02004, doi: 10.1029/2008JG000772.
- Brandt, L. A., King, J. Y., and Milchunas, D. G. (2007). Effects of ultraviolet radiation on litter decomposition depend on precipitation and litter chemistry in a shortgrass steppe ecosystem. *Global Change Biol.*, 13:2193–2205.
- Brownell, D. K., Moore, R. M., and Cullen, J. J. (2010). Production of methyl halides by *Prochlorococcus* and *Synechococcus*. *Global Biogeochem. Cy.*, 24. doi:10.1029/2009GB003671.
- Bruhn, D., Mikkelsen, T. N., Øbro, J., Willats, W. G. T., and Ambus, P. (2009). Effects of temperature, ultraviolet radiation and pectin methyl esterase on aerobic methane release from plant material. *Plant Biol.*, 11:43–48.
- Butler, J. H. (1994). The potential role of the ocean in regulating atmospheric CH₃Br. *Geophys. Res. Lett.*, 21(3):185–188.
- Butler, J. H. (2000). Better budgets for methyl halides? *Nature*, 403:260–261.
- Cahill, T. M., Seaman, V. Y., Charles, M. J., Holzinger, R., and Goldstein, A. H. (2006). Secondary organic aerosols formed from oxidation of biogenic volatile organic compounds in the Sierra Nevada Mountains of California. *J. Geophys. Res.*, 111. D16312, doi: 10.1029/2006JD007178.
- Campbell, N. A. and Reece, J. B. (2002). *Biology*. Benjamin Cummings, sixth edition.
- Chameides, W. L., Lindsay, R. W., Richardson, J., and Kiang, C. S. (1988). The role of biogenic hydrocarbons in urban photochemical smog: Atlanta as a case study. *Science*, 241(4872):1473–1475.
- Cheburkin, A. K. and Shotyk, W. (1996). An energy-dispersive miniprobe multielement analyzer (EMMA) for direct analysis of Pb and other trace elements in peats. *Fresen. J. Anal. Chem.*, 354:688–691.
- Claeys, M., Graham, B., Vas, G., Wang, W., Vermeylen, R., Pashynska, V., Guyon, J., Andreae, M. O., Artaxo, P., and Maenhaut, W. (2004). Formation of secondary organic aerosols through photooxidation of isoprene. *Science*, 303:1173–1176.
- Cogley, J. G. (2003). Gghydro - global hydrographic data, release 2.3. Trent Technical Note 2003-1, Department of Geography, Trent University, Peterborough, Ontario, Canada. Revised January 2007. 8p., data files.

- Conrad, R. and Seiler, W. (1982). Arid soils as a source of atmospheric carbon monoxide. *Geophys. Res. Lett.*, 9(12):1353–1356.
- Conrad, R. and Seiler, W. (1985a). Characteristics of abiological carbon monoxide formation from soil organic matter, humic acids and phenolic compounds. *Environ. Sci. Technol.*, 19(12):1165–1169.
- Conrad, R. and Seiler, W. (1985b). Influence of temperature, moisture, and organic carbon on the flux of H₂ and CO between soil and atmosphere: field studies in subtropical regions. *J. Geophys. Res.*, 90(D3):5699–5709.
- Cox, M. L., Sturrock, G. A., Fraser, P. J., Siems, S. T., Krummel, P. B., and O'Doherty, S. (2003). Regional sources of methyl chloride, chloroform and dichloromethane identified from AGAGE observations at Cape Grim, Tasmania, 1998 - 2000. *J. Atmos. Chem.*, 45:79–99.
- Dagar, J. C. and Gurbachan, S. (2007). Biodiversity of saline and waterlogged environments. Documentation, Utilization and Management. NBA Scientific Bulletin Number - 9, National Biodiversity Authority, Chennai, TamilNadu, India.
- Day, T. A., Zhang, E. T., and Ruhland, C. T. (2007). Exposure to solar UV-B radiation accelerates mass and lignin loss of *Larrea tridentata* litter in the Sonoran Desert. *Plant Ecol.*, 193:185–194.
- Dekking, F. M., Kraaikamp, C., Lopuhaä, H. P., and Meester, L. E. (2005). *A modern introduction to probability and statistics*. Springer, second edition.
- DiCarlo, P., Martinez, W. H., Harder, H., Leshner, R., Ren, X., Thornberry, T., Carroll, M. A., Young, V., Shepson, P. B., Riemer, D., Apel, E., and Campbell, C. (2004). Missing OH reactivity in a forest: Evidence for unknown reactive biogenic VOCs. *Science*, 304:722–725.
- Dimmer, C. H., Simmonds, P. G., Nickless, G., and Bassford, M. R. (2001). Biogenic fluxes of halomethanes from Irish peatland ecosystems. *Atmos. Environ.*, 35:321–330.
- Dumelin, E. E. and Tappel, A. L. (1977). Hydrocarbon gases produced during in vitro peroxidation of polyunsaturated fatty acids and decomposition of preformed hydroperoxides. *Lipids*, 12(11):894–900.
- Ehhalt, D. H. and Rohrer, F. (2009). The tropospheric cycle of H₂: a critical review. *Tellus*, 61B:500 – 535.
- Elliott, S. and Rowland, S. (1993). Nucleophilic substitution rates and solubilities for methyl halides in seawater. *Geophys. Res. Lett.*, 20(11):1043–1046.
- Ganzeveld, L., Lelieveld, J., and Roelofs, G.-J. (1998). A dry deposition parametrization for sulfur oxides in a chemistry and general circulation model. *J. Geophys. Res.*, 103(D5):5679–5694.

BIBLIOGRAPHY

- Gebhardt, S., Colomb, A., Hofmann, R., Williams, J., and Lelieveld, J. (2008). Halogenated organic species over the tropical South American rainforest. *Atmos. Chem. Phys.*, 8:3185–3197.
- Gola, A. A., D’Anna, B., Feilburg, K. L., Sellevag, S. R., Bache-Andreassen, L., and Nielsen, C. J. (2005). Kinetic isotope effects in the gas phase reactions of OH and Cl with CH₃Cl, CD₃Cl and ¹³CH₃Cl. *Atmos. Chem. Phys.*, 5:2395–2402.
- Graedel, T. E. and Keene, W. C. (1995). Tropospheric budget of reactive chlorine. *Global Biogeochem. Cy.*, 9(1):47–77.
- Gray, C. M., Monson, R. K., and Fierer, N. (2010). Emissions of volatile organic compounds during the decomposition of plant litter. *J. Geophys. Res.*, 115(G03015). doi:10.1029/2010JG001291.
- Halliwell, B. and Gutteridge, J. M. C. (2008). *Free radicals in biology and medicine*. Oxford university press, fourth edition.
- Hamilton, J. T. G., McRoberts, W. C., Keppler, F., Kalin, R. M., and Harper, D. B. (2003). Chloride methylation by plant pectin: An efficient environmentally significant process. *Science*, 301:206–209.
- Hardacre, C. J., Blei, E., and Heal, M. R. (2009). Growing season methyl bromide and methyl chloride fluxes at a sub-arctic wetland in sweden. *Geophys. Res. Lett.*, 36. L12401, doi: 10.1029/2009GL038277.
- Harper, D. B. (1985). Halomethane from halide ion - a highly efficient fungal conversion of environmental significance. *Nature*, 315:55–57.
- Harper, D. B., Hamilton, J. T. G., Ducrocq, V., Kennedy, J. T., Downey, A., and Kalin, R. M. (2003). The distinctive isotopic signature of plant-derived chloromethane: possible application in constraining the atmospheric chloromethane budget. *Chemosphere*, 52:433–436.
- Hatanaka, A. (1993). The biogeneration of green odour by green leaves. *Phytochem.*, 34:1201–1218.
- Hellebrand, H. J. and Schade, G. W. (2008). Carbon monoxide from composting due to thermal oxidation of biomass. *J. Environ. Qual.*, 37:592–598.
- Hellén, H., Hakola, H., Pystynen, K.-H., Rinne, J., and Haapanala, S. (2006). C₂ – C₁₀ hydrocarbon emissions from a boreal wetland and forest floor. *Biogeoscience*, 3:167–174.
- Holzinger, R., Lee, A., Paw, K. T., and Goldstein, A. H. (2005). Observations of oxidation products above a forest imply biogenic emissions of very reactive compounds. *Atmos. Chem. Phys.*, 5:67–75.
- Hopkins, W. G. (1999). *Introduction to Plant Physiology*. John Wiley and Sons, Inc., second edition.

- Huijnen, V., Williams, J., van Weele, M., van Noije, T., Krol, M., Dentener, F., Segers, A., Houweling, S., Peters, W., de Laat, J., Boersma, F., Bergamaschi, P., Velthoven, P., Sager, P. L., Eskes, J., Alkemade, J., Scheele, R., Nédélec, P., and Pätz, H.-W. (2010). The global chemistry transport model TM5: description and evaluation of the tropospheric chemistry version 3.0. *Geosci. Model Dev.*, 3:445–473. doi: 10.5194/gmd-3-445-2010.
- IPCC, editor (2007). *Contribution of Working Group I to the Fourth Assessment Report of the Intergovernmental Panel on Climate Change*. Cambridge University Press, Cambridge, United Kingdom and New York, NY, USA.
- Isidorov, V. and Jdanova, M. (2002). Volatile organic compounds from leaves litter. *Chemosphere*, 48:975–979.
- Isidorov, V. A., Smoleska, M., Purzyńska-Pugacewicz, A., and Tyszkiewicz, Z. (2010). Chemical composition of volatile and extractive compounds of pine and spruce leaf litter in the initial stages of decomposition. *Biogeoscience*, 7:2785–2794.
- John, W. W. and Curtis, R. W. (1977). Isolation and identification of the precursor of ethane in *Phaseolus vulgaris* L. *Plant Physiol.*, 79:521–522.
- Kasera, K. P. and Mohammed, S. (2010). Ecology of inland saline plants. In Ramawat, K. G., editor, *Desert Plants*. Springer Berlin Heidelberg.
- Keene, W. C., Khalil, M. A. K., III, D. J. E., McCulloch, A., Graedel, T. E., Lobert, J. M., Aucott, M. L., Gong, S. L., Harper, D. B., Kleiman, G., Midgley, P., Moore, R. M., Seuzaret, C., Sturges, W. T., Benkovitz, C. M., Koropalov, V., Barrie, L. A., and Li, Y. F. (1999). Composite global emissions for reactive chlorine from anthropogenic and natural sources: Reactive Chlorine Emission Inventory. *J. Geophys. Res.*, 104(D7):8429–8440.
- Keppler, F., Boros, M., Frankenberg, C., Lelieveld, J., McLeod, A., Pirttilä, A. M., Röckmann, T., and Schnitzler, J.-P. (2009). Methane formation in aerobic environments. *Environ. Chem.*, 6:459–465.
- Keppler, F., Eiden, R., Nledan, V., Pracht, J., and Schöler, H. F. (2000). Halocarbons produced by natural oxidation processes during degradation of organic matter. *Nature*, 403:298–301.
- Keppler, F., Harper, D. B., Röckmann, T., Moore, R. M., and Hamilton, J. T. G. (2005). New insight into the atmospheric chloromethane budget gained using stable carbon isotope ratios. *Atmos. Chem. Phys.*, 5:2402–2411.
- Keppler, F., Kalin, R. M., Harper, D. B., McRoberts, W. C., and Hamilton, J. T. G. (2004). Carbon isotope anomaly in the major plant C1 pool and its global biogeochemical implications. *Biogeoscience*, 1(2):123–131.

BIBLIOGRAPHY

- Khalil, M. A. K., Moore, R. M., Harper, D. B., Lobert, J. M., Erickson, D. J., Koropalov, V., Sturges, W. T., and Keene, W. C. (1999). Natural emissions of chlorine-containing gases: Reactive Chlorine Emissions Inventory. *J. Geophys. Res.*, 104(D7):8333–8346.
- Khalil, M. A. K. and Rasmussen, R. A. (1999). Atmospheric methyl chloride. *Atmos. Environ.*, 33:1305–1321.
- Khalil, M. A. K. and Rasmussen, R. A. (2000). Soil-atmosphere exchange of radiatively and chemically active gases. *Environ. Sci. Pollut. Res.*, 7(2):79–82.
- Khan, M. A. H., Rhew, R. C., Whelan, M. E., Zhou, K., and Deverel, S. J. (2011). Methyl halide and chloroform emissions from a subsiding Sacramento-San Joaquin Delta island converted to rice fields. *Atmos. Environ.*, 45:977–985.
- Kimmerer, T. W. and Kozlowski, T. T. (1982). Ethylene, ethane, acetaldehyde, and ethanol production by plants under stress. *Plant Physiol.*, 69:840–847.
- Konze, J. R. and Elstner, E. F. (1978). Ethane and ethylene formation by mitochondria as indication of aerobic lipid degradation in response to wounding of plant tissue. *Biochim. Biophys. Acta.*, 528:213–221.
- Krol, M. C., Houweling, S., Bregman, B., van den Broek, M., Segers, A., van Velthoven, P., Peters, W., Dentener, F., and Bergamaschi, P. (2005). The two-way nested global chemistry-transport zoom model TM5: algorithm and applications. *Atmos. Chem. Phys.*, 5:417–432.
- Lee-Taylor, J. M., Brasseur, G. P., and Yokouchi, Y. (2001). A preliminary three-dimensional global model study of atmospheric methyl chloride distributions. *J. Geophys. Res.*, 106(D24):34221–34233.
- Leff, J. W. and Fierer, N. (2008). Volatile organic compound (VOC) emissions from soil and litter samples. *Soil Biol. Biochem.*, 40:1629–1636.
- Leri, A. C. and Myneni, S. C. B. (2010). Organochlorine turnover in forest ecosystems: the missing link in the terrestrial chlorine cycle. *Glob. Biogeochem. Cy.*, 24. GB4021, doi:10.1029/2010GB003882.
- Lobert, J. M., Keene, W. C., Logan, J. A., and Yevich, R. (1999). Global chlorine emissions from biomass burning: Reactive Chlorine Emission Inventory. *J. Geophys. Res.*, 104(D7):8373–8389.
- Manley, S. L., Wang, N.-Y., Walser, M. L., and Cicerone, R. J. (2006). Coastal salt marshes as global methyl halide sources from determinations of intrinsic production by marsh plants. *Glob. Biogeochem. Cy.*, 20. GB3015, doi:10.1029/2005GB002578.
- Marcum, K. B. (1999). Salinity tolerance mechanisms of grasses in the subfamily Chloridoideae. *Crop Science*, 39(4):1153–1160.

- Matthews, E. (1989). Global data bases on distribution, characteristics and methane emission of natural wetlands: documentation of archived data tape. NASA TM-4153. National Aeronautics and Space Administration. Washington, D.C.
- Matthews, E. (1997). Global litter production, pools, and turnover times: Estimates from measurement data and regression models. *J. Geophys. Res.*, 102(D20):18771–18800.
- Matthews, E. and Fung, I. (1987). Methane emission from natural wetlands: global distribution, area and environmental characteristics of sources. *Global Biogeochem. Cycles*, 1:61–86.
- McAnulla, C., McDonald, I. R., and Murrell, J. C. (2001). Methyl chloride utilising bacteria are ubiquitous in the natural environment. *FEMS Microbiol. Lett.*, 201:151–155.
- McCulloch, A., Aucott, M. L., Benkovitz, C. M., Graedel, T. E., Kleiman, G., Midgley, P. M., and Li, Y.-F. (1999). Global emissions of hydrogen chloride and chloromethane from coal combustion, incineration and industrial activities: Reactive Chlorine Emission Inventory. *J. Geophys. Res.*, 104(D7):8391–9403.
- McDonald, I. R., Warner, K. L., McAnulla, C., Woodall, C. A., Oremland, R. S., and Murrell, J. C. (2002). A review of bacterial methyl halide degradation: biochemistry, genetics and molecular ecology. *Environ. Microbiol.*, 4(4):193–203.
- McKinlay, A. F. and Diffey, B. L. (1987). A reference action spectrum for ultraviolet induced erythema in human skin. *CIE Research Note*, 6(1):17–22.
- McLeod, A. R., Fry, S. C., Loake, G. J., Messenger, D. J., Reay, D. S., Smith, K. A., and Yun, B.-W. (2008). Ultraviolet radiation drives methane emissions from terrestrial plant pectins. *New Phytol.* doi: 10.1111/j.1469-8137.2008.02571.x.
- Meirink, J. F., Bergamaschi, P., and Krol, M. C. (2008). Four-dimensional variational data assimilation for inverse modelling of atmospheric methane emissions: method and comparison with synthesis inversion. *Atmos. Chem. Phys.*, 8:6341–6353.
- Messenger, D. J., McLeod, A. R., and Fry, S. C. (2009). The role of ultraviolet radiation, photosensitizers, reactive oxygen species and ester groups in mechanisms of methane formation from pectin. *Plant, Cell and Environ.*, 32:1–9.
- Miller, L. G., Warner, K. L., Baesman, S. M., Oremland, R. S., McDonald, I. R., Radajewski, S., and Murrell, J. C. (2004). Degradation of methyl bromide and methyl chloride in soil microcosms: Use of stable C isotope fractionation and stable isotope probing to identify reactions and the responsible microorganisms. *Geochim. Cosmochim. Ac.*, 68(15):3271–3283. doi: 10.1111/j.1469-8137.2008.02571.x.
- Moore, R. M. (2000). The solubility of a suite of low molecular weight organochlorine compounds in seawater and implications for estimating the marine source of methyl chloride to the atmosphere. *Chemosphere - Global Change Science*, 2:95–99.

BIBLIOGRAPHY

- Moore, R. M. (2008). A photochemical source of methyl chloride in saline water. *Environ. Sci. Technol.*, 42:1933–1937.
- Myneni, S. C. B. (2002). Formation of stable chlorinated hydrocarbons in weathering plant material. *Science*, 295:1039–1041.
- Natale, E., Zalba, S. M., Oggero, A., and Reinoso, H. E. (2010). Establishment of *Tamarix ramosissima* under different conditions of salinity and water availability: Implications for its management as an invasive species. *J. Arid Environ.*, 74(11):1399–1407.
- Novelli, P. C., Lang, P. M., Masarie, K. A., Hurst, K. A., Myers, R., and Elkins, J. W. (1999). Molecular hydrogen in the troposphere: Global distribution and budget. *J. Geophys. Res.*, 104:30427 – 30444.
- Ooki, A., Tsuda, A., Kameyama, S., Takeda, S., Itoh, S., Suga, T., Tazoe, H., Okubo, A., and Yokouchi, Y. (2010). Methyl halides in surface seawater and marine boundary layer of the northwest Pacific. *J. Geophys. Res.*, 115. C10013, doi:10.1029/2009JC005703.
- Patra, P. K., Houweling, S., Krol, M., Bousquet, P., Belikov, D., Bergmann, D., Bian, H., Cameron-Smith, P., Chipperfield, M. P., Corbin, K., Fortems-Cheiney, A., Fraser, A., Gloor, E., Hess, P., Ito, A., Kawa, S. R., Law, R. M., Loh, Z., Maksyutov, S., Meng, L., Palmer, P. I., Prinn, R. G., Rigby, M., Saito, R., and Wilson, C. (2011). TransCom model simulations of CH₄ and related species: linking transport, surface flux and chemical loss with CH₄ variability in the troposphere and lower stratosphere. *Atmos. Chem. Phys.*, 11:12813–12837.
- Pieterse, G., Krol, M. C., Batenburg, A. M., Steele, L. P., Krummel, P. B., Langenfeld, R. L., and Röckmann, T. (2011). Global modelling of H₂ mixing ratios and isotopic composition with the TM5 model. *Atmos. Chem. Phys. Discuss.*, 11:5811 – 5866.
- Poisson, N., Kanakidou, M., and Crutzen, P. J. (2000). Impact of non-methane hydrocarbons on tropospheric chemistry and the oxidizing power of the global troposphere: 3-dimensional modelling results. *J. Atmos. Chem.*, 36:157–230.
- Pozzer, A., Pollmann, J., Taraborrelli, D., Jöckel, P., Helmig, D., Tans, P., Hueber, J., and Lelieveld, J. (2010). Observed and simulated global distribution and budget of atmospheric C₂–C₅ alkanes. *Atmos. Chem. Phys.*, 10:4403–4422.
- Ramadan, T. (2001). Dynamics of salt secretion by *Sporobolus spicatus*(Vahl) Kunth from sites of differing salinity. *Ann. Bot.*, 87(2):259–266.
- Redeker, K. R., Wang, N.-Y., Low, J. C., McMillan, A., Tyler, S. C., and Cicerone, R. J. (2000). Emissions of methyl halides and methane from rice paddies. *Science*, 290:966–969.
- Rhew, R. and Mazéas, O. (2010). Gross production exceeds gross consumption of methyl halides in northern California salt marshes. *Geophys. Res. Lett.*, 37. L18813, doi:10.1029/2010GL044341.

- Rhew, R. C. and Abel, T. (2007). Measuring simultaneous production and consumption fluxes of methyl chloride and methyl bromide in annual temperate grasslands. *Environ. Sci. Technol.*, 41:7837 – 7843.
- Rhew, R. C., Aydin, M., and Saltzman, E. S. (2003). Measuring terrestrial fluxes of methyl chloride and methyl bromide using a stable isotope tracer technique. *Geophys. Res. Lett.*, 30(21). doi:10.1029/2003GL018160.
- Rhew, R. C., Chen, C., Teh, Y. A., and Baldocchi, D. (2010). Gross fluxes of methyl chloride and methyl bromide in a California oak-savanna woodland. *Atmos. Environ.*, 44(21):2054–2061.
- Rhew, R. C., Miller, B. R., and Weiss, R. F. (2000). Natural methyl bromide and methyl chloride emissions from coastal salt marshes. *Nature*, 403:292–295.
- Saito, T. and Yokouchi, Y. (2006). Diurnal variation in methyl halide emission rates from tropical ferns. *Atmos. Environ.*, 40:2806–2811.
- Saito, T. and Yokouchi, Y. (2008). Stable carbon isotope ratio of methyl chloride emitted from glasshouse-grown tropical plants and its implication for the global methyl chloride budget. *Geophys. Res. Lett.*, 35. L08807, doi:10.1029/2007GL032736.
- Salinas, M. J., Blanca, G., and Romero, A. T. (2000). Riparian vegetation and water chemistry in a basin under semiarid Mediterranean climate, Andarax River, Spain. *Environmental Management*, 26:539–552.
- Sander, S. P., Friedl, R. R., Golden, D. M., Kurylo, M. J., Moortgat, G. K., Keller-Rudek, H., Wine, P. H., Ravishankara, A. R., Kolb, C. E., Molina, M. J., Finlayson-Pitts, B. J., Huie, R. E., and Orkin, V. L. (2003). Chemical kinetics and photochemical data for use in atmospheric studies. Evaluation No. 15, JPL Publication 06-2, Jet propulsion Laboratory, Pasadena, Calif.
- Sanhueza, E., Dong, Y., Scharffe, D., Lobert, J. M., and Crutzen, P. J. (1998). Carbon monoxide uptake by temperate forest soils: the effect of leaves and humus layers. *Tellus*, 50B:51–58.
- Sanhueza, E., Donoso, L., Scharffe, D., and Crutzen, P. J. (1994). Carbon monoxide fluxes from natural, managed, or cultivated savannah grasslands. *J. Geophys. Res.*, 99(D8):16421–16427.
- Sauvage, S., Plaisance, H., Locoge, N., Wroblewski, A., Coddeville, P., and Galloo, J. C. (2009). Long term measurements and source apportionment of non-methane hydrocarbons in three French rural areas. *Atmos. Environ.*, 43:2430–2441.
- Schade, G. W. and Crutzen, P. J. (1999). CO emissions from degrading plant matter (2). Estimate of a global source strength. *Tellus*, 51B:909–918.
- Schade, G. W., Hofman, R.-M., and Crutzen, P. J. (1999). CO emissions from degrading plant matter (1). Measurements. *Tellus*, 51B:889–908.

BIBLIOGRAPHY

- Scheeren, H. A., Lelieveld, J., de Gouw, J. A., van der Veen, C., and Fischer, H. (2002). Methyl chloride and other chlorocarbons in polluted air during INDOEX. *J. Geophys. Res.*, 107(D19). 10.1019/2001JD001121.
- Scheeren, H. A., Lelieveld, J., Williams, J., Fischer, H., and C. Warneke (2003). Measurements of reactive chlorocarbons over the Surinam tropical rain forest: indications of strong biogenic emissions. *Atmos. Chem. Phys. Discuss.*, 3:5469–5512.
- Schönknecht, G., Brown, J. E., and Verchot-Lubicz, J. (2008). Plasmodesmata transport of GFP alone or fused to potato virus X TGBp1 is diffusion driven. *Protoplasma*, 232:143–152.
- Seinfeld, J. H. and Pandis, S. N. (2006). *Atmospheric chemistry and physics: From air pollution to climate change*. John Wiley and Sons, Inc., second edition.
- Shorter, J. H., Kolb, C. E., Crill, P. M., Kerwin, R. A., Talbot, R. W., Hines, M. E., and Harriss, R. C. (1995). Rapid degradation of atmospheric methyl bromide in soils. *Nature*, 377:717–719.
- Sionkowska, A., Kaczmarek, H., Vicini, S., Pedemonte, E., and Wisniewski, M. (2002). The influence of camphorquinone on the photochemical stability of cellulose. *Polymer Degradation and Stability*, 78:175–182.
- Smythe-Wright, D., Peckett, C., Boswell, S., and Harrison, R. (2010). Controls on the production of organohalogenes by phytoplankton: effect of nitrate concentration and grazing. *J. Geophys. Res.*, 115. G03020, doi:10.1029/2009JG001036.
- Song, J., Feng, G., Tian, C.-Y., and Zhang, F.-S. (2006). Osmotic adjustment traits of *Suaeda physophora*, *Haloxylon ammodendron* and *Haloxylon persicum* in field or controlled conditions. *Plant Sci.*, 170(1):113–119.
- Spivakovsky, C. M., Logan, J. A., Montzka, S. A., Balkanski, Y. J., Foreman-Fowler, M., Jones, D. B. A., Horowitz, L. W., Fusco, A. C., Brenninkmeijer, C. A. M., Prather, M. J., Wofsy, S. C., and McElroy, M. B. (2000). Three-dimensional climatological distribution of tropospheric OH: update and evaluation. *J. Geophys. Res.*, 105:8931–8980.
- Stein, O. and Rudolph, J. (2007). Modeling and interpretation of stable carbon isotope ratios of ethane in global chemical transport models. *J. Geophys. Res.*, 112. doi:10.1029/2006JD008062.
- Tarr, M. A., Miller, W. L., and Zepp, R. G. (1995). Direct carbon monoxide photoproduction from plant matter. *J. Geophys. Res.*, 100(D6):11403–11413.
- Teh, Y. A., Mazéas, O., Atwood, A. R., Abel, R., and Rhew, R. C. (2009). Hydrological regulation of gross methyl chloride and methyl bromide uptake from Alaskan Arctic tundra. *Global Change Biol.*, 15:330–345. doi:10.1111/j.1365-2486.2008.01749.x.

- Van der Werf, G. R., Randerson, J. T., Giglio, L., Collatz, G. J., Mu, M., Kasibhatla, P. S., Morton, D. C., DeFries, R. S., Jin, Y., and van Leeuwen, T. T. (2010). Global fire emissions and the contribution of deforestation, savanna, forest, agricultural, and peat fires (1997-2009). *Atmos. Chem. Phys.*, 10:11707–11735.
- Vigano, I., Holzinger, R., Keppler, F., Greule, M., Brand, W. A., Geilmann, H., van Weelden, H., and Röckmann, T. (2010). Water drives the deuterium content of the methane emitted from plants. *Geochim. Cosmochim. Ac.*, 74:3865–3873.
- Vigano, I., Röckmann, T., Holzinger, R., van Dijk, A., Keppler, F., Greule, M., Brand, W. A., Geilmann, H., and van weelden, H. (2009). The stable isotope signature of methane emitted from plant material under UV radiation. *Atmos. Environ.*, 43:5637–5646.
- Vigano, I., van Weelden, H., Holzinger, R., Keppler, F., McLeod, A., and Röckmann, T. (2008). Effect of UV radiation and temperature on the emission of methane from plant biomass and structural components. *Biogeosciences*, 5:973–947.
- Warneke, C., Karl, T., Judmaier, H., Hansel, A., Jordan, A., Lindinger, W., and Crutzen, P. J. (1999). Acetone, methanol, and other partially oxidized volatile organic emissions from dead plant matter by abiological processes: Significance for atmospheric HOx chemistry. *Glob. Biogeochem. Cy.*, 13(1):9–17.
- Watling, R. and Harper, D. B. (1998). Chloromethane production by wood-rotting fungi and an estimate of the global flux to the atmosphere. *Mycol. Res.*, 102(7):769–787.
- Wesely, M. L. (1989). Parametrization of surface resistances to gaseous dry deposition in regional-scale numerical models. *Atmos. Environ.*, 23:1293–1304.
- Wishkerman, A., Gebhardt, S., McRoberts, C. W., Hamilton, J. T. G., Williams, J., and Keppler, F. (2008). Abiotic methyl bromide formation from vegetation and its strong dependence on temperature. *Environ. Sci. Technol.* doi: 10.1021/es800411j.
- World Meteorological Organization, editor (2010). *Scientific Assessment of Ozone Depletion*, chapter 1: Ozone-depleting substances (ODSs) and related chemicals. World Meteorological Organization.
- Xiao, X., Prinn, R. G., Fraser, P. J., Simmonds, P. G., Weiss, R. F., O'Doherty, S., Miller, D. R., Salameh, P. K., Harth, C. M., Krummel, P. B., Porter, L. W., Mühle, J., Grevilly, B. R., Cunnold, D., Wang, R., Montzka, S. A., Elkins, J. W., Dutton, G. S., Thompson, T. M., Butler, J. H., Hall, B. D., Reimann, S., Vollmer, M. K., Stordal, F., Lunder, C., Maione, M., Arduini, J., and Yokoucki, Y. (2010). Optimal estimation of the surface fluxes of methyl chloride using a 3-D global chemical transport model. *Atmos. Chem. Phys.*, 10:5515–5533.
- Yassah, N., Wishkerman, A., Keppler, F., and Williams, J. (2009). A method for the fast determination of methyl chloride and methyl bromide emissions from plant matter and soil samples using HS-SPME and GC-MS. *Environ. Chem.*, 6:311–318.

BIBLIOGRAPHY

- Yates, E. L., Derwent, R. G., Simmonds, P. G., Grealley, B. R., O'Doherty, S., and Shallcross, D. E. (2010). The seasonal cycles and photochemistry of C₂–C₅ alkanes at Mace Head. *Atmos. Environ.*, 44:2705–2713.
- Yokouchi, Y., Ikeda, M., Inuzuka, Y., and Yukawa, T. (2002). Strong emission of methyl chloride from tropical plants. *Nature*, 416:163–165.
- Yokouchi, Y., Noijiri, Y., Barrie, L. A., Toom-Sauntry, D., Machida, T., Inuzuka, Y., Akimoto, H., Li, H. J., Fujinuma, Y., and Aoki, S. (2000). A strong source of methyl chloride to the atmosphere from tropical coastal land. *Nature*, 403:295–298.
- Yokouchi, Y., Saito, T., Ishigaki, C., and Aramoto, M. (2007). Identification of methyl chloride-emitting plants and atmospheric measurements on a subtropical island. *Chemosphere*, 69:549–553.
- Yoshida, Y., Wang, Y., Shim, C., Cunnold, D., Blake, D. R., and Dutton, G. S. (2006). Inverse modeling of the global methyl chloride sources. *J. Geophys. Res.*, 111. D16307, doi: 10.1029/2005JD006696.
- Yoshida, Y., Wang, Y., and Zeng, T. (2004). A three-dimensional global model study of atmospheric methyl chloride budget and distribution. *J. Geophys. Res.*, 109. D24309, doi: 10.1029/2004JD004951.
- Zar, J. H. (2007). *Biostatistical analysis*. Pearson Education, USA, 5th edition.
- Zepp, R. G., Miller, W. L., Burke, R. A., Parsons, D. A. B., and Scholes, M. C. (1996). Effects of moisture and burning on soil-atmosphere exchange of trace carbon gases in a southern African savanna. *J. Geophys. Res.*, 101(D19):23699–23706.